Late Barremian–early Aptian ammonite bioevents from the Urgonian-type series of Provence, southeast France: Regional stratigraphic correlations and implications for dating the peri-Vocontian carbonate platforms

Camille Frau, Anthony J.-B. Tendil, Cyprien Lanteaume, Jean-Pierre Masse, Antoine Pictet, Luc Bulot, Tim Luber, Jonathan Redfern, Jean Borgomano, Philippe Leonide, et al.

Late Barremian–early Aptian ammonite bioevents from the Urgonian-type series of Provence, southeast France

DOI:
10.1016/j.cretres.2018.04.008

Document Version
Accepted author manuscript

Late Barremian–early Aptian ammonite bioevents from the Urgonian-type series of Provence, southeast France: regional stratigraphic correlations and implications for dating the peri-Vocontian carbonate platforms

Camille Frau[1,*], Anthony J.-B. Tendil[2], Cyprien Lanteaume[2], Jean-Pierre Masse[2], Antoine Pictet[3,4], Luc G. Bulot[2,5], Tim L. Luber[5], Jonathan Redfern[5], Jean R. Borgomano[2], Philippe Léonide[2], François Fournier[2] and Gérard Massonnat[6]

[1] Groupement d'Intérêt Paléontologique, Science et Exposition, 60 bd Georges Richard, 83000 Toulon, France

[2] Aix Marseille Université, CNRS, IRD, Collège de France, CEREGE, Marseille St-Charles, France

[3] University of Geneva, Department of Earth Sciences, 13 Rue des Maraîchers, 1205 Geneva, Switzerland

[4] Present address: Musée cantonal de géologie, BFSH-2, 1015 Lausanne, Switzerland

[5] University of Manchester, School of Earth and Environmental Sciences, North Africa Research Group, M13 9PL, Manchester, UK

[6] TOTAL S.A., Centre Scientifique & Technique Jean Féger, Avenue Larribau, 64018 Pau, France

[*] corresponding author, E-mail address: camille_frau@hotmail.fr (Camille Frau)

Abstract

This work provides a new ammonite age-calibration of the rudistid limestones of the Urgonian-type Provence carbonate platform (Southeast France) based on sampling along three ~200 km-long platform-to-basin transects and re-examination of historical collections. Ammonite key findings indicate that the first rudistid platform stage (including the *Agriopleura* and requieniid–monopleurid beds) develops and spreads northward through the *Toxancyloceras vandenheckii–Gerhardtia sartousiana* zones interval (lower upper Barremian). This stage is interrupted by the tectonically-induced deepening of the southern Provence domain during the *Imerites giraudi* Zone while the northern regions records the massive deposition of *Palorbitolina–Heteraster* beds. Recovery of the rudistid carbonate system is illustrated by the development of caprinid-bearing rudistid limestones in the North Provence domain through the *Martelites sarasini* Subzone (lower *Martelites sarasini* Zone, uppermost Barremian), which shows a bidirectional progradation toward the South Provence and Vocontian basins. The

caprinid-bearing limestones terminate at a short-term exposure and are overlain by cherty–oobioclastic deposits spanning the *Pseudocrioceras waagenoides* Subzone (upper *M. sarasini* Zone) to the lower *Deshayesites forbesi* Zone. A regional-wide flooding of the study area is illustrated by the abrupt change to a marl-dominated regime occurring in the upper *D. forbesi* Zone. Compared to the previous datings, the Barremian/Aptian boundary should be relocated in the lower part of the post-caprinid, cherty–oobioclastic deposits although its precise level cannot be fixed due to the lack of a continuous ammonite record. Ammonite age-calibration of the surrounding Urgonian rudistid platform series is discussed and gives evidence of a comparable twofold demise of the peri-Vocontian rudistid biota during the uppermost Barremian. Accordingly, the link between the final demise of the peri-Vocontian rudistid biota and the onset and/or culmination of the mid-early Aptian Oceanic Anoxic Event (OAE) 1a should be reconsidered.

Keywords

Urgonian; Carbonate Platform; Ammonite; OAE 1a; Cretaceous; Southeast France.

1. Introduction

Urgonian carbonate platforms of Barremian–Aptian age are extensively recorded in southeast France which hosts the unit-stratotype at Orgon (Alpilles Massif, Bouches-du-Rhône) as introduced by d'Orbigny (1850, 1852). At this time, the Urgonian platforms of Provence, Bas-Vivarais, Subalpine Chains and Swiss–French Jura record their maximum spatial extent and enclose the Vocontian Basin; i.e. forming a horseshoe-shaped marginal sea opened eastward to the Alpine Tethys Ocean (Arnaud, 2005a and references therein). In the existing models, the extensive growth of peri-Vocontian Urgonian carbonate platforms is first interrupted by a major shift from rudist–coral carbonate accumulation to mixed orbitolinid-dominated siliciclastic–carbonate deposition at, or close, to the putative Barremian/Aptian (B/A) boundary. This refers to the *Palorbitolina–Heteraster* guide level of the North Provence (Masse, 1976), the V4 episode of the Bas-Vivarais (Lafarge, 1978), the Lower *Orbitolina* Beds of the Subalpine regions (Arnaud et al., 1998) and the Poet Beds of Swiss–French Jura (Pictet et al., 2016). The recovery of the rudistid biota, dominated by caprinid rudists, supposedly unfolds in the lowermost Aptian but it subsequently collapses with large-scale exposure that ends the rudistid regime throughout the peri-Vocontian platforms (e.g. Masse, 1976, 1995, 2003; Masse et al., 1999; Masse & Fenerci-Masse, 2011, 2013a-b;

Arnaud-Vanneau & Arnaud, 1990; Arnaud-Vanneau et al., 2005; Arnaud & Arnaud-Vanneau, 1991; Arnaud et al., 1998, 2017; Chartrousse, 1998; Clavel et al., 2002, 2007; 2013, 2014; Embry, 2005; Linder et al., 2006; Léonide et al., 2008, 2012, 2014; Bastide, 2014; Pictet et al., 2015, 2016; Huck et al., 2011, 2013; Huck & Heimhofer, 2015; Godet et al., 2016a) and eastern Switzerland as well (Wissler et al., 2002, 2003; Föllmi, 2008, 2012; Föllmi & Gainon, 2008; Föllmi et al., 1994; 2006, 2007; Stein et al., 2012a). Integrated approaches developed in the latter contributions, coupling sedimentology, palaeoenvironmental proxies and shallow-water biostratigraphy (viz. rudists, orbitolinid, dasycladaceans and charophytes), addressed the timing and causal relationships of the final demise of the Urgonian rudistid regime with the onset and/or culmination of the mid-early Aptian Oceanic Anoxic Event (OAE) 1a. Unfortunately, the lack of coeval biological markers across the B/A boundary limits the correlation of the Urgonian series with the Barremian- and Aptian-type basinal sections of the nearby Vocontian Basin. Here, various bio- (Dauphin, 2002; Herrle & Mutterlose, 2003), litho- (Bréhéret, 1997; Cotillon et al., 2000; Cotillon, 2010) and geochemical (Westermann et al., 2013) expressions of the OAE 1a have been constrained to the Mediterranean ammonite zonations; successively developed by the IUGS Lower Cretaceous Ammonite Working Group (Reboulet et al., 2011, 2014). This lack of robust biostratigraphic constrain caused a number of disputes in the literature about the calibration of shallow-water biological markers or correlation of major unconformities into the basin and their correspondence with major sea-level changes, which ultimately introduced significant confusion on the timing and predominant controlling factors of the stepwise demise of the Urgonian carbonate production.

Over the past decades, external calibration by means of chemostratigraphy (i.e. $\delta^{13}C$, $\delta^{18}O$, Sr) has emerged and imposed itself as a powerful tool of stratigraphic significance for correlating and dating carbonate units (Scholle & Arthur, 1980). The carbon signature of the Urgonian platform series of SE France and Switzerland has been, therefore, intensively investigated in order to refine platform-to-basin correlations and palaeoenvironmental interpretations (e.g. Masse et al., 1999; Raddadi, 2005; Godet et al., 2006; Föllmi et al., 2006; Huck et al., 2011, 2013; Stein et al., 2012b; Léonide et al., 2014; Huck & Heimhofer, 2015); enough to enable the authors to come to the conclusion that chemostratigraphy has the potential to provide an independent control on the controversial dating based on biological markers (Huck et al., 2013). The uppermost Barremian is characterised by a global, sharp negative excursion in $\delta^{13}C$ values in basinal sections (Kuhnt et al., 2000; Godet et al., 2006; Stein et al., 2011, 2012a-b). From this observation, several authors have characterised this time interval in the Urgonian platform successions by assuming a contemporaneous negative excursion in C-isotope signal observed at, or just below, the orbitolinid-rich episodes of the peri-Vocontian platforms (Raddadi, 2005;

Arnaud-Vanneau et al., 2005; Huck et al., 2011, 2013; Léonide et al., 2014). However, such trends may result from documented subaerial exposure surfaces (Masse & Fenerci-Masse, 2011; Huck et al., 2014) and their subsequent diagenetic alteration (Allan & Matthews, 1977; Joachimski, 1994; Fouke et al., 1995; Léonide et al., 2014) which strongly affect the isotope signature of Urgonian carbonates (Godet et al., 2016b).

A limited number of works focused on the Sr-Isotope Stratigraphy (SIS), of the Urgonian platform series of SE France (Huck et al., 2011, Huck & Heimhofer, 2015) and Switzerland (Godet et al., 2011). SIS was expected to improve the existing ammonite-based age models for the Barremian–Aptian time interval (Masse & Steuber, 2007). Unfortunately, Frau et al. (accepted) highlight that SIS provide limited utility for intervals with little or no variations through time, such as the Barremian–Aptian transition. Its low resolution has led to the inconsistent stratigraphic dating of the Urgonian limestones of Provence (cf. Huck & Heimhofer, 2015). The foregoing considerations show that bio- and chemostratigraphic markers are frequently in conflict when dating the Urgonian platform series of SE France and Switzerland and do not allow to accurately pinpoint the uppermost Barremian (*Imerites giraudi–Martelites sarasini* zones interval) to earliest Aptian (*Deshayesites oglanlensis–Deshayesites forbesi* zones interval) time interval.

To address this issue, new *in situ* ammonite findings along three ~200km-long platform-to-basin transects of the Provence platform are reported in this paper, together with a re-examination of the collection of one of us (J.-P. Masse). This allows a critical review of the ammonite age-calibration of the Urgonian-type series with respect to the standard Mediterranean ammonite zonation (Fig. 1). Our data pinpoint a late Barremian stepwise demise of the Urgonian rudistid regime throughout the peri-Vocontian carbonate platforms.

2. Current ammonite age-calibration of the Provence platform

According to the stratigraphical model developed in the past decades by Masse (1993, 1995, 2003), Masse & Fenerci-Masse (2011, 2013a-c) and Léonide et al. (2012), the Provence rudistid platform records its maximum northward progradation at the lower/upper Barremian transition and extends up into the mid-lower Aptian (*D. forbesi* Zone), from the southern (Calanques and Nerthe massifs) to the northern (Monts de Vaucluse and Rissas–Bluye Mountains) Provence where it plunges into the Vocontian Basin. Contrary to the Orgon unit-stratotype, the Monts de Vaucluse in northern Provence house complete Urgonian-type series (Masse & Fenerci-Masse, 2013a), which was historically divided into three informal lithostratigraphic units; U^1 (bioclastic), U^2 (rudistid) and U^3 (bioclastic) *sensu* Leenhardt (1883). Three distinct rudistid episodes are recognised in the North

Provence rudist-bearing limestones (= U^2 *lato sensu*); these are from oldest to youngest; the (*i*) *Agriopleura* (Martigues fauna); (*ii*) requieniid–monopleurid (Orgon fauna) and (*iii*) caprinid (Rustrel fauna) rudistid faunas (see Tendil et al., accepted). The caprinid-bearing limestones (= U^2 *stricto sensu*) can be easily distinguished in the field since they usually overly the *Palorbitolina–Heteraster* guide level, traceable in the Monts de Vaucluse (Masse & Fenerci-Masse, 2011; Léonide et al., 2012) and adjacent settings of the Bas-Vivarais platform (Lafarge, 1978; Masse, 1995, Masse & Fenerci-Masse, 2011).

For the time being, only a handful of ammonite occurrences have contributed to the dating of the Urgonian-type limestones. Isolated occurrence of upper Barremian hemihoplitid and heteroceratid taxa have been documented in drowning discontinuities of the U^1 formation (Fahy, 1965; Masse, 1976; Léonide et al., 2008, 2012) or the basinward equivalent of the *Palorbitolina–Heteraster* guide level in pre-Vocontian settings (e.g. Masse, 1976; Monier, 1986; Conte, 1989; Delanoy, 1997a; Masse & Fenerci-Masse, 2011). These ammonite occurrences supported the location of the B/A boundary within the rudist-bearing U^2 *l.s.* formation but its precise location has been repeatedly questioned over the last two centuries (Leenhardt, 1883; Kilian, 1896; Pellat, 1903; Paquier, 1905; Pellat & Cossmann, 1907; Douvillé, 1918; Goguel, 1932; Rivier, 1960; Faure, 1965; Fahy, 1965; Maillard, 1965; Masse, 1976; Masse et al., 1999; Masse & Fenerci-Masse, 2011, 2013a-c; Léonide et al., 2012, 2014) (Fig. 2), and still remains a challenging issue in the understanding of the demise of the rudistid biota in peri-Vocontian Urgonian platforms (Frau et al., 2017). Unfortunately, a comprehensive review of the ammonite occurrences of the Provence platform had not previously been undertaken and no ammonite had been described from the overlying U^3 formation of North Provence, which might have provided a direct calibration.

3. Geological setting

3.1. Geographical context

In this study, we examine classical and new localities of the Provence platform covering parts of the Bouches-du-Rhône (Calanques, Nerthe, Fare and Alpilles massifs), Vaucluse (western Monts de Vaucluse) and Alpes-de-Haute-Provence (eastern Monts de Vaucluse, Albion Plateau and Monges Massif) regions (Fig. 3). The study area is bounded by the Rhône River valley to the west and by the Durance River valley to the east, the Mediterranean coast to the south and the Ventoux–Lure mountains to the north.

151

152 *3.2. Palaeogeography*

153

154 In southern Provence, the Urgonian platform regime developed between the lower Valanginian and the
155 upper Barremian at a palaeo-latitude of ~27–28° N (Masse, 1976, 1993; Masse et al. 2000; Masse & Fenerci-
156 Masse, 2011, 2013b), and records successive phases of northward progradation and southward backstepping
157 towards the Vocontian Basin (Masse, 1993) (Fig. 4). The maximum northward progradation of the Provence
158 rudistid platform occurred during the lower upper Barremian (Fig. 4A and B), with the spreading of the
159 *Agriopleura* and requieniid–monopleurid episodes south to the N100-trending Mont Ventoux–Lure axis (Masse,
160 1976), which marks the palaeogeographic transition with the neighbouring Vocontian basinal setting (Kandel,
161 1992). A progressive deepening, whose spatial extent remains unknown (Fig. 4C), is recorded in the Saint-
162 Chamas area (Masse & Fenerci-Masse, 2013b) and precedes the regional collapse of the southern part of the
163 Provence platform during the upper Barremian *Imerites giraudi* Zone (Masse & Fenerci-Masse, 2011; Frau et
164 al., 2016). This event leads to the installation of the ammonite-rich, intra-shelf South Provençal Basin from the
165 latest Barremian onward (*M. sarasini* Zone – Fig. 4C) up into the upper Aptian (Moullade et al., 2000a; Frau et
166 al., submitted). The corresponding drowning sequence and lowermost basinal series are known to record short-
167 lived, dys- to anoxic episodes (Machhour et al., 1998; Masse & Machhour, 2000), which are supposed to be
168 coeval with the massive outbreak of *Palorbitolina–Heteraster* communities in northern Provence and adjacent
169 settings of the Bas-Vivarais (Masse & Fenerci-Masse, 2011).

170 In northern Provence, recovery of the rudistid regime occurs and corresponds to the spreading of the
171 caprinid biota (Fig. 4E), whose corresponding platform stage exhibits a bidirectional progradation toward the
172 South Provence and Vocontian basins (Masse, 1976, 1993, 1995, 2003; Embry, 2005; Masse & Fenerci-Masse,
173 2011; Léonide et al., 2008, 2012). The progradation of the North Provence platform *sensu* Masse (1993) is
174 abruptly interrupted at a short-termed emersion surface herein dated to the uppermost Barremian (*M. sarasini–P.*
175 *waagenoides* subzonal boundary) which ends the Urgonian rudistid regime through the study area. This
176 discontinuity is overlain by a thick succession (~20 to 100 m) of calcarenites and cherty limestones (U^3
177 formation) in the North Provence (Fig. 4F), with a *Palorbitolina*–coral episode at its base (Masse & Fenerci-
178 Masse, 2011; Léonide et al., 2012). As shown by Frau et al. (2017), the U^3 formation is partly coeval with the
179 limestone-dominated basinal series (Fig. 4F), referred to the Calcareous Mb. (*sensu* Moullade et al., 2000b) in

180 the South Provence Basin and the Barremian–Bedoulian Limestones Fm. (*sensu* Delanoy, 1995a-b) in the
181 Vocontian Basin.

182 A regional deepening event terminates the deposition of the U^3 platform calcarenites (Fig. 4G) and leads
183 to the deposition of a thick (~ 80 m), marl-dominated succession of mid-early (Frau et al., 2017) to late Aptian
184 age in the North Provence (Dutour, 2005; Moullade et al., 2012). This succession was itself divided into three
185 units (A^1 to A^3) by Leenhardt (1883) and forms the Aptian-type series of the Apt–Gargas area (Moullade, 1965).
186 A minor discontinuity evidenced by a glauconitic horizon is documented between the yellowish A^1 and the blue–
187 grey A^2 marls, which includes the OAE 1a time interval (i.e. culmination of the black shale deposits) dated to the
188 uppermost *D. forbesi*–lower *D. deshayesi* zones interval (Frau et al., 2017 and references therein). This regional
189 deepening is coeval with a change toward a marl-dominated regime in the South Provence (Marly-limestone
190 Mb.) and Vocontian (Blue Marls Fm.) basins which continues up into the Albian (Bréhéret, 1995; Dauphin,
191 2002).
192
193 **4. Material and methods**
194
195 This paper deals with a coupled sedimentological–palaeontological study based on field observations
196 and ammonite sampling obtained from 20 reference profiles of Provence described in the joint contribution of
197 Tendil et al. (accepted). The ammonites were collected by the three first authors (C.F., A.J.-B.T., C.L.), but we
198 also re-examined additional specimens collected by J.-P. Masse during his seminal study (Masse, 1976). A
199 systematic description of the studied ammonite taxa is provided below. We recognised eight ammonite bioevents
200 of regional significance which span the upper Barremian–lower Aptian and provide an improved age-calibration
201 for the North Provence platform settings. The ammonite bioevents are here interpreted as Opportunity Faunal
202 Uniformity Horizons (O-FUH) *sensu* Bulot (1993), and mainly correspond to mixed shelf–basin ammonite
203 assemblages following major flooding events.

204 The direct recognition of the ammonite bioevents, or their derived stratigraphic correlations, enable us
205 to reconstruct three platform-to-basin transects of the Provence platform (Fig. 5, 6, 7). Occurrence of ammonite
206 faunas in platform settings are tentatively tied to the relative sea-level variations documented at that time in the
207 Vocontian Basin and its margins (Arnaud, 2005b, fig. 88) (see also Fig. 2), and compared to the ammonite
208 abundance changes of the Barremian-type series of Angles (Delanoy, 1995a-b, 1997a-b; Bréhéret, 1997;
209 Vermeulen, 2005; Bert et al., 2008), and the Nice topographic high (Delanoy, 1992, Arnaud, 2005b, fig. 89).

5. Systematic palaeontology

This palaeontological appendix discusses and illustrates the ammonite taxa that are of biostratigraphic relevance for dating the studied sections of the Provence platform. The following palaeontological notes are by no means to be considered as definitive and many taxa are left in open nomenclature pending the collection of better preserved and/or more abundant material. Unless otherwise mentioned, all specimens and/or duplicates are deposited in the Frau collection at the Musée de Paléontologie de Provence (MPP – Aix-Marseille Université, France). The other acronyms of repositories indicate: FSL – Faculté des Sciences, Université Claude Bernard–Lyon-I, Lyon and UJF-ID – Institut Dolomieu, Université Joseph Fournier, Grenoble. Suprageneric classification is limited to the family level.

Family Ancyloceratidae Gill, 1871

Genus *Moutoniceras* Sarkar, 1955

Moutoniceras sp.

Fig. 8A–B

Material. One specimen, FSL.85850 from Roque Pourquière (Fontaine-de-Vaucluse).

Description. Shaft fragment of a *Moutoniceras* relatives marked by a compressed sub-oval whorl section bearing uniform ribs that are thickened and nodular on the upper flanks and venter.

Genus *Toxancyloceras* Delanoy, 2003

Toxancyloceras vandenheckii (Astier, 1851)

Fig. 8C

Material. Two specimens, MPP-V-MV.7 and V-MV.8 from the Mont Ventoux (Monts de Vaucluse).

Description. Specimen MPP-V-MV.7 is represented by a large-sized, sub-complete ancyloceratid ammonite lacking its spire. Growth rate is moderately low and marked by a long and massive, straight shaft terminated by a

moderately long, U-shaped hook. Its ornamentation is composed of the alternation of straight to slightly prorsiradiate, trituberculate primary ribs and variable number of atuberculate secondaries through most part of the shaft. As growth increase, primary ribs are enlarged and bears stronger tubercles. In the adult, the ornamentation changes into strong, spaced, sharp ribs with smooth interspaces.

Toxancyloceras sp.

Fig. 8D–E

Material. One specimen, MPP-A.45 (Masse *in* Frau coll.) from Roque Pourquière (Fontaine-de-Vaucluse).

Description. Poorly-preserved fragment tentatively assigned to the late part of a *Toxancyloceras* spire. It is marked by a compressed sub-oval whorl section bearing differentiated ribs; tri-tuberculate main ribs alternated with one to three fine, atuberculate intercalatories.

Genus *Kutatissites* Kakabadze, 1970

Kutatissites gr. *chreithiensis* Kakabadze, 1981

Fig. 9A–B

Material. Two specimens, n°28720 (private collection of G. Delanoy) and UJF-ID. 10590. We re-examined the specimen illustrated by Delanoy & Ebbo (1997) from Redortiers, ~4km north to Banon. It originates from the lateral equivalent of the basinal succession overlying the northward termination of the caprinid-bearing limestones represented by fine-grained calcisiltites at Banon. The specimen UJF-ID. 10590 (Gidon coll.) previously referred to *Ancyloceras* gr. *matheronianum* by Arnaud et al. (1998, pl. 7, fig. 7) is here referred to *K.* gr. *chreithiensis*.

Description. The specimen n°28720 has been precisely described by Delanoy & Ebbo (1997, p. 5-6) to which the reader is referred. The specimen UJF-ID. 10590 closely resembles the Delanoy's specimen by its morphological and ornamental features. It differs slightly by its robust tripartite coiling.

Kutatissites gr. *pouponi* Delanoy, Ropolo, Gonnet & Ebbo, 2000

Fig. 9C–D

Material. One specimen, MPP-V-SC.C.1 from Saint Christol (Plateau d'Albion). It originates from the lateral equivalent of the second lithological unit of the Sault section (see supplementary data).

Description. Specimen MPP-V-SC.C.1 is represented by a medium-sized, inflated shaft of a tripartite *Kutatissites* characterised by irregular alternation of trituberculate primary ribs, sometimes bifurcated, and variable number of simple secondaries. As growth increases, secondary ribs disappear while primary ribs strengthen and develop peri-ventral clavis. Whorl section is rounded to sub-hexagonal with a flattened venter on the shaft.

Genus *Pseudocrioceras* Spath, 1924

Pseudocrioceras sp.

Fig. 9E–G

Material. One specimen, MPP-A.113 (Masse *in* Frau coll.) from the Conque Verte Valley, Gorges de La Nesque (Monts de Vaucluse).

Description. MPP-A.113 corresponds to a large-sized, body chamber of an ancyloceratid ammonite. Whorl height increases rapidly with a compressed, higher than wide, sub-oval whorl section which become sub-rounded in the adult. The ornamentation of the shaft and lower part of the hook is marked by spaced, thick, slightly prorsiradiate, trituberculate ribs with smooth interspaces. The internal and external lateral tubercles are strong with a rounded base while the latero-ventral ones are elongated and form elevated clavi delimiting a ventral furrow. Near the aperture, the ornamentation changes into thick, spaced rounded atuberculate ribs. Suture line is of ancyloceratid type. By its morphology (ancyloceratid coiling) and ornamentation (trituberculate primary ribs ended by elongated clavi), the specimen belongs to *Pseudocrioceras*, but the lack of the spire prevents its specific identification.

Family Hemihoplitidae Spath, 1924

Subfamily Hemihoplitinae Spath, 1924

Genus *Camereiceras* Delanoy, 1990

Camereiceras limentinum (Thieuloy, 1979)

Fig. 10A, B–C, H–I

Material. Seven specimens, MPP-A.102 (*Masse* in Frau coll.) from La Redde, Gorges de La Nesque (Monts de Vaucluse); MPP-V-MV.5, 6, 9, 10, 11 from the Mont Ventoux section (Monts de Vaucluse); MPP-APH-BAU.R0.1 *ex situ* from Baudinard (Monges Massif). We also re-examined the specimen illustrated by Léonide et al. (2012, fig. 6G) from the Cire section Gorges de La Nesque (Monts de Vaucluse).

Description. Small- to large-sized, evolute, dimorphic hemihoplitids. Ontogeny encompasses the three stages defined by Bert et al. (2006, p. 181) to which the reader is referred.

Genus *Janusites* Bert & Delanoy, 2000

Janusites janus (Thieuloy, 1979)

Fig. 10D–E

Material. One specimen, MPP-V-MV.4 from the Mont Ventoux (Monts de Vaucluse).

Description. Small-sized, evolute hemihoplitid bearing the three ornamental stages described by Bert & Delanoy (2000, p. 71) to which the reader is referred.

Genus *Hemihoplites* Spath, 1924

Hemihoplites sp. gr. *feraudianus* (d'Orbigny, 1841)

Fig. 11A–B, C

Material. Six specimens, MPP-SC-S.1, 2, 3, 4, 5 and MPP-A.14335 (Masse *in* Frau coll.) from Saint-Chamas (Fare Massif)

Description. The collected specimens are represented by large-size body chambers whose inner whorls are generally crushed or lacking. This prevents a direct comparison with the plastolectotype MNHN-R723

designated by Busnardo *in* Gauthier et al. (2006) based on a small-sized, macroconch morphotype from the basinal series of the Vocontian Basin. Nevertheless, the species is also known by a certain number of large-sized macroconch forms illustrated by Delanoy (1990) which perfectly match the specimens at our disposal.

Genus *Imerites* Rouchadzé, 1933

Imerites giraudi (Kilian, 1888)

Fig. 11D, E–F

Material. Two specimens, MPP-AHP-BAU.R28m+1.1 from Baudinard (Monges Massif); FSL.85837 (80) (Masse *in* Busnardo coll.) from Piedmoure, Sault (Plateau d'Albion).

Description. Small-sized, imericone, dimorphic hemihoplitids whose ontogenetic stages matches well the microconch variability illustrated by Delanoy (1997a).

Family Heteroceratidae Spath, 1922

Genus *Heteroceras* d'Orbigny, 1849

Heteroceras emericianum (d'Orbigny, 1842)

Fig. 11G

Material. One specimen, FSL.85842 (86) (Masse *in* Busnardo coll.) from Sault (Plateau d'Albion).

Description. A poorly-preserved fragment of retroversum which perfectly matches the morphological and ornamental features of the species known by numerous, complete specimens from the Lure Mountains (Delanoy, 1997a) to which the reader is referred.

Genus *Martelites* Conte, 1989

Martelites gr. *sarasini* (Rouchadzé, 1933) – *marteli* Conte, 1989

Fig. 12A, B–C, D, 13A–B, C, 14A–B, C–D, E, F

Material. Thirteen specimens, MPP-BAN.1, 2, 3, 4, 6, MPP-BAN-BRX.1 and MPP-A.36-15 from Banon; MPP-V-MS.1 from Montsalier; MPP-SC-AA.1 from Saint-Christol (Plateau d'Albion); MPP-V-SV.1 from Savoillan and MPP-V-BR.1 from Brantes (Rissas–Bluye Massif); MPP-APH-BAU.R33.1 and BAU.R33.2 from Baudinard (Monges Massif).

Description. The material at our disposal is composed of small- to large-sized complete martelicone ammonite which either typologically belong to *M. sarasini* or *M. marteli* depending their turricone and size, as well as their density and strength of the ribs in the adult. It seems unnecessary to kept separate the two species in the present contribution since they both co-occur during two peak abundance episodes in the Provence platform

Martelites sp. gr. *sarasini* (Rouchadzé, 1933) – *marteli* Conte, 1989

Fig. 14G-H

Material. One specimen, MPP-A.88 (Masse in Frau coll.) from Les Estèves, Simiane-La-Rotonde (Plateau d'Albion).

Description. Incomplete body chamber of a middle-sized *Martelites*. The coiling seems to be moderately involute, with a compressed, higher than wide, sub-oval whorl section with bulged venter, convex flanks and low, rounded umbilical wall. The ornamentation is composed of slightly rursiradiate, single or bifurcate ribs that branch on the umbilical margin. Irregular intercalatory ribs are observed. Ribs cross the venter in thickening. Suture lines are hardly distinguishable.

Family Pulchelliidae Douvillé, 1890

Genus *Gerhardtia* Hyatt, 1903

Gerhardtia galeatoides (Karsten, 1858)

Fig. 10F, G

Material. Five specimens, MPP-V-MV.12, 13, 14, 15, 16 from the Mont Ventoux (Monts de Vaucluse)

Description. Small-sized pulchellid ammonites with an evolute, quasi-scaphitid coiling in the adult and compressed, higher than wide, whorl section. Ornamentation composed of slightly flexuous, broad and flattened simple, and rare intercalatory, ribs. They sometimes branch on peri-umbilical bullae with a marked retrocurvature. Ribs terminates as elongated ridge-like clavi on the peri-ventral margin and define a narrow ventral furrow.

Family Deshayesitidae Stoyanow, 1949

Genus *Deshayesites* Kazansky, 1914

Deshayesites aff. *euglyphus* Casey, 1964 *in* Delanoy, 1995b

Fig. 15A, B, ?C

Material. Three specimens, MPP-B-VC. 20 and 24 from bed 107 and MPP-B-EM.250 from bed 123 of the Bedoulian-type series.

Description. Small-sized, moderately evolute, deshayesitids characterised by regular alternation of slightly flexuous, simple, or rarely bifurcate, primary and generally one secondary ribs. All termination of the ribs show a smooth thickening on the peri-ventral margin and venter.

Deshayesites gr. *luppovi* Bogdanova, 1983

Fig. 15D, E, ?F

Material. MPP-B-VC.15 and 25 from bed 107 of the Bedoulian-type series and i*n-situ* specimens observed at Savoillan and Brantes.

Description. Small-sized, moderately evolute, deshayesitids characterised by alternation of flexuous, simple and bifurcate primary ribs with irregular single secondary one. Point of furcation commonly falls at mid-flank. All ribs are dense and gracile but can be spaced and slightly flattened on the upper flank near the aperture.

Deshayesites sp.

Fig. 15G-H

418

419 Material. One specimen, MPP-V-FDV.1 from Fontaine-de-Vaucluse (Monts de Vaucluse).

420

421 Description. Small-sized fragment of a deshayesitid whorl composed of flexuous ribs which form distinct
422 bulging in crossing the venter. Despite its poor state of preservation, it may belong to *Deshayesites* aff.
423 *euglyphus*.

424

425 Family Desmoceratidae Zittel, 1895

426 Genus *Pseudohaploceras* Hyatt, 1900

427 *Pseudohaploceras matheroni* (d'Orbigny, 1841)

428 Fig. 15I–J

429

430 Material. One specimen, MPP-V-PF.2 from Petit Fribouquet (Monts de Vaucluse)

431

432 Description. Medium-sized desmoceratid ammonite with a moderately involute and compressed coiling, convex
433 flanks and rounded venter. Ornamentation is composed of distinct, straight to slightly sinuous, constrictions
434 collated in fine, branching ribs which cross the venter.

435

436 Family Macroscaphitidae Hyatt, 1900

437 Genus *Macroscaphites* Meek, 1876

438 *Macroscaphites yvani* (Puzos, 1832)

439 Fig. 15K–L

440

441 Material. Two specimens, MPP-V-PF.3 and V-PF.4 from the Petit Fribouquet (Monts de Vaucluse).

442

443 Description. Medium-sized, markedly evolute ammonites with dense, radial, rarely bifurcated, ribs interrupted
444 by sporadic constrictions. The two specimens belong to macroconch morphotype by their size and
445 ammoniticonic coiling.

446

447 Family Douvilleiceratidae Parona & Bonarelli, 1897

448 Genus *Prochelonicera*s Spath, 1923

449 *Prochelonicera*s *sporadicum* (Rouchadzé, 1933)

450 Fig. 16A-B

451

452 Material. Two specimens, MPP-A17 (Masse *in* Frau coll.) from Sault (Plateau d'Albion); MPP.APH-BAN.5 *ex*
453 *situ* from Banon (Plateau d'Albion).

454

455 Description. Fragment of a medium-sized douvilleiceratid ammonite showing a moderately evolute coiling and a
456 depressed, sub-rounded whorl section. Ornamentation is composed of spaced, straight, simple ribs, strengthened
457 on the venter.

458

459 *Prochelonicera*s sp. gr. *dechauxi* (Kilian & Reboul, 1915)

460 Fig. 16C

461

462 Material. MPP-V-PF.1 from the Petit Fribouquet (Monts de Vaucluse).

463

464 Description. Medium-sized, poorly-preserved douvilleiceratid ammonite with a depressed, cadicone whorl
465 section. Cast of its inner whorls shows a deep umbilicus whose ornamentation is composed of strong, radial,
466 single or bifurcate, primary ribs, enlarged on the peri-umbilical margin, and smoothed interspaces.
467 Ornamentation of its body chamber is composed of broad and spaced ribs, sharp on the venter, which branch on
468 thick, peri-umbilical bullae.

469

470 **6. Key ammonite bioevents of the Provence Platform**

471

472 *6.1. The Toxancyloceras vandenheckii bioevent*

473

474 The Ancyloceratidae *T. vandenheckii* (Fig. 8C) was collected in the first marlstone episode cropping out
475 in the south facing side of the Mont Ventoux together with numerous Barremitidae. In the current state of
476 knowledge, *T. vandenheckii* defines the base of the upper Barremian in the Vocontian basinal settings which
477 marks a deep renewal in ammonite assemblage with the increase of the Ancyloceratidae, followed by the

478 inception of the Hemihoplitidae (Bert et al., 2008). Unfortunately, the *T. vandenheckii* bioevent was not detected
479 in the other pre-Vocontian settings surveyed (Brantes, Savoillan, Banon) due to limited outcrop exposure at this
480 time interval.

481 An equivalent of the *T. vandenheckii* bioevent crops out in the outer platform deposits underlying the U^1
482 calcarenites of the Fontaine-de-Vaucluse–Sénanque area. Here, the ammonites *Moutoniceras* sp. (Fig. 8A–B),
483 *Pseudovaldedorsella* sp., and *Toxancyloceras* sp. (Fig. 8D–E), dating the *Moutoniceras moutonianum–T.*
484 *vandenheckii* zones interval, occur between the Unit 1e and 1h of the Roque Pourquière series *sensu* Masse
485 (1976, fig. 14). These ammonites were misidentified by Busnardo *in* Masse (1976, p. 39) who alleged a late to
486 latest Barremian age for the U^1 calcarenites (see also Léonide et al., 2012). The lack of the two age-diagnostic
487 dasycladaceans *Piriferella paucicalcarea* and *Salpingoporella genevensis* in the corresponding interval supports
488 our ammonite age-calibration (see Masse, 1976, fig. 14) since their extinction occurs in the middle part of the
489 lower Barremian (Masse & Fenerci-Masse, 2013c; Clavel et al., 2014; see discussion in §6.1).

490 This dating differs southward since the LO of the two abovementioned dasycladaceans is documented
491 in the calcarenites underlying the onset of the rudistid (*Agriopleura*-dominated) beds in the Alpilles (~150m) and
492 Fare (~40m) massifs (Masse & Fenerci-Masse, 2013c; Clavel et al., 2014). The occurrence of the age-diagnostic
493 caprinid rudist *Offneria simplex* just below the first rudistid limestones in the Fare Massif pinpoints the *M.*
494 *moutonianum* Zone by comparison with the Bas-Vivarais record (Masse & Fenerci-Masse, 2013c; Tendil et al.,
495 accepted; see discussion in §6.1). This suggests that the installation of rudistid regime in these areas is slightly
496 older than the northern Provence settings and merely occurs at, or close to, the base of the upper Barremian.

497 The putative location of this boundary in the Calanques–Nerthe series was previously fixed in the lower
498 part of the Port-Miou–Cassis Unit *sensu* Masse (1976) where it overlies the outbreak of the *Agriopleura*-bearing
499 beds. Unfortunately, this assumption has not been yet confirmed by the lack of ammonite evidence and the
500 recent thesis of Bastide (2014) failed to provide a comprehensive litho- and biostratigraphy of the southern
501 Provence series with respect to the lithostratigraphic nomenclature introduced by Masse (1976).

502

503 *6.2. The Camereiceras limentinum bioevent*

504

505 The Hemihoplitidae *C. limentinum* (Fig. 10A, B–C) and *Janusites janus* (Fig. 10D–E) were found in the
506 second marlstone episode on the south-facing side of the Mont Ventoux and its eastward equivalent (Banon)
507 together with the Pulchellidae *Gerhardtia galeatoides* (10F, G) and numerous Barremitidae. The species has a

widespread record in pre-Vocontian setting (Thieuloy, 1979; Arnaud et al., 1998), and forms a regional-wide correlative bioevent in deeper settings of the Vocontian Basin dating the lower *G. sartousiana* Zone (Bert et al., 2008). The *C. limentinum* acme is accompanied by a minor faunal turnover in the pulchelliid stock, together with a peak abundance of numerous hemihoplitid, desmoceratid, lytoceratid and macroscaphitid ammonites in the Barremian-type series (Vermeulen, 2005).

The *C. limentinum* bioevent has been previously detected in the northern part of the Monts de Vaucluse as illustrated by the collection of the corresponding species in the Gorges de La Nesque (Léonide et al., 2012, fig. 6G, plus our own record on Fig. 10H–I). Its occurrence falls 150m below the northernmost progradation of the *Agriopleura*-bearing beds (Masse, 1976). Unfortunately, this bioevent was not detected southward and prevents the direct calibration of the *T. vandenheckii–G. sartousiana* zonal boundary in the South Provence.

6.3. The Hemihoplites feraudianus bioevent

In the Fare Massif (Saint-Chamas), the *Agriopleura*-bearing limestones are overlain by a cherty marlstone interval which exposes an ammonite-rich bed (1.5 m-thick) at its base. The presence of glauconite and abraded bivalve–rhynchonellid shells prove that it is a condensed bed, itself bracketed by two distinct hardground surfaces (Masse & Fenerci-Masse, 2011). This bed yields the Hemihoplitidae *Hemihoplites* sp. gr. *feraudianus* (Fig. 11A–B, C) and the nautiloid *Cymatoceras* sp.

According to Bert et al. (2008), the acme of *H. feraudianus* marks the lower part of the *H. feraudianus* Subzone (upper *G. sartousiana* Zone) in the nearby Vocontian basinal settings which includes the sequence boundary of the B4 depositional sequence *sensu* Arnaud (2005b). The lack of the requieniid–monopleurid rudistid beds in this area, replaced by a condensed, ammonite-bearing bed seemingly relates to the fault-induced formation of the Saint-Chamas corridor as assumed by Masse & Fenerci-Masse (2013a, fig. 3–6). Supposed temporal equivalence between the *H. feraudianus* Subzone dated deposits of the Fare Massif and the requieniid–monopleurid rudistid beds of the Provence platform conforms to the dating of the regional termination of the rudist genus *Agriopleura* in the upper *G. sartousiana* Zone (Masse & Fenerci-Masse, 2013a, 2015). Note that the Last Appearance Datum (LAD) of *Agriopleura* is associated to a short-term emersion surface through the inner Provence platform settings that merely relates to the SbB4 of the Vocontian basinal settings. Interestingly, a deep ammonite faunal turnover occurs at that time with the worldwide LO of the Pulchelliidae, subsequently balanced by the appearance of the Heteroceratidae during the *H. feraudianus* Subzone (Bert et al., 2008).

538

539 *6.4. The Heteroceras bioevent*

540

541 In the Vocontian basinal settings, the deposition of a basin-wide, marl-dominated wedge relates to the
542 maximum sea-level rise of the B4 depositional sequence *sensu* Arnaud (2005b). This marlstone episode is
543 commonly referred as the *Heteroceras* Marls *sensu* Paquier (1900) since it records the diversification and
544 predominance of the Heteroceratidae, together with the acme of the late Hemihoplitidae *Imerites giraudi* (Fig.
545 11D) marking the base of the *I. giraudi* Zone. This marlstone episode has an extensive record in pre-Vocontian
546 settings (Brantes, Savoillan, Mont Ventoux and Banon) and yields a rich heteroceratid fauna in the Lure
547 Mountains (Kilian, 1888; Delanoy, 1997). It can be traced up to the northern Provence platform settings where it
548 changes into skeletal–peloidal limestones with abundant cherts (Sault) and further to mixed calcarenite–
549 oobioclastic limestones with coral bodies overlying the requieniid–monopleurid beds (Gorges de la Nesque). The
550 occurrence of ammonites dating the *I. giraudi* Zone has long been recognised at Sault (Conte, 1989, p. 40–41;
551 Delanoy, 1997a), as illustrated by poorly-preserved specimens of the index species (Fig. 11E–F) and
552 *Heteroceras emericianum* (Fig. 11G).

553 In the South Provence, this time interval corresponds to the fault-induced, drowning of the requieniid–
554 monopleurid beds which initiates the opening of the intra shelf South Provence Basin (Masse & Fenerci-Masse,
555 2011, 2013b; Frau et al., 2016). The drowning sequence records deep changes in the environmental conditions
556 indicated by a positive $\delta^{13}C$ shift and massive kaolinite input (Stein et al., 2012b). According to the previous
557 authors, both signals convincingly reflect a shift toward a warm and humid climate. This enhanced burial of
558 isotopically light organic carbon triggering episodes of dys- to anoxic conditions at that time illustrated by
559 extensive organic-rich black shale horizons (Machhour et al., 1998; Masse & Machhour, 2000; Stein et al.,
560 2012a). These litho- and geochemical signals are also documented in the Vocontian Basin (Godet et al., 2006,
561 2008) during the *I. giraudi* Zone but only discrete organic-rich horizons are observed in this basin (De Renéville
562 & Raynaud, 1981). These environmental perturbations are seemingly responsible for the drop in ammonite
563 abundance and diversity observed in the upper *I. giraudi* Zone in both the South Provence (Frau et al., 2016) and
564 Vocontian basins (Delanoy, 1995a, 1997a-b; Vermeulen, 2005; Bert et al., 2008). These perturbations are
565 convincingly responsible for the massive outbreak of *Palorbitolina–Heteraster* communities above the
566 requieniid–monopleurid unit through the North Provence (Masse & Fenerci-Masse, 2011).

567

568 *6.5. The first Martelites bioevent*

569

570 Above the *Heteroceras* Marls, the B4 depositional sequence progressively returns towards a limestone-
571 dominated succession in the Vocontian basinal settings (Arnaud, 2005b), which records the peak abundance of
572 the recoiled Heteroceratidae *Martelites sarasini* (Fig. 12B–C). The species characterises the last zone of the
573 Barremian in both the South Provençal (Delanoy et al., 1997; Ropolo et al., 1999, 2000a-b; Frau et al., 2016) and
574 Vocontian basins (Delanoy, 1995a; 1997a-b). This event is also well-developed in pre-Vocontian settings as
575 demonstrated by the common record of *Martelites* of the *sarasini–marteli* group (Fig. 12D and 13A–B), together
576 with *Heteroceras baylei* and *Macroscaphites yvani*, as well as rare *Kutatissites* spp. (Delanoy & Ebbo, 1997, fig.
577 1; plus our own record Fig. 9C–D) and *Procheloniceras* of the *sporadicum* group (Fig. 16A–B) at the Brantes,
578 Savoillan, Mont Ventoux, Sault and Banon sections.

579 Representatives of *Martelites* gr. *sarasini–marteli* have also been previously reported from around of
580 distal platform settings of the Monts de Vaucluse (Sault, Saint-Christol, Rissas) but they have long been
581 confused with lower Aptian Deshayesitidae (Masse, 1976; Monier, 1986). Only the *Martelites* specimens from
582 Sault have been subsequently illustrated by Conte (1989) and Delanoy (1997a, pl. 52 to pl. 62). According to
583 Delanoy (1997a, p. 252), an additional specimen of *M. marteli* was misidentified as *Prodeshayesites* sp. by
584 Monier (1986, pl. 2, fig. f) from the Rissas Massif. In all localities listed above, the *Martelites*-bearing levels
585 underlie coral build-up deposits considered to represent the basinward prograding termination of the caprinid-
586 bearing limestones (Masse, 1976, 1995; Masse & Fenerci-Masse, 2011). This lateral variation can be tracked *in*
587 *situ* along the south facing side of the Toulourenc syncline in the Rissas Massif (Arnaud-Vanneau et al., 1972;
588 Masse, 1976; Monier, 1986; Masse & Fenerci-Masse, 2011), and prove that the *Martelites*-bearing levels
589 represent a time equivalent of the topmost part of the *Palorbitolina–Heteraster* guide level.

590 For the time being, no ammonite has been collected in the *Palorbitolina–Heteraster* guide level
591 cropping out in the southwestern Monts de Vaucluse. Nevertheless, we collected poorly-preserved fragments of
592 *Martelites* gr. *sarasini–marteli* (Fig. 13C) and the nautiloids *Cymatoceras neocomiense* and *Eucymatoceras*
593 *plicatum* in the orbitolinid-rich beds at Azé Aven, ~1.2km southwest to Saint-Christol interpreted as the distal
594 equivalent of the guide level (Blanc et al., 1973). This consequently implies that the *Palorbitolina–Heteraster*
595 guide level strictly encompasses the *I. giraudi* Zone and lowermost *M. sarasini* Zone.

596

597 *6.6. The second Martelites bioevent*

598

599 For the first time, age-diagnostic ammonites, here assigned to *Pseudocrioceras* sp. (Fig. 9E–G) and
600 *Martelites* sp. (Fig. 14G–H), have been collected from the bottom part of the U^3 formation from the northwestern
601 (Gorges de La Nesque) and southeastern (Simiane-la-Rotonde) Monts de Vaucluse, above the last caprinid-
602 bearing beds. The co-occurrence of *Martelites* and *Pseudocrioceras* relatives are documented at the base of the
603 *P. waagenoides* Subzone in the South Provençal Basin (Delanoy et al., 1997; Ropolo et al., 1999, 2000a-b)
604 which marks the upper *M. sarasini* Zone. At Simiane-la-Rotonde, *Martelites* sp. originate from a level overlying
605 a thin (~ 10cm) orbitolinid-rich horizon and a rudstone bed that represent the northward prograding termination
606 of the post-caprinid, *Palorbitolina*-rich limestones of the southeastern Monts de Vaucluse (Masse & Fenerci-
607 Masse, 2011; Léonide et al., 2012). This indicates that the demise of the North Provence rudistid biota, and its
608 *Palorbitolina*-rich cover, is markedly older than previously assumed (see discussion §6.3), and falls in the
609 uppermost Barremian.

610 In pre-Vocontian settings (Mont Ventoux, Savoillan and Banon sections), the second *Martelites*
611 bioevent (Fig. 15A–B, C–D, E, F) was identified in a set of alternating marl-limestone beds unconformably
612 overlying a coarse to fine-grained bioclastic unit. This unit may represent the basinward expression of the
613 exposure topping the caprinid-bearing U^2 *s.s.* limestones (see discussion in Tendil et al., accepted).

614 In deeper Vocontian settings, the B/A boundary interval suffers from low-resolution dating since this
615 time interval records a significant drop in ammonite abundance above the lower part of the *M. sarasini* Subzone
616 (Delanoy, 1995a, 1997a-b; Vermeulen, 2005; Bert et al., 2008). This low abundance spans most of the B5
617 depositional sequence as defined by Arnaud (2005b) and prevents the direct recognition of the *P. waagenoides*
618 Subzone in the Vocontian Basin (Vermeulen, 2005). Note that a potential hiatus including part of the upper *M.*
619 *sarasini* Zone merely occurs in Vocontian basinal settings (see Frau et al., 2018; and discussion in §5.3).

620

621 *6.7. The first Deshayesites event*

622

623 From southern (Fontaine-de-Vaucluse–Sénanque) to northern (Pié Gros–Petit Fribouquet) platform
624 settings of the Monts de Vaucluse, a drowning discontinuity is detected in the upper part of the U^3 formation. It
625 can be either sealed by cherty calcisiltites or biocalcarenites (Masse & Fenerci-Masse, 2011; Frau et al., 2017).
626 In the southern Monts de Vaucluse, this discontinuity corresponds to a serpulid-rich, firmground surface which
627 yields poorly-preserved fragments of *Deshayesites* sp. (Fig. 15G–H) and *Macroscaphites* sp. at Fontaine-de-

628 Vaucluse. Its northwestern counterpart (Petit Fribouquet) also contains *Pseudohaploceras matheroni* (Fig. 15I–
629 J), *Macroscaphites yvani* (Fig. 16K–L) and *Procheloniceras* sp. gr. *dechauxi* (Fig. 16C).
630 In pre-Vocontian settings (Brantes, Savoillan, Mont Ventoux), this discontinuity is represented by a
631 metre-thick marly episode cropping out in the lower part of the chert-rich limestones of the Calcaires de Vaison
632 Fm. *sensu* Leenhardt (1883). This layer contains the taxa listed above as well as *Deshayesites* aff. *euglyphus* and
633 *Deshayesites* gr. *luppovi* (Fig. 15F) that were previously assigned to *D. deshayesi* by Monier (1986) at Brantes.
634 In the Vocontian Basin, both *Deshayesites* aff. *euglyphus* and *D.* gr. *luppovi* occur in an ammonite peak
635 abundance observed in the upper part of the Barremian–Bedoulian Limestones Fm. (Delanoy, 1995b, fig. 3)
636 which is associated to the MFS of the A1 depositional sequence *sensu* Arnaud (2005b). Its southern counterpart
637 in the South Provence Basin refers to the marlstone episode known as the Niveau Toucas *sensu* Moullade et al.
638 (2000b) cropping out in the upper part of the Calcareous Mb. *D.* aff. *euglyphus* has also been collected there and
639 throughout the rest of the Calcareous Mb. (Fig. 16A, B). In the Niveau Toucas, it also co-occurs with the *D.* gr.
640 *luppovi* (Fig. 16D, E) which marks the uppermost *D. oglanlensis* Zone (Reboulet et al., 2011, 2014). Transitional
641 form seemingly links both forms (Fig. 16C). As a result, the MFS of the A1 sequence occurs close to the *D.*
642 *oglanlensis–D. forbesi* zonal boundary as currently defined by Frau et al. (2015) in the Bedoulian-type series and
643 forms a regional-wide correlative bioevent in Provence.
644
645 *6.8. The second Deshayesites event*
646
647 The U^3 platform carbonates of the North Provence platform are topped by a distinct hardground surface
648 and capped by the ammonite-bearing A^1 marls in southwestern and southeastern Monts de Vaucluse which yield
649 common *Deshayesites forbesi* (see Frau et al., 2017, fig. 8–10). According to these authors, this species dates the
650 upper (but non-uppermost) part of the *D. forbesi* Zone and characterises the lower part of the Marly-limestone
651 Mb. in the South Provençal Basin (Moullade et al., 2000b). This time interval refers to depositional sequence
652 BA2 *sensu* Arnaud (2005b), including the spreading of the OAE 1a-related oceanic anoxia (Frau et al., 2017).
653 The top of the A^1 marls is interrupted by a burrowed, glauconitic firmground including the OAE 1a time interval,
654 and overlain by the blue-grey A^1 marls whose base is dated to the upper *D. deshayesi* Zone by means of
655 ammonites (Dutour, 2005; Frau et al., 2017).
656 In the Vocontian Basin and its margins, this time interval is generally lacking due to non-deposition gap
657 and/or resedimentation at the transition between the limestone- (Barremian–Bedoulian Limestones) and marl-

dominated (Blue Marls) formations (Cotillon, 2010; Cotillon et al., 2000). Usually, only the upper *D. deshayesi* and/or *D. furcata* zones directly lies above eroded or slumped Barremian–Bedoulian limestones Fm.; except in few localities (Bréhéret, 1995).

6. Biostratigraphic significance and regional implications

Our revised calibration substantially modifies the datings of the North Provence platform developed in the five last decades. A comparative scheme is given in Fig. 17. Major results are discussed below.

6.1. Installation of the North Provence rudistid biota

Although its timing remains poorly constrained in the Calanques–Nerthe massifs, the outbreak of rudistid beds in the South Provence series, dominated by *Agriopleura* spp., is likely associated to its northward progradation during the *T. vandenheckii* in the Fare and Alpilles massifs, and delayed up into the *G. sartousiana* zones interval throughout Monts de Vaucluse. An orbitolinid-rich horizon underlies the deposition of the first *Agriopleura*-bearing beds at Fontaine-de-Vaucluse and can be seemingly tracked up to the Gorges de La Nesque area (Léonide et al., 2012; Tendil et al., accepted). This horizon and its overlying *Agriopleura*-bearing beds are enclosed between the *C. limentinum* and *H. feraudianus* ammonite bioevents which constrain the installation of the rudistid biota in northern Provence to the middle part of the *G. sartousiana* Zone. According to Arnaud (2005b), this time interval includes the maximum flooding surface of the Vocontian B3 depositional sequence, evidenced by the record of an ammonite peak abundance dominated by pulchelliid and hemihoplitid taxa in the *G. provincialis* Subzone (Vermeulen, 2005). The wide extent (~20 km) and stratigraphic location of the orbitolinid-rich horizon make it as a potential candidate for the local expression of the corresponding MFS. This supports the concomitant northernmost progradation of the *Agriopleura*-bearing biota during the *G. provincialis* Subzone.

6.2. Dating of the Palorbitolina–Heteraster guide level

In previous contributions, the B/A boundary was located within, or at the top, of the *Palorbitolina–Heteraster* guide level, assigning *de facto* an early Aptian age to the overlying caprinid-bearing limestones of the

North Provence platform. This assumption involved the record of three alleged age-diagnostic bio- and chemostratigraphic markers in the guide level; these are:

(*i*) The co-occurrence of the orbitolinids *Palorbitolina lenticularis* and *Orbitolinopsis* spp. considered to be indicative of the lowermost Aptian (Arnaud et al., 1998; Arnaud-Vanneau et al., 2005);

(*ii*) The unfigured report of lowermost Aptian ammonites [*D. bedouliensis* and *Deshayesites* aff. *consobrinus*] in the cherty marlstones underlying the caprinid-bearing limestones in the Fare Massif (Masse, 1995; Masse & Fenerci-Masse, 2011; Clavel et al., 2013);

(*iii*) The record of a negative carbon shift at the base of the guide level attributed to the latest Barremian negative carbon excursion (Léonide et al., 2014).

As discussed below, none of these arguments is reliable for the recognition of the B/A boundary within the *Palorbitolina–Heteraster* guide level:

(*i*) The orbitolinid zonation of the Urgonian-type series follows those developed in the nearby Subalpine platform series by Arnaud et al. (1998) and Arnaud-Vanneau et al. (2005). According to their foraminiferal distribution chart, the association of *P. lenticularis* and *Orbitolinopsis* spp. in the Lower *Orbitolina* Beds would be indicative of the lowermost Aptian. In line with previous contributions of Clavel et al. (2007, 2013, 2014), Granier et al. (2013) recently brought new light on the vertical range of Barremian–Aptian Orbitolinidae in southeast France by the study of reworked assemblages in the base-of-slope, ammonite-constrained Vocontian section (l'Estellon, Drôme). These authors suggested that the first co-occurrence of *P. lenticularis* and *Orbitolinopsis* spp. dates back to the lower Barremian (*N. pulchella* Zone) and these taxa are, therefore, of little help for defining the B/A boundary.

The early Aptian age assigned to the association of *P. lenticularis* and *Orbitolinopsis* spp. was also supported by the supposed co-occurrence of lower Aptian ammonites referred to *Ancyloceras* gr. *matheronianum*, *Deshayesites* gr. *weissi* and *Toxoceratoides* sp. in the Lower *Orbitolina* Beds of the Chartreuse and Vercors massifs (Gidon, 1952; Moret & Deleau, 1960; Arnaud et al., 1998). Re-investigation of the palaeontological collections of the Grenoble University failed to retrieve the specimens of *Deshayesites* sp. and *Toxoceratoides* sp. Their systematic assignments, therefore, remain doubtful in the absence of illustration. The ancyloceratid ammonite originally referred to *A.* gr. *matheronianum* and illustrated by Arnaud et al. (1998, pl. 7, fig. 7) is still kept in the Gidon collection under the catalogue number UJF-ID.10590. Our re-examination highlights that it lacks the typical adult ornamentation (i.e. regular alternation of trituberculate primaries and

718 inerme, secondaries ribs) and elongated coiling which typifies the genus *Ancyloceras*. The robust quadrate to
719 depressed subhexagonal whorl section and irregular ribbing rather suggest that this specimen closely matches the
720 body chamber of *Kutatissites* gr. *chreithiensis* (Fig. 9A–B). This taxon reaches its acme in the lowermost *M.*
721 *sarasini* Zone in the North Provence platform and gives evidence of the potential coevality between the Lower
722 *Orbitolina* Beds of the Subalpine Chains and the North Provence *Palorbitolina–Heteraster* guide level which
723 both record *Kutatissites* peak abundance.

724 (*ii*) According to Masse (1976) and Masse & Fenerci-Masse (2011), the occurrence of lowermost
725 Aptian Deshayesitidae in the cherty marlstones of the Saint-Chamas section supports the location of the B/A
726 boundary below the caprinid-bearing limestones. However, Masse & Fenerci-Masse (2013a) revised the
727 taxonomy of these ammonites subsequently referred to upper Barremian Hemihoplitidae. The authors also
728 indicated that they originate from the condensed bed at the base of the cherty marlstones, herein dated to the *H.*
729 *feraudianus* Subzone (see discussion in §6.3). Extensive fieldwork in the Fare Massif confirms the lack of any
730 Aptian ammonites in the cherty marlstones of the Fare Massif.

731 (*iii*) According to Stein et al. (2012b), the negative $\delta^{13}C$ shift documented in the Lower *Orbitolina* Beds
732 of the Subalpine Chains (Raddadi, 2005; Arnaud-Vanneau et al., 2005, fig. 50) and the *Palorbitolina–Heteraster*
733 guide level of the North Provence (Léonide et al., 2014) are coeval and correlate to the sharp negative carbon
734 excursion of latest Barremian age observed across the Tethyan basins (Stein et al., 2012a). However, Frau et al.
735 (2018) highlighted that the correlation of this negative carbon excursion was so far based on inaccurate
736 ammonite age-calibration in basinal settings, thus questioning its correlation in shallow-water carbonates.
737 Indeed, Masse & Fenerci-Masse (2011, p. 671) pointed out that the $\delta^{13}C$ shift of the Lower *Orbitolina* Beds
738 merely relates to the existence of an emersion surface whose carbon signal is diagenetically overprinted.
739 Moreover, one of us (A.J.-B.T.) detected a significant lag between the vertical distribution of the carbon values
740 and the litho-log of Fontaine-de-Vaucluse where the negative $\delta^{13}C$ shift was documented by Léonide et al.
741 (2014). His correction suggests that the 2‰ negative carbon shift falls within a requieniid–monopleurid bed,
742 approximately 8m below the basal surface of the *Palorbitolina–Heteraster* guide level. It seemingly relates to
743 the expression of a parasequence-related emersion surface typical for this part of the Urgonian-type series
744 (Masse et al., 2001). As a result, the record of the latest Barremian negative peak in the Urgonian-type Provence
745 platform is not substantiated by C-isotope data.
746

In the present contribution, the North Provence *Palorbitolina–Heteraster* guide level is correlated to the *I. giraudi* Zone and lowermost *M. sarasini* Subzone (Fig. 17), in agreement with ammonite findings and geological mapping. The overlying caprinid-bearing limestones, and its *Palorbitolina*-rich cover are strict time equivalent of the *M. sarasini* Subzone since they are overlain by the U^3 formation bearing ammonites of the *P. waagenoides* Subzone at its base. The latter is unanimously considered to be the last ammonite subzone of the Barremian (Delanoy et al., 1997; Ropolo et al., 1999; 2000a-b; Bert et al., 2008; Reboulet et al., 2014). As a result, the B/A boundary should be re-located in the lowermost part of post-caprinid U^3 formation, although its precise level cannot be fixed due to the lack of a continuous ammonite record. Relocation of this boundary above the North Provence rudistid limestones represents a return to the conceptions first developed by Faure (1965), Fahy (1965) and Maillard (1965) (see also Fig. 2).

6.3. Demise of the North Provence caprinid biota (Fig. 18)

According to our calibration, the North Provence caprinid-bearing U^2 *s.s.* limestones develop above the *Palorbitolina–Heteraster* guide level and record a bidirectional progradation toward the South Provence and the Vocontian basins during the *M. sarasini* Subzone *pro parte*. This unit is covered by a short-term epikarstic surface, indicated by minor dissolution of both low-Mg calcitic and aragonitic rudist shell layers (Masse, 1976; Masse & Fenerci-Masse, 2011; Léonide et al., 2012), that interrupted the overall progradation of caprinid-bearing deposition. This emersion is also confirmed by the record of a strong negative spike in the C-isotope signal indicating an influence of meteoric diagenesis (Léonide et al., 2014). In North Provence, this discontinuity is overlain by bioclastic–cherty limestones (U^3 formation). Its expression is less conspicuous in the southwestern Monts de Vaucluse since the last caprinid-rich levels give way, transitionally, to *Palorbitolina*-rich limestones including decametre-width coral mounds, and then to cherty, *Palorbitolina*-bearing limestones (Tendil et al., accepted). These *Palorbitolina*-rich limestones thin northward and disappear along a NW–SE bulge, i.e. the so-called Flassan–Rustrel ridge *sensu* Masse & Fenerci-Masse (2011, fig. 11). As indicated by the record of the second *Martelites* bioevent, the demise of the caprinid episode, and subsequent deposition of its *Palorbitolina*-rich cover, occur in the uppermost *M. sarasini* Subzone.

In the South Provence, the *M. sarasini* Subzone marks the onset of the basinal sedimentary conditions above the drowning sequence (Frau et al., 2016). This time interval is characterised by the alternation of laminated organic-rich black shales and highly burrowed, shelly limestones, reflecting successive anoxic to

777 dysoxic/oxic depositional conditions at that time (Stein et al., 2012a). The high rate of accumulation and
778 preservation of the organic matter is consistent with the proposed model of a restricted intra-shelf basin bordered
779 by a shallow-water carbonate platform acting as an additional feeding sources of organic matter (Machhour et
780 al., 1998). The *M. sarasini* Subzone records the peak abundance of micromorphic heteroceratid ammonite fauna
781 showing a favourable adaptation to oxygen-depleted, sea-water conditions (Frau et al., 2016).

782 The transition between the *M. sarasini* and *P. waagenoides* subzones in the Bedoulian-type series (beds
783 44–45 *sensu* Moullade et al., 2000b) consists of a serpulid-rich, wavy discontinuity which is approximately
784 coeval with the faunal replacement of the Heteroceratidae by the Ancyloceratidae *Pseudocrioceras* (see Ropolo
785 et al., 1999; 2000a). This bed interval is marked by a strong negative oxygen and carbon isotope shift (~1.5‰),
786 seen in paired organic matter and carbonate carbon (Kuhnt et al., 2000; Masse & Fenerci-Masse, 2011; Stein et
787 al., 2012a). Isotopic excursions give evidence of a short-termed, syn-depositional hiatus. In the absence of
788 platform-derived material in the corresponding discontinuity, the negative carbon excursion may result from
789 seawater enrichment by isotopically-light, dissolved inorganic carbon derived from intense weathering of the
790 hinterland during the emersion of the platform. This interval is also characterised by a productivity increase
791 (Bergen, 2000), maximum TOC values (~18%), and phosphorus enrichment (Stein et al., 2012a).

792 By contrast, the uppermost Barremian (*P. waagenoides* Subzone) and lowermost Aptian (*D. oglanlensis*
793 Zone) of the South Provence Basin records the progressive recovery toward oxic palaeoenvironmental conditions
794 illustrated by the deposition of regular, blue–grey basinal limestones lacking any redox sensitive trace elements
795 anomaly (Stein et al., 2012a). This recovery is coeval with the abrupt termination of the *Pseudocrioceras* stock
796 replaced by the peak abundance of the *Deshayesites* which marks the base of the Aptian Stage by means of
797 ammonites (Delanoy et al., 1997; Cecca et al., 1999, 2000; Ropolo et al., 1999, 2000a-b, 2006; Reboulet et al.,
798 2011, 2014).

799 In the Vocontian Basin, the B/A boundary is located in the Barremian–Bedoulian Limestones Fm. but
800 its precise level remains unclear since the corresponding time interval records a marked drop in abundance and
801 diversity of ammonite taxa above the lowermost part of the *M. sarasini* Subzone (Delanoy, 1995a, 1997a-b;
802 Vermeulen, 2005; Bert et al., 2008). The putative boundary was fixed at the minimum value of a distinct
803 negative $\delta^{13}C$ excursion (Godet et al., 2006; Huck et al., 2011), considered to be the local expression of the latest
804 Barremian negative excursion of the Bedoulian-type series by the latter authors. This negative $\delta^{13}C$ excursion
805 falls at the base of a bundle of thick limestone beds traceable throughout the basin (i.e. Thick Bundle *sensu*
806 Delanoy, 1995b; beds 201–206 *sensu* Vermeulen, 2005), which yields few specimens of lower (but non-

lowermost) Aptian deshayesitids (Delanoy, 1995b). Following Frau et al. (2018), the record of the latest Barremian negative carbon excursion just below *Deshayesites*-bearing beds outlines the existence of a minor temporal hiatus, including, at least, the *P. waagenoides* Subzone, and (?) the lowermost part of the *D. oglanlensis* Zone. If this should prove correct, one may wonder if the lack of ammonite evidences of the *P. waagenoides* Subzone can really be explained by the deep water depth of the Vocontian settings (Bert et al., 2008) or is linked to the presence of a hiatus temporally linked to the demise of the North Provence platform.

7. Comparison with peri-Vocontian Urgonian platforms

7.1. Bas-Vivarais (Fig. 19)

Along the western margin of the Vocontian Basin (Cévenole margin), the innermost known settings of the Urgonian Bas-Vivarais platform deposits (Col de la Serre–Serre de Tourre sections) expose three main rudist-rich units pinching out toward the Vocontian Basin:

(*i*) Above ammonite-bearing shelf deposits, the installation of Urgonian platform carbonates consists of calcarenite enriched in rudists upward, i.e. *Agriopleura*–requieniid beds (Lafarge, 1978; Masse and Fenerci-Masse, 2013b). The rudistid beds terminate at a distinct emersion surface overlain by mixed, rudist-poor, marls–carbonates (V3 *sensu* Elmi et al., 1996), including the Caribbean caprinid rudist *Offneria simplex* (see Chartrousse & Masse, 1998; Masse & Fenerci-Masse, 2013b). According to Clavel et al. (2007, 2013, 2014) and Masse & Fenerci-Masse (2013c), the first platform stage develops through the *K. nicklesi–N. pulchella* zones interval since it overlies ammonite-bearing marly-limestones of latest Hauterivian to earliest Barremian age and underlies the V3 episode which yields rare ammonites assigned to the upper *N. pulchella–M. moutonianum* zones interval.

We fully support the dating of the underlying shelf deposits but alternative dating of the V3 episode arises from ongoing studies by A. Pictet and P.-O. Mojon (unpublished data), who found new ammonites and re-examined specimens illustrated by Clavel and his collaborators. From the Serre de Tourre to outermost platform settings of the Bas-Vivarais, the V3 episode contains several ammonite-bearing horizons dating the *K. compressissima*, *M. moutonianum* and *T. vandenheckii* zones. The apparent lack of ammonite evidence from the *N. pulchella* Zone is consistent with the record of Vocontian marginal settings in which this zone is highly condensed (Delanoy et al., 2012; Vermeulen et al., 2013; Arnaud, 2005b) or lacking (Delanoy, 1992; Arnaud,

837 2005b). Given these considerations, the *Agriopleura*–requieniid beds of the Middle Urgonian Mb. should rather
838 be assigned to the upper *K. nicklesi* Zone. The *N. pulchella* Zone merely lacks as a result of a short-term
839 emersion hiatus.

840 (*ii*) Above the V3 episode, massive recovery of the Urgonian rudistid biota occurs as illustrated by the
841 development of *Agriopleura*-, and requieniid–monopleurid beds (thickness comprised between ~25 and 50 m).
842 This series conforms to the northward progradation of the Provence platform during the *T. vandenheckii–G.*
843 *sartousiana* zones interval. As further evidence, the *Agriopleura*-bearing beds terminates at an epikarstic
844 discontinuity (Masse & Fenerci-Masse, 2011); herein dated to the *G. provincialis–H. feraudianus* subzonal
845 boundary.

846 (*iii*) The Bas-Vivarais requieniid–monopleurid beds are overlain by *Palorbitolina*-rich beds (V4 *sensu*
847 Elmi et al., 1996) which represent the local equivalent of the North Provence *Palorbitolina–Heteraster* guide
848 level (Lafarge, 1978; Masse & Fenerci-Masse, 2011; Frau et al. 2017). This is furthermore confirmed by the
849 occurrence of poorly-preserved heteroceratid ammonites dating the *I. giraudi–M. sarasini* zones interval *pro*
850 *parte* in the Vallon Pont d'Arc region (Pascal collection deposited at the University of Claude Bernard – Lyon I).

851 (*iv*) Above the guide level, the last platform stage consists of caprinid-bearing limestones (Lafarge,
852 1978; Masse, 1995), which displays the maximum eastward progradation of the Bas-Vivarais platform toward
853 the Vocontian Basin (Masse & Fenerci-Masse, 2011; Frau et al., 2017, fig. 11). According to Masse & Fenerci-
854 Masse (2013b), the caprinid-bearing limestones were connected to their North Provence counterpart although the
855 two domains are now disconnected by the N40 sinistral, strike-slip Nîmes fault (Masse & Fenerci-Masse,
856 2013b).

857 Exception made for the lower Barremian, the spatial evolution of the Bas-Vivarais Urgonian limestones
858 formation strictly conforms to the northward progradation of the Provence platform during the *G. sartousiana*–
859 lower *M. sarasini* zones interval. Nevertheless, a westward pinching out of the North Provence U^3 formation is
860 documented into the discontinuity topping the caprinid-bearing limestones in eastern Bas-Vivarais (Frau et al.,
861 2017). As a result, the more proximal Bas-Vivarais settings experienced a longer exposure including the
862 uppermost Barremian (upper *M. sarasini* Zone) up into the lowermost Aptian (lower *D. forbesi* Zone). This long-
863 term exposure is reflected by the three generations of infills in epikarstic cavities documented by Pictet et al.
864 (2015).

865 The emersion surface is regionally drowned by three successive, or conjugated, ammonite-bearing
866 deepening-up phases (Chabert and Frayol formations *sensu* Pictet et al., 2015) spanning the upper *D. forbesi*

867 Zone to the *D. furcata* Zone (Pictet & Delanoy, 2016). This dating is consistent with those of the post-Urgonian
868 marly cover (A^1–A^2 units) of the North Provence (Frau et al., 2017), although it differs by its continuous
869 succession across the OAE 1a-related time interval in the Bas-Vivarais settings. This new calibration challenges
870 the recent studies which limited the duration of the final Urgonian emersion to the lower *D. forbesi* Zone (e.g.
871 Masse, 1995; Masse & Fenerci-Masse, 2011; Bastide, 2014; Clavel et al., 2013, 2014; Pictet et al., 2015; Pictet
872 & Delanoy, 2016).
873
874 *7.2. Subalpine Chains (Fig. 20)*
875
876 The Urgonian platform series extending from the Swiss–French Jura to the Subalpine Chains have been
877 intensively studied over the past decades but its dating is part of a long-lived debate for which two main
878 biostratigraphic models (Grenoble vs. Genève university conceptions) based on distinct orbitolinid scales have
879 been developed and still await validation.
880 In the pioneering Grenoble model of Arnaud-Vanneau & Arnaud (1990) and Arnaud & Arnaud-
881 Vanneau (1991) updated by Arnaud et al. (1998, 2017) and Godet et al. (2016a), the Urgonian series outcropping
882 of the Subalpine platform includes two successive stratigraphic formations, i.e. the bioclastic-dominated
883 Glandasse Fm. of early to early late Barremian age and the rudist-bearing Urgonian limestones Fm. of latest
884 Barremian to early Aptian age. The latter consists of two rudist accumulation units (i.e. Lower and Upper
885 Urgonian members) separated by the Lower *Orbitolina* Beds, which form a regional-wide correlative event
886 (Arnaud et al., 1998). According to this model, "*the Glandasse Fm. is restricted to the southern part of the*
887 *Vercors and pinches out northward, whereas the Urgonian Formation spreads over the entire subalpine domain*
888 *including the French-Swiss Jura where it overlies directly Hauterivian platform limestones*" (Richet, 2011). The
889 datings of the Urgonian limestones Fm. would be supported by correlation with ammonite-bearing, drowning
890 discontinuities followed into basinward settings of the southern Vercors and Diois regions (Arnaud et al., 1998,
891 fig. 36-38). For example, the recognition of the *G. sartousiana* Zone dated deposits below the Urgonian
892 limestones Fm. in the southern Vercors was used as evidence for the latest Barremian inception of the rudistid
893 limestones throughout the Subalpine Chains.
894 In the Genève University model developed over the past decades (Clavel et al., 1995, 2002, 2007, 2010,
895 2013, 2014; Charollais et al., 2008; Granier et al., 2013), "*the Arnaud's Glandasse Fm. grades northwards to*
896 *rudist bearing limestones, which implies that the Glandasse and the lower part of the Urgonian formation are*

stratigraphically equivalent, and essentially early Barremian in age" (Richet, 2011). This assumption relies on the record of upper Hauterivian to lowermost Barremian ammonites below the Arnaud's Glandasse Fm., which furthermore contains lower Barremian age-diagnostic dasycladaceans and orbitolinids (Clavel et al., 2007, 2010, 2013, 2014). A similar shallow-water assemblage is also documented in the Lower Urgonian Mb. and gives evidence of its coevality with part of the Arnaud's Glandasse Fm. cropping out in the southern Vercors (Clavel et al., 2014 and references therein). Most recent sedimentological studies tend to corroborate the Genève University model but the lack of continuous high-resolution mapping of outcrop cliffs in the northeastern Vercors prevent to draw a general conclusion (Richet, 2011).

Preliminary review of the published data is summarised below and give new insight into the growth and demise of the Subalpine rudistid biota:

(*i*) In proximal settings of the Swiss–French Jura (Rocher des Hirondelles type section), the installation of the rudistid regime seemingly occurs in the upper Hauterivian and continues southward through the lowermost Barremian. Although no direct ammonite occurrence is presently known, this scenario is supported by the integration of shallow-water biological markers (Masse et al., 1998; Clavel et al., 2007, 2013, 2014). This conforms to the southward inception of the Urgonian facies in the Subalpine Chains, which are seemingly delayed up into the (?)lower *K. nicklesi* Zone in the northern Vercors as indicated by the record of the ammonites *Emericiceras* sp. gr. *koechlini* and *Torcapella* sp. in an underlying marly episode at the Grands Goulets section (Clavel et al., 2014, pl. 1, fig. 5). Note that none evidence of sedimentary hiatus occurs between this marly episode and the first rudistid limestones (Clavel et al., 2014, see discussion on p. 37-38), as assumed in the Grenoble model (SbB3 *sensu* Arnaud et al., 1998).

(*ii*) In the southern part of the Swiss–French Jura, the rudistid regime is ended by a prominent karstic discontinuity, forming incised valleys infilled by *Palorbitolina–Heteraster* limestones locally referred as the Poet Beds in the Valserine Valley (Pictet et al., 2016). The Poet Beds previously yielded an ammonite specimen referred to *Deshayesites* gr. *saxbyi* by Martín-Closas et al. (2009), and recently figured in Pictet et al. (2016, Fig. 7 f3; FSL.105033). Re-examination of this specimen highlights that it can be confidently assigned to *Martelites* sp. juv. This ammonite gives evidence of the likely coevality between the Poet Beds and the Lower *Orbitolina* Beds of the Subalpine Chains and the *Palorbitolina–Heteraster* guide level of the North Provence–Bas-Vivarais regions which all delivered ammonites dating the lowermost *M. sarasini* Subzone at their top. In the current state of knowledge, the early Barremian age *pro parte* of the underlying rudistid limestones indicates the presence of a major hiatus including part of the upper lower and lower upper Barremian at their top, i.e. (?) up to the *I. giraudi*

927 Zone according to Martín-Closas et al. (2009) and Clavel et al. (2007, 2013, 2014). However, ongoing studies of
928 A. Pictet and P.-O. Mojon (unpublished data) suggest that the rudistid limestones of the Swiss-French Jura may
929 locally have reached the uppermost Barremian, although this dating would contradict with dasycladale and rudist
930 occurrences of older significance.

931 (*iii*) The Lower Urgonian Mb. of the Chartreuse and northern Vercors includes three main exposure
932 surfaces –SbB4, SbB5 and SbA1 – whose ammonite age-calibration strongly varies between the two existing
933 models. The Lower Urgonian Mb. encompasses the mid-upper Barremian to lowermost Aptian in the Grenoble
934 model while it strictly spans the lower Barremian *pro parte* (*T. hugii* to *K. compressissima* zones interval) in the
935 Genève one. Considering that the extinction of the age-diagnostic dasycladales *S. genevensis* and *P.*
936 *paucicalcarea* occurs several tens of meters below the SbA1 while the rudist genus *Agriopleura* reaches the top
937 of the member (Arnaud-Vanneau, 1980), the dating of the Lower Urgonian Mb. better conforms to the age-
938 assignment of the Genève model. However, it has been documented in the seminal thesis of Richet (2011) that
939 rudistid limestones develop below *G. sartousiana* zone dated deposits in the southern Vercors. If the early
940 Barremian age of the Lower Urgonian Mb. proves correct, geometry of the platform across the lower/upper
941 Barremian boundary is more complex than actually assumed. Note that the SbA1 topping the Lower Urgonian
942 Mb. is of lesser importance compared to its northward counterpart although it is similarly overlain by Lower
943 *Orbitolina* Beds herein assigned to the *I. giraudi* and lowermost *M. sarasini* zones (see discussion §6.2*i*).

944 (*v*) As for the North Provence–Bas Vivarais record, the recovery of the rudistid regime above the
945 Lower *Orbitolina* Beds (i.e. Upper Urgonian Mb.) is expressed by the development of caprinid-bearing
946 limestones, which also marks the maximum progradation of the Subalpine platform (Arnaud-Vanneau, 1980).
947 Both Grenoble and Genève models so far assigned an early Aptian age *pro parte* to the Upper Urgonian Mb. by
948 comparison with the North Provence record (e.g. Arnaud et al., 1998; Clavel et al., 2013, 2014). According to
949 our recalibration, this member should be re-assigned to the *M. sarasini* Subzone.

950 In accordance with the proximal Bas-Vivarais platform settings, the Upper Urgonian Mb. is topped by
951 a major exposure event ending the Urgonian rudistid regime. It is characterised by intense karstification
952 processes which can form deeply, incised palaeovalleys infilled by a new episode of *Palorbitolina*-rich
953 marlstones (locally referred as the Upper *Orbitolina* Beds) and capped by calcarenites (the Lumachelle). These
954 levels yield ammonites of late early Aptian age (i.e. upper *Deshayesites deshayesi* and *D. furcata* zones) in the
955 Upper *Orbitolina* Beds, and at the base of the Lumachelle (Thieuloy & Girod, 1964; Delamette et al., 1997;
956 Pictet, unpublished data). As herein understood, the minimum duration of the hiatus related to the end of the

957 Urgonian rudistid regime (SbA2 in the Grenoble model) straddles the upper *M. sarasini* to the (?)lower *D.*
958 *deshayesi* zones. This new calibration challenges both the Grenoble and Genève models which limited the
959 duration of the SbA2 emersion to part of the lower *D. forbesi* Zone (Arnaud et al., 1998; Clavel et al., 2007,
960 2013, 2014 amongst others).
961 (*vii*) The Upper Urgonian Mb. disappears northward since it has no equivalent in the Swiss–French
962 Jura. In these areas, the Poet Beds are also topped by an emersive discontinuity and overlain by stacked units of
963 variegated, detrital, marls and sandstones (i.e. Perte-du-Rhône Fm. *sensu* Pictet et al., 2016) dated to the upper
964 *D. forbesi* to *D. furcata* zones interval by its ammonite content (Pictet et al., 2016). As a result, the associated
965 hiatus topping the Poet Beds conforms well to the duration of the SbBA2-related hiatus in the Subalpine Chains.
966 Above this discontinuity, this region acts as a topographic high whose sedimentary succession only records
967 flooding events of third order significance, interrupted by an ammonite-bearing, condensed phosphoritic
968 horizons spanning the upper Aptian to the lower Cenomanian (Pictet et al., 2016).
969
970 In summary, the installation of the rudistid biota in the Swiss–French Jura and its southward
971 progradation in the Subalpine Chains during the Hauterivian–Barremian transition conforms to other record of
972 the peri-Vocontian platforms. However, intra-Urgonian correlations with the Provence–Bas-Vivarais
973 depositional sequences are made difficult due to an imprecise ammonite age-calibration and a complex
974 accommodation history of the Subalpine regions. We hope that these preliminary results will stimulate new
975 detailed investigations on the platform-to-basin correlations of the Subalpine platform.
976
977 **8. Conclusion**
978
979 Revised ammonite age-calibration of the Urgonian-type, Provence platform series leads to two main
980 regional implications:
981 (*i*) The northward progradation of rudistid limestones in North Provence is, strictly, of late Barremian
982 age and spans the *T. vandenheckii* to the lower *M. sarasini* zones;
983 (*ii*) The Urgonian rudistid limestones record a twofold demise. The first event corresponds to the
984 tectonically-induced collapse of the South Provence domain during the *I. giraudi* Zone coeval with the North
985 Provence *Palorbitolina* mass accumulation (*Palorbitolina–Heteraster* guide level). The second one terminates
986 the Urgonian regime at the *M. sarasini–P. waagenoides* subzonal boundary.

Comparison with the peri-Vocontian Urgonian platforms pinpoints coeval demise of the rudistid biota in the uppermost Barremian:

(*i*) The first demise refers to the likely coeval, massive outbreak of a *Palorbitolina*-rich limestones of the Bas-Vivarais (V4 episode) and Subalpine platforms (Lower *Orbitolina* Beds) with the North Provence *Palorbitolina–Heteraster* guide level. This contrasts with the diachronous nature (~1 to 1.2 Myr offset) assumption developed by Huck et al. (2011, 2013, 2014) and gives evidence of large-scale environmental perturbations in both platform and basin settings during this time interval.

(*ii*) The second demise refers to the termination of the Urgonian caprinid episode at a regional exposure event. The associated hiatus occurs at the *M. sarasini–P. waagenoides* subzonal boundary (North Provence) but it can include a longer duration in reaching the middle part of the lower Aptian (as minimum constrained age) in most proximal settings (Western Bas-Vivarais, Subalpine Chains).

Acknowledgments

This work is a contribution to the PhD thesis project of one of us (A.J.-B.T.). It is part of the ALBION research project initiated by TOTAL S.A. whose financial support is gratefully acknowledged. Gérard Delanoy (Nice Sophia Antipolis Université), Bernard Clavel (Messery), Christina Ifrim (Ruprecht-Karls-Universität) and Émile Hourqueig (Nantes) greatly contributed by their fruitful discussions during the course of this study. Special thanks are due to Axel Arnoux (Aix–Marseille University), Emmanuel Robert (Université Claude Bernard–Lyon I) and Fabienne Giraud (Grenoble Alpes Université) who allowed us access to the collections in their care. This work greatly benefits from the insightful review of Josep A. Moreno-Bedmar (Universidad Nacional Autónoma de México) and Serge Ferry (Université Claude Bernard–Lyon I), as well as those of the editor-in-chief, Eduardo Koutsoukos. Last but not least, we wish to express our warmest thanks to the families of the first two authors for their help and continuous support during the preparation of this work.

References

Allan, J.R., Matthews, R.K., 1982. Isotope signatures associated with early meteoric diagenesis. Sedimentology 29, 797–817.

1017 Arnaud, H., Arnaud-Vanneau, A., 1991. Les calcaires urgoniens des massifs subalpins septentrionaux et du Jura
1018 (France) : âge et discussion des données stratigraphiques. Géologie Alpine 67, 63–79.
1019 Arnaud, H., Arnaud-Vanneau, A., Blanc-Alétru, M.-C., Adatte, T., Argot, M., Delanoy, G., Thieuloy, J.-P.,
1020 Vermeulen, J., Virgone, A., Virlouvet, B., Wermeille, S., 1998. Répartition stratigraphique des
1021 orbitolinidés de la plate-forme urgonienne subalpine et jurassienne (SE de la France). Géologie Alpine
1022 74, 3–89.
1023 Arnaud, H., 2005a. The South-East France Basin (SFB) and its Mesozoic evolution. In: Adatte, T., Arnaud-
1024 Vanneau, A., Arnaud, H., Blanc-Alétru, M.-C., Bodin, S., Carrio-Schaffauser, E., Föllmi, K., Godet, A.,
1025 Raddadi, M.C., Vermeulen, J., 2005. The Hauterivian lower Aptian sequence stratigraphy from Jura
1026 platform to Vocontian basin: a multidisciplinary approach. Field-trip of the 7th International symposium
1027 on the Cretaceous (September 1–4, 2005). Géologie Alpine, Colloques et excursions 7, 181 pp.
1028 Arnaud, H., 2005b. Sequence stratigraphy interpretation. In: Adatte, T., Arnaud-Vanneau, A., Arnaud, H., Blanc-
1029 Alétru, M.-C., Bodin, S., Carrio-Schaffauser, E., Föllmi, K., Godet, A., Raddadi, M.C., Vermeulen, J.,
1030 2005. The Hauterivian lower Aptian sequence stratigraphy from Jura platform to Vocontian basin: a
1031 multidisciplinary approach. Field-trip of the 7th International symposium on the Cretaceous (September
1032 1–4, 2005). Géologie Alpine, Colloques et excursions 7, 181 pp.
1033 Arnaud, H., Arnaud-Vanneau, A., Godet, A., Adatte, T., Massonnat, G., 2017. Barremian platform carbonates
1034 from the eastern Vercors Massif, France: Organization of depositional geometries. American Association
1035 of Petroleum Geologists Bulletin 101, 485–493.
1036 Arnaud-Vanneau, A., 1980. Micropaléontologie, paléoécologie et sédimentologie d'une plate-forme carbonatée
1037 de la marge passive de la Téthys : l'Urgonien du Vercors septentrional et de la Chartreuse (Alpes
1038 occidentales). Géologie Alpine, Mémoire Hors-Série 11, 1–874.
1039 Arnaud-Vanneau, A., Arnaud, H., 1990. Hauterivian to Lower Aptian carbonate shelf sedimentation and
1040 sequence stratigraphy in the Jura and northern Subalpine chains (southeastern France and Swiss Jura), in:
1041 Tucker, M.E., Wilson, J.L., Crevello, P.D., Sarg, J.R., Read, J.F. (Eds.), Carbonate Platforms: Facies,
1042 Sequences and Evolution. Blackwell Scientific Publications, pp. 203–233.
1043 Arnaud-Vanneau, A., Arnaud, H., Foury, G., Masse, J.-P, 1972. Excursion sur l'Urgonien de Haute--Provence et
1044 du Vercors (9-12 octobre 1972). Livret-Guide de l'Excursion du GFC pour 1972, 69 pp.
1045 Arnaud-Vanneau, A., Arnaud, H., Carrio-Schaffhauser, E., Raddadi, M.C., 2005. Urgonian deposits and
1046 Barremian–early Aptian sequence stratigraphy in the Vercors Massif. In: Adatte, T., Arnaud-Vanneau, A.,

1047 Arnaud, H., Blanc-Alétru, M.-C., Bodin, S., Carrio-Schaffauser, E., Föllmi, K., Godet, A., Raddadi, M.C.,
1048 Vermeulen, J., 2005. The Hauterivian lower Aptian sequence stratigraphy from Jura platform to
1049 Vocontian basin: a multidisciplinary approach. Field-trip of the 7th International symposium on the
1050 Cretaceous (September 1–4, 2005). Géologie Alpine, Colloques et excursions 7, 181 pp.
1051 Astier, J.-E., 1851. Catalogue descriptif des *Ancyloceras* appartenant à l'étage Néocomien d'Escragnolles et des
1052 Basses-Alpes. Annales des Sciences Physiques et Naturelles, d'Agriculture et d'Industrie 3, 435–456.
1053 Bastide, F., 2014. Synthèse de l'évolution de la plateforme urgonienne (Barrémien tardif à aptien précoce) du
1054 Sud-Est de la France : Faciès, micropaléontologie, géochimie, géométries, paléotectonique et
1055 géomodélisation. Ph.D. thesis ISTerre Grenoble–UNIL, 300 pp.
1056 Bergen, J.A., 2000. Calcareous nannofossils from the lower Aptian historical stratotype at Cassis–La Bédoule
1057 (SE France). In: Moullade, M., Tronchetti, G., Masse, J.-P., (Eds.), Le stratotype historique de l'Aptien
1058 inférieur (Bédoulien) dans la région de Cassis–La Bédoule (S.E. France). Géologie méditerranéenne 25
1059 (1998), 227–255.
1060 Bert, D., Delanoy, G., 2000. Considérations nouvelles sur quelques représentants barremiens des Puchelliidae
1061 Douvillé, 1890 et des Hemihoplitidae Spath, 1924 (Ammonoidea). Annales du Muséum d'Histoire
1062 Naturelle de Nice 15, 63–89.
1063 Bert, D., Delanoy, G., Bersac, S., 2006. Descriptions de représentants nouveaux ou peu connus de la famille des
1064 Hemihoplitidae SPATH, 1924 (Barrémien supérieur, Sud-est de la France) : conséquences taxinomiques
1065 et phylétiques. Annales du Muséum d'Histoire Naturelle de Nice 21, 179–253.
1066 Bert, D., Delanoy, G., Bersac, S., 2008. Nouveaux biohorizons et propositions pour le découpage biozonal
1067 ammonitique du Barrémien supérieur du Sud-Est de la France. Carnets de Géologie/Notebooks on
1068 Geology, Article 2008/03 (CG2008_A03), 18 pp.
1069 Bert, D., Delanoy, G., Canut, L., 2009. L'origine des *Imerites* Rouchadze, 1933 : résultats d'une innovation chez
1070 les Gassendiceratinae Bert, Delanoy et Bersac, 2006 (Ammonoidea, Ancyloceratina). Annales de
1071 Paléontologie 95, 21–35.
1072 Blanc, J.-J., Weydert, P., Masse, J.P., Roux, M., de Peyronnet, P., Rouire, J., 1973. Notice explicative et carte
1073 géologie de la France 1/50 000, feuille Sault-de-Vaucluse 942. Orléans, BRGM, 15 pp.
1074 Bogdanova, T.N., 1983, [*Deshayesites tuarkyricus* Zone - the lower zone of the Aptian in Turkmenia].
1075 Ezhegondik Vsesoyuznogo Paleontologicheskogo Obshchestva 26, 128–147. (in Russian)

1076 Bréhéret, J.-G., 1995. L'Aptien et l'Albien de la Fosse vocontienne (des bordures au bassin). Évolution de la
1077 sédimentation et enseignements sur les événements anoxiques. Société Géologique du Nord 25, 614 pp.
1078 Bulot, L.G., 1993. Stratigraphical implications of the relationship between ammonites and facies; examples from
1079 the Lower Cretaceous (Valanginian-Hauterivian) of the western Tethys. Systematic Association, Special
1080 Volume 47, 243–265.
1081 Casey, R., 1964. A monograph of the Ammonoidea of the Lower Greensand, part V. Palaeontographical Society,
1082 289–398.
1083 Cecca, F., Ropolo, P., Gonnet, R., 1999. The appearance of the genus *Deshayesites* (Kazansky, 1914,
1084 Ammonoidea) in the lowermost Aptian (Lower Cretaceous) of La Bédoule (SE France). Rivista Italiana
1085 di Paleontologia e Stratigrafia 105, 267–286.
1086 Cecca, F., Ropolo, P., Gonnet, R., 2000. La base de l'Aptien à Cassis–La Bédoule (SE France). In: Moullade, M.,
1087 Tronchetti, G., Masse, J.-P., (Eds.), Le stratotype historique de l'Aptien inférieur (Bédoulien) dans la
1088 région de Cassis–La Bédoule (S.E. France). Géologie méditerranéenne 25 (1998), 149–157.
1089 Charollais, J., Clavel, B., Busnardo, R., 2008. Biostratigraphie et découpage séquentiel des formations du
1090 Crétacé Inférieur de la plateforme Jurassienne (France, Suisse). A Terra: Conflitos e ordem, Homenagem
1091 ao Professor Ferreira Soares, 197–207.
1092 Chartrousse, A., 1998. Les Caprinidae (rudistes) du Crétacé inférieur. Thèse Université de Provence, 289 p.
1093 Chartrousse, A., Masse, J.-P., 1998. *Offneria simplex* nov. sp. (rudiste, Caprinidae) du Barrémien du Sud-Est de
1094 la France et de Cuba. Implications sur la biostratigraphie et l'évolution du genre *Offneria*. Bulletin de la
1095 Société Géologique de France 6, 841–860.
1096 Clavel, B., Charollais, J., Schroeder, R., Busnardo, R., 1995. Réflexions sur la biostratigraphie du Crétacé
1097 inférieur et sur sa complémentarité avec l'analyse séquentielle : exemple de l'Urgonien jurassien et
1098 subalpin. Bulletin de la Société géologique de France 166, 663–680.
1099 Clavel, B., Schroeder, R., Charollais, J., Busnardo, R., Martín-Closas, C., Decrouez, D., Sauvagnat, J., Cherchi,
1100 A., 2002. Les "couches inférieures à orbitolines" (Chaînes subalpines septentrionales): mythe ou réalité?
1101 Revue de Paléobiologie 21, 865–871.
1102 Clavel, B., Charollais, J., Conrad, M., Jan du Chêne, R., Busnardo, R., Gardin, S., Erba, E., Schroeder, R.,
1103 Cherchi, A., Decrouez, D., Granier, B., Sauvagnat, J.,Weidmann, M., 2007. Dating and progradation of
1104 the Urgonian limestone from the Swiss Jura to South-East France. Zeitschrift der Deutschen Gesellschaft
1105 für Geowissenschaften 158, 1025–1062.

1106 Clavel, B., Busnardo, R., Charollais, J., Conrad, M.A., Granier, B., 2010. Répartition biostratigraphique des
1107 orbitolinidés dans la biozonation à ammonites (plate-formeurgonienne du Sud-Est de la France) Partie 1 :
1108 Hauterivien supérieur - Barrémien basal. Carnets de Géologie/Notebooks on Geology, Article 2010/06
1109 (CG2010_ A06) 53 pp.
1110 Clavel, B., Conrad, M-A., Busnardo, R., Charollais, J., Granier, B., 2013. Mapping the rise and demise of
1111 Urgonian platforms (Late Hauterivian–Early Aptian) in southeastern France and the Swiss Jura.
1112 Cretaceous Research 39, 29–46.
1113 Clavel, B., Charollais, J., Busnardo, R., Granier, B., Conrad, M., Desjaques, P., Metzger, J., 2014. La plate-
1114 forme carbonatée urgonienne (Hauterivien supérieur–Aptien inférieur) dans le Sud-Est de la France et en
1115 Suisse : synthèse. Archives des Sciences 67, 1–97.
1116 Conte, G., 1989. Fossiles du plateau d'Albion. Les Alpes de Lumière 99, 1–72.
1117 Cotillon, P., 2010. Sea bottom current activity recorded on the southern margin of the Vocontian basin (southeast
1118 France) during the Lower Aptian. Evidence for a climatic signal. Bulletin de la Société Géologique de
1119 France 181, 3–18.
1120 Cotillon, P., Banvillet, M., Gaillard, C., Grosheny, D., Olivero, D., 2000. Les surfaces à Rhizocorallium de
1121 l'Aptien inférieur sur la bordure méridionale du bassin vocontien (France Sud-Est), marqueurs de
1122 dynamiques locales; leur relation avec un événement anoxique global. Bulletin de la Société Géologique
1123 de France 171, 229–238.
1124 Dauphin, L., 2002. Litho-, bio-, et chronostratigraphie comparées dans le Bassin Vocontien à l'Aptien. Ph.D.
1125 thesis of the Université de Lille, 451 pp.
1126 Delamette, M., Charollais, J., Decrouez, D., Caron, M., 1997. Les grès verts helvétiques (Aptien moyen –
1127 Albien supérieur) de Haute-Savoie, Valais et Vaud (Alpes occidentales franco-suisses). Publications du
1128 Département de la Géologie et Paléontologie, Université Genève 23, 400 pp.
1129 Delanoy, G. 1990. *Camereiceras* nov. gen. (Ammonoidea, Ancyloceratina) du Barrémien supérieur du Sud-Est
1130 de la France. Géobios 23, 71–93.
1131 Delanoy, G., 1992. Les ammonites du Barrémien Supérieur de Saint-Laurent de l'Escarène (Alpes-Maritimes,
1132 Sud-Est de la France). Annales du Muséum D'Histoire Naturelle de Nice 9, 1–148.
1133 Delanoy, G., 1995a. Les zones à Feraudianus, Giraudi et Sarasini du Barrémien supérieur de la région
1134 stratotypique d'Angles–Barrême–Castellane (Sud-Est de la France). Géologie Alpine, Mémoire Hors-
1135 Série 20 (1994), 279–319.

1136 Delanoy, G., 1995b. About some significant ammonites from the Lower Aptian (Bedoulian) of the Angles–
1137 Barrême area (South-East France). Memori Descrittive della Carta Geologica d'Italia 51, 65–101.
1138 Delanoy, G. 1997a. Biostratigraphie des faunes d'Ammonites à la limite Barrémien–Aptien dans la région
1139 d'Angles–Barrême–Castellane. Étude particulière de la famille des Heteroceratina Spath, 1922
1140 (Ancyloceratina, Ammonoidea). Annales du Muséum d'Histoire Naturelle de Nice 12, 1–270.
1141 Delanoy, G., 1997b. Biostratigraphie haute résolution du Barrémien supérieur du Sud-Est de la France. Comptes
1142 Rendus de l'Académie des Sciences, Paris, Sciences de la Terre et des Planètes 325, 689–694.
1143 Delanoy, G., 2003. *Toxancyloceras* gen. nov. (Ammonoidea, Ancyloceratina) un nouveau genre du Barrémien
1144 supérieur. Annales du Muséums d'Histoire Naturelle de Nice 18, 1–19.
1145 Delanoy, G., Ebbo, L., 1997. Révision de l'holotype d'*Ancyloceras urbani* var. *paquieri* Kilian & Reboul, 1915
1146 et réflexions sur le genre *Kutatissites* Kakabadze, 1970 (Ammonoidea, Ancyloceratina). Géologie Alpine
1147 73, 3–21.
1148 Delanoy, G., Ropolo, P., Gonnet, R., Ebbo, L., 2000. Le genre *Kutatissites* Kakabadze, 1970 (Ammonoidea,
1149 Ancyloceratina) dans le Barrémien supérieur/Aptien basal de la Bédoule (Sud-Est de la France). Annales
1150 du Muséum d'Histoire Naturelle de Nice 15, 19–61.
1151 Delanoy, G., Baudouin, C., Gonnet, R., Conte, G., Frau, C., 2012. Sur la présence des genres *Heminautilus*
1152 Spath, 1927 et *Eucymatoceras* Spath, 1927 (Nautilida, Nautilaceae) dans le Barrémien inférieur du Gard
1153 (sud-est de la France). Annales du Musée d'Histoire naturelle de Nice 27, 155–195.
1154 Delanoy, G., Busnardo, R., Ropolo, P., Gonnet, R., Conte, G., Moullade, M., Masse, J.-P., 1997. The
1155 '*Pseudocrioceras* beds' at La Bédoule (SE France) and the position of the Barremian–Aptian boundary in
1156 the historical lower Aptian stratotype. Comptes Rendus de l'Académie des Sciences, Série IIA Earth
1157 Planetary Sciences 325, 593–599.
1158 Douvillé, H., 1890. Sur la classification des Cératites de la Craie. Bulletin de la Société Géologique de France,
1159 Série 3, 18, 275–292.
1160 Douvillé, H., 1918. Le Barrémien supérieur de Brouzet; Troisième Partie : Les Rudistes. Mémoires de la Société
1161 Géologique de France, Paléontologie, Mémoire 52, 28 pp.
1162 Dutour, Y., 2005. Biostratigraphie, évolution et renouvellements des ammonites de l'Aptien supérieur
1163 (Gargasien) du bassin vocontien (Sud-Est de la France). Ph.D thesis Université Claude Bernard–Lyon 1,
1164 302 pp.

1165 Elmi, S., Busnardo, R., Clavel, B., Camus, G., Kieffer, G., Bérard, P., Michaely, B., 1996. Notice explicative de
1166 la feuille Aubenas à 1/50.000, Editions du BRGM. Service géologique national 170 p.
1167 Embry, J.C., 2005. Paléoécologie et architecture stratigraphique en haute résolution des plates-formes
1168 carbonatées du Barrémien–Aptien de la Néo-Téthys (Espagne, Suisse, Provence–Vercors). Impact
1169 respectif des différents facteurs de contrôle. Ph.D thesis Institut Français du Pétrole, 298 pp.
1170 Fahy, J., 1965. Contribution à l'étude de la région du Mont Ventoux contact avec le massif de Suzette et les
1171 Baronies. Ph.D thesis Université de Grenoble, 192 pp.
1172 Faure, D., 1965. Le Barrémien du Sud du couloir rhodanien. In: Colloque sur le Crétacé inférieur (Lyon,
1173 Septembre 1963). Mémoire du Bureau de Recherches Géologiques et Minières 34, pp. 139–146.
1174 Föllmi, K.B., 2008. A synchronous, middle Early Aptian age for the demise of the Helvetic Urgonian platform
1175 related to the unfolding oceanic anoxic event 1a (Selli event). Comment on the article «Sur la présence de
1176 grands foraminifères d'âge aptien supérieur dans l'Urgonien de la Nappe du Wildhorn (Suisse centrale).
1177 Note préliminaire» by R. Schroeder, K. Schenk, A. Cherchi & B. Schwizer, Revue de Paléobiologie,
1178 2007, 665-669. Revue de Paléobiologie 27, 461–468.
1179 Föllmi, K.B., 2012. Early Cretaceous life, climate and anoxia. Cretaceous Research 35, 230–257.
1180 Föllmi, K.B., Gainon, F., 2008. Demise of the northern Tethyan Urgonian carbonate platform and subsequent
1181 transition towards pelagic conditions: The sedimentary record of the Col de la Plaine Morte area, central
1182 Switzerland. Sedimentary Geology 205, 142–159.
1183 Föllmi, K.B., Weissert, H., Bisping, M., Funk, H., 1994. Phosphogenesis, carbon-isotope stratigraphy, and
1184 carbonate-platform evolution along the Lower Cretaceous northern Tethyan margin. Geological Society
1185 of America Bulletin 106, 729–746.
1186 Föllmi, K.B., Godet, A., Bodin, S., Linder, P., 2006. Interactions between environmental change and shallow
1187 water carbonate buildup along the northern Tethyan margin and their impact on the Early Cretaceous
1188 carbon isotope record. Paleoceanography 21, PA4211, 1–16.
1189 Föllmi, K.B., Bodin, S., Godet, A., Linder, P., Van de Schootbrugge, B., 2007. Unlocking paleo-environmental
1190 information from Early Cretaceous shelf sediments in the Helvetic Alps: stratigraphy is the key! Swiss
1191 Journal of Geosciences 100, 349–369.
1192 Fouke, B.W., Zwart, E.W., Everts, A.J.W., Schlager,W., 1995. Carbonate platform stratal geometries and the
1193 question of subaerial exposure. Sedimentary Geology 97, 9–19.

1194 Frau, C., Delanoy, G., Hourqueig, E., 2015. Le genre *Macroscaphites* Meek, 1876 (Ammonoidea) dans l'Aptien
1195 inférieur de Cassis–La Bédoule (Bouches-du-Rhône, France). Proposition d'un nouveau schéma zonal
1196 pour la série stratotypique. Revue de Paléobiologie 34, 45–57.
1197 Frau, C., Delanoy, G., Masse, J.-P., Lanteaume, C., Tendil, A.J.B., 2016. New Heteroceratidae (Ammonoidea)
1198 from the late Barremian deepening succession of Marseille (Bouches-du-Rhône, France). Acta Geologica
1199 Polonica 66, 205–225.
1200 Frau, C., Pictet, A., Spangenberg, J., Masse, J.-P., Tendil, A.J.B.T., Lanteaume, C., 2017. New insights on the
1201 age of the post-Urgonian marly cover of the Apt region (Vaucluse, SE France) and its implications on the
1202 demise of the North Provence carbonate platform. Sedimentary Geology 359, 44–61.
1203 Frau, C., Bulot, L.G., Delanoy, G., Moreno-Bedmar, J.A., Masse, J.-P., Lanteaume, C., Tendil, A.J.-B.T., 2018.
1204 The candidate Aptian GSSP at Gorgo a Cerbara (Central Italy): an alternative interpretation of the bio-,
1205 litho- and chemostratigraphic markers. Newsletters on Stratigraphy in press.
1206 Frau, C., Masse, J.-P., Fenerci-Masse, M., Tendil, A.J.-B., Pictet, A., Lanteaume, C., accepted. Is Strontium
1207 isotope stratigraphy a reliable tool for dating the Barremian–Aptian transition in shallow water carbonate
1208 settings? Examples from North Tethyan case studies. Carnets de Géologie/Notebooks on Geology.
1209 Gauthier, H., Busnardo, R., Combémorel, R., Delanoy, G., Fischer, J.–C., Guérin–Franiatte, S., Joly, B.,
1210 Kennedy, W.J., Sornay, J., Tintant, H., 2006. Volume IV. Céphalopodes crétacés. In: Fischer, J.-C., (Ed.),
1211 Révision critique de la Paléontologie Française d'Alcide d'Orbigny. Backhuys Publishers BV, Leiden,
1212 pp. 1–292.
1213 Gidon, P., 1952. Une ammonite de l'Urgonien en Grande-Chartreuse. Comptes Rendus Sommaires de la Société
1214 Géologique de France 1952, p. 237.
1215 Gill, T., 1871. Arrangement of the families of mollusks. Smithsonian Miscellaneous Collections 227, xvi + 1–49.
1216 Godet, A., Bodin, S., Föllmi, K.B., Vermeulen, J., Gardin, S., Fiet, N., Adatte, T., Berner, Z., Stüben, D., Van de
1217 Schootbrugge, B., 2006. Evolution of the marine stable carbon isotope record during the early
1218 Cretaceous: a focus on the late Hauterivian and Barremian in the Tethyan realm. Earth Planetary Sciences
1219 Letters 242, 254–271.
1220 Godet, A., Bodin, S., Adatte, T., Föllmi, K.B., 2008. Platform-induced clay-mineral fractionation along a
1221 northern Tethyan basin-platform transect: implications for the interpretation of Early Cretaceous climate
1222 change (Late Hauterivian-Early Aptian). Cretaceous Research 29, 830–847.

1223 Godet, A., Föllmi, K.B., Stille, P., Bodin, S., Matera, V., Adatte, T., 2011. Reconciling Strontium isotope and K–
1224 Ar ages with biostratigraphy: the case of the Urgonian platform, Early Cretaceous of the Jura Mountains,
1225 Western Switzerland. Swiss Journal of Geosciences 104, 147–160.
1226 Godet, A., Adatte, T., Arnaud-Vanneau, A., Arnaud, H., Carrio-Schaffauser, E., Vermeulen, J., 2016a. Approche
1227 multidisciplinaire des séries hauteriviennes à aptiennes: étude d'un transect allant de la plateforme
1228 jurasienne et du Vercors au bassin Vocontien. Field-trip of the Excursion du Groupe Français du Crétacé
1229 (October 2–5, 2016), 155 pp.
1230 Godet, A., Durlet, C., Spangenberg, J.E., Föllmi, K.B., 2016b. Estimating the impact of early diagenesis on
1231 isotope records in shallow-marine carbonates: A case study from the Urgonian platform in western Swiss
1232 Jura. Palaeogeography, Palaeoclimatology, Palaeoecology 454, 125–138.
1233 Goguel, J., 1932. Sur l'extension des faciès urgoniens dans les Monts de Vaucluse. Bulletin de la Société
1234 Géologique de France 5, 445–464.
1235 Granier, B., Clavel, B., Moullade, M., Busnardo, R., Charollais, J., Tronchetti, G., Desjacques, P., 2013.
1236 L'Estellon (Baronnies, France), a "Rosetta Stone" for the Urgonian biostratigraphy. Carnets de
1237 Géologie/Notebooks on Geology, Article 2013/04 (CG2013_ A04) 163–207.
1238 Herrle, J.O., Mutterlose, J., 2003. Calcareous nannofossils from the Aptian - early Albian of SE France:
1239 Paleoecological and biostratigraphic implications. Cretaceous Research 24, 1–22.
1240 Huck, S., Heimhofer, U., 2015. Improving shallow water carbonate chemostratigraphy by means of rudist
1241 bivalve sclerochemistry. Geochemistry, Geophysics, Geosystems 16, doi:10.1002/2015GC005988, 1–18.
1242 Huck, S., Rameil, N., Korbar, T., Heimhofer, U., Wieczorek, T.D., Immenhauser, A., 2010. Latitudinally
1243 different responses of Tethyan shoal-water carbonate systems to the Early Aptian oceanic anoxic event
1244 (OAE 1a). Sedimentology 57, 1585–1614.
1245 Huck, S., Heimhofer, U., Immenhauser, A., 2012. Early Aptian algal bloom in a neritic proto-North Atlantic
1246 setting: Harbinger of global change related to OAE1a? Geological Society of America Bulletin 124,
1247 1810–1825.
1248 Huck, S., Heimhofer, U., Rameil, N., Bodin, S., Immenhauser, A., 2011. Strontium and carbon-isotope
1249 chronostratigraphy of Barremian–Aptian shoal water carbonates: Northern Tethyan platform drowning
1250 predates OAE 1a. Earth and Planetary Sciences Letters 304, 547–558.

1251 Huck, S., Heimhofer, A., Immenhauser, A., Weissert, H., 2013. Carbon-isotope stratigraphy of early Cretaceous
1252 (Urgonian) shoal water deposits: diachronous changes in carbonate-platform production in the north-
1253 western Tethys. Sedimentary Geology 290, 157–174.
1254 Huck, S., Stein, M., Immenhauser, A., Skelton, P.W., Christ, N., Föllmi, K.B., Heimhofer, U., 2014. Response of
1255 proto-North Atlantic carbonate platform ecosystems to OAE1a-related stressors. Sedimentary Geology
1256 313, 15–31.
1257 Hyatt, A., 1900. Cephalopoda. In: Zittel, von K. (Ed.), Textbook of Palaeontology, English ed., translated by
1258 C.R. Eastman. Macmillan. London & New York, pp. 502-592.
1259 Hyatt, A., 1903. *Pseudoceratites* of the Cretaceous. Monographs of the United States Geological Survey 44, 352
1260 pp.
1261 Joachimski, M.M., 1994. Subaerial exposure and deposition of shallowing upward sequences: evidence from
1262 stable isotopes of Purbeckian peritidal carbonates (basal Cretaceous), Swiss and French Jura Mountains.
1263 Sedimentology 41, 805–824.
1264 Kakabadze M.V., 1970. New genus *Kutatissites* gen. nov. from Lower Cretaceous deposits of Western Georgia
1265 Bulletin of the Academy of Sciences of the Georgian SSR 58, 733–736. (In Russian)
1266 Kakabadze, M.V., 1981. The Ancyloceratids of the southern of the USSR and their stratigraphical significance.
1267 Trudy Geologicheskogo Instituta Akademii Nauk GSSR 71, 1–221. (In Russian)
1268 Kandel, D., 1992. Analyse paléotectonique de la plate-forme méridionale du bassin vocontien et de ses bordures,
1269 durant l'intervalle Barrémo-albien (Ventoux-Lure-Baronnies, chaines subalpines méridionales, France).
1270 Tectonique. Ph.D thesis, Université Pierre et Marie Curie - Paris VI, 318 pp.
1271 Karsten, H. 1858. Über die geognostischen Verhältnisse des westlichen Columbien, der heutigen Republiken
1272 Neu-Granada und Equador. Amtlicher Bereich über die Versammlung Deutscher Naturforscher und
1273 Aerzte (1856), 80–117.
1274 Kazansky, P.A., 1914. Description d'une collection des Céphalopodes des terrains Crétacés du Daghestan.
1275 Tomsk. 127 pp. (in Russian)
1276 Kilian, W., 1888. Description géologique de la Montagne de Lure (Basses-Alpes). Thèse, Paris, 460 pp.
1277 Kilian, W., 1896. Sur quelques céphalopodes nouveaux ou peu connus de la période secondaire. Travaux du
1278 Laboratoire de Géologie de la Faculté des Sciences de Grenoble, 285–296.
1279 Kilian, W., Reboul, P., 1915. Contribution à l'étude des faunes paléocrétacées du Sud-Est de la France. I. La
1280 faune de l'Aptien inferieur des environs de Montélimar (Drôme). II. Sur quelques ammonites de

1281 l'Hauterivien de la Bégude (Basses Alpes). Mémoires pour Servir à l'Explication de la Carte géologique
1282 Détaillée de la France, 288 pp.
1283 Kuhnt, W., Moullade, M., Masse, J.-P., Erlenkeuser, H., 2000. Carbon isotope stratigraphy of the lower Aptian
1284 historical stratotype at Cassis-La Bédoule. Géologie Méditerranéenne XXV, 3-4 (1998), 63–79.
1285 Lafarge, D., 1978. Étude géologique du plateau de Saint-Remèze, Ardèche. Stratigraphie, cartographie,
1286 sédimentologie, tectonique. Ph.D thesis Université Claude Bernard–Lyon, 119 pp.
1287 Leenhardt, F., 1883. Étude géologique de la région du Mont-Ventoux. Ph.D thesis Université de Montpellier,
1288 273 pp.
1289 Léonide, P., Doublet, S., Masse, J.-P., Borgomano, J., 2008. Modélisation géologique et pétrophysique des
1290 réservoirs et des unités d'écoulement dans les carbonates de la plate-forme du Crétacé inférieur
1291 (Barrémien-Aptien) de Provence - Stratigraphie et sédimentologie des carbonates d'âge Barrémien -
1292 Aptien inférieur de la région des Monts de Vaucluse. Unpublished report of the Laboratoire de Géologie
1293 des Systèmes et des Réservoir Carbonatés, Université de Provence, 197 + 40 pp.
1294 Léonide, P., Borgomano, J., Masse, J.-P., Doublet, S., 2012. Relation between stratigraphic architecture and
1295 multi-scale heterogeneities in carbonate platforms: the Barremian–lower Aptian of the Monts de
1296 Vaucluse, SE France. Sedimentary Geology 265, 87–109.
1297 Léonide, P., Fournier, F., Reijmer, J.J.G., Vonhof, H.B., Borgomano, J., Dijk, J., Rosenthal, M., van Goethem,
1298 M., Cochard, J., Meulenaars, K., 2014. Diagenetic patterns and pore space distribution along a platform to
1299 outer-shelf transect (Urgonian limestone, Barremian–Aptian, SE France). Sedimentary Geology 306, 1–
1300 23.
1301 Linder, P., Gigandet, J., Hüsser, J.-L., Gainon, F., Föllmi, K.B., 2006. The Early Aptian Grünten Member:
1302 Description of a new lithostratigraphic unit of the helvetic Garschella Formation. Eclogae Geologicae
1303 Helvetiae 99, 327–341.
1304 Machhour, L., Masse, J.-P., Oudin, J.L., Lambert, B., Lapointe, P., 1998. Petroleum potential of dysaerobic
1305 carbonate source rocks in an intrashelf basin: the Lower Cretaceous of Provence, France. Petroleum
1306 Geosciences 4, 139–146.
1307 Maillard, J., 1965. Le passage Barrémien–Aptien et ses rapports avec l'Urgonien dans le couloir rhodanien (entre
1308 Valence et Avignon). In colloque Sur le Crétacé inferieur, Lyon 1963. Mémoire du Bureau de Recherches
1309 Géologiques et Minières 34, 147–156.

1310 Martín-Closas, C., Clavel, B., Schroeder, R., Charollais, J., Conrad, M.A., 2009. Charophytes from the
1311 Barremian-lower Aptian of the Northern Subalpine Chains and Jura Mountains, France: correlation with
1312 associated marine assemblages. Cretaceous Research 30, 49–62.
1313 Masse, J.-P., 1976. Les calcaires urgoniens de Provence (Valanginien–Aptien inférieur). Stratigraphie,
1314 paléontologie, les paléoenvironnements et leur évolution. Ph.D. thesis Université d'Aix–Marseille II, 445
1315 pp.
1316 Masse, J.-P., 1993. Valanginian to early Aptian carbonate platforms from Provence (SE France). In: Simo, A.,
1317 Scott, R.W., Masse, J.-P. (Eds.), Cretaceous Carbonate Platforms. American Association of Petroleum
1318 Geologists, Memoir 5, 363–374.
1319 Masse, J.-P., 1995. Lower Cretaceous Rudist Biostratigraphy of Southern France, a Reference for Mesogean
1320 Correlations. Revista Mexicana de Ciencias Geológicas 12, 236–256.
1321 Masse, J.-P., 2003. Integrated stratigraphy of the Lower Aptian and applications to carbonate platforms: a state
1322 of the art. In: Gili, E., Negra, M.H., Skelton, P.W. (Eds.), North African Cretaceous Carbonate Platform
1323 Systems. NATO Science Series, IV. Earth and Environmental Sciences 28. Kluwer Academic Publishers,
1324 203–214.
1325 Masse, J.-P., Steuber, T., 2007. Strontium isotope stratigraphy of early Cretaceous rudist bivalves. In: Cretaceous
1326 rudists and carbonate platforms: environmental feedback. SEPM Special Publication 87, Society for
1327 Sedimentary Geology, 159–165.
1328 Masse, J.-P., Fenerci-Masse, M., 2011. Drowning discontinuities and stratigraphic correlations in platform
1329 carbonates. The late Barremian–Early Aptian record of South-East France. Cretaceous Research 32, 659–
1330 684.
1331 Masse, J.-P., Fenerci-Masse, M., 2013a. Stratigraphic updating and correlation of late Barremian–early Aptian
1332 Urgonian successions and their marly cover, in their type region (Orgon–Apt, SE France). Cretaceous
1333 Research 39, 17–28.
1334 Masse, J.-P., Fenerci-Masse, M., 2013b. Drowning events, development and demise of carbonate platforms and
1335 controlling factors: The Late Barremian–Early Aptian record of Southeast France. Sedimentary Geology
1336 298, 28–52.
1337 Masse, J.-P., Fenerci-Masse, M., 2013c. Bioevents and palaeoenvironmental changes in carbonate platforms: the
1338 record of Barremian "Urgonian" limestones of SE France. Palaeogeography, Palaeoclimatology,
1339 Palaeoecology 381, 637–661.

1340 Masse, J.-P., Fenerci-Masse, M., 2015. Evolution of the rudist bivalve *Agriopleura* Kühn (Radiolitidae,
1341 Hippuritida) from the Mediterranean region. Palaeontology 58, 71–100.
1342 Masse, J.-P., Machhour, L., 2000. La matière organique dans la série du stratotype historique de l'Aptien
1343 inférieur de Cassis–La Bédoule (SE France). Géologie Méditerranéenne XXV, 3-4 (1998), 55–62.
1344 Masse, J.-P., Gourrat, C., Orbette, D., Schmuck, D., 1998. Hauterivian rudist faunas of Southern Jura (France).
1345 In: Masse, J.-P., Skelton, P.W. (Eds.), Quatrième Congrès international sur les Rudistes. Geobios, M.S.
1346 22, 225–233.
1347 Masse, J.-P., El Albani, A., Erlenkeuser, H., 1999. Stratigraphie isotopique ($\delta^{13}C$) de l'Aptien inférieur de
1348 Provence (SE France): applications aux corrélations plateforme - bassin. Eclogae geologiae Helvetiae 92,
1349 25–263.
1350 Masse, J.-P., Bouaziz, S., Amon, E.O., Baraboshkin, E., Tarkowski, R., Bergerat, F., Sandulescu, M., Canérot, J.,
1351 Guiraud, R., Poisson, A., Ziegler, M., Rimmele, G., 2000. Early Aptian. In: Dercourt, J., Gaetani, M., et
1352 al. (Eds.), Atlas Peritethys, Palaeogeographical Maps. CCGM/CGMW, Paris, Map.
1353 Masse, J.-P., Fenerci, M., Borgomano, J., 2001. Levelling pattern in peritidal carbonates, Late Barremian from
1354 Cassis (Marseille region, SE France). Anatomic implications. Géologie Méditerranéenne 28, 117–120.
1355 Meek, F.B., 1876. A report on the invertebrate Cretaceous and Tertiary fossils of the upper Missouri country. In:
1356 Hayden, F.V. (Ed.), Report of the United States Geological Survey of the Territories 9, lxiv + pp. 629 pp.
1357 Monier, P., 1986. De la plate-forme urgonienne provençale au bassin vocontien: étude stratigraphique,
1358 cartographique et paléogéographique de la série crétacée du Mont Ventoux et Chaînes Subalpines
1359 méridionales du Sud-Est de la France. Ph.D thesis, Université Claude Bernard–Lyon 1, 186 pp.
1360 Moret, L., Deleau, P., 1960. Notes de paléontologie savoisienne : découverte d'ammonites dans le Berrias et
1361 l'urgonien des environs d'Annecy (Haute-Savoie). Travaux du Laboratoire de Géologie de Grenoble 36
1362 (1960), 43–44.
1363 Moullade, M., 1965. Révision des stratotypes de l'Aptien: Gargas (Vaucluse). Colloque sur le Crétacé inférieur
1364 (Lyon, septembre 1963). Mémoire Bureau Recherches Géologiques et Minières 34, 201–214.
1365 Moullade, M., Masse, J.-P., Tronchetti, G., Kuhnt, W., Ropolo, P., Bergen, J.A., Masure, E., Renard, M., 2000a.
1366 Le stratotype historique de l'Aptien inférieur (région de Cassis–La Bédoule, SE France): synthèse
1367 stratigraphique. In: Moullade, M., Tronchetti, G., Masse, J.-P., (Eds.), Le stratotype historique de l'Aptien
1368 inférieur (Bédoulien) dans la région de Cassis - La Bédoule (S.E. France). Géologie Méditerranéenne
1369 XXV, 3-4 (1998), 289–298.

1370 Moullade, M., Tronchetti, G., Busnardo, R., Masse, J.-P., 2000b. Description lithologique des coupes types du
1371 stratotype historique de l'Aptien inférieur dans la région de Cassis – La Bédoule (SE France). In:
1372 Moullade, M., Tronchetti, G., Masse, J.-P., (Eds.), Le stratotype historique de l'Aptien inférieur
1373 (Bédoulien) dans la région de Cassis - La Bédoule (S.E. France). Géologie Méditerranéenne 26, 15–29.
1374 Moullade, M., Tronchetti, G., Balme, C., Mauroux, P., 2012. A new upper Bedoulian section in the Aptian
1375 stratotypic area: Croagnes (5 km NW of Gargas, Vaucluse, SE France). Carnets de Géologie, Letter
1376 2012/03, 193–199.
1377 Orbigny, d'A., 1849-1852. Cours élémentaire de paléontologie et de géologie stratigraphique. Masson. Paris. I-
1378 (1849) 1–299; II-(1851) 1–382; III-(1852): 383–847.
1379 Orbigny, d' A., 1840–1842. Paléontologie française, Description zoologique et géologique de tous les animaux
1380 mollusques et rayonnés fossiles de France. Terrains Crétacés, Vol. 1. Céphalopodes. Masson, Paris 662
1381 pp.
1382 Orbigny, d' A., 1850. Prodrome de Paléontologie stratigraphique universelle des animaux mollusques et
1383 rayonnes. Volume 2, Masson, Paris, 428 pp.
1384 Orbigny, d' A., 1852. Prodrome de Paléontologie stratigraphique universelle des animaux mollusques et
1385 rayonnés et table alphabétique et synonymique des genres et des espèces contenus dans le Prodrome de
1386 Paléontologie stratigraphique universelle. Volume 3, Masson, Paris, 196 + 191 pp.
1387 Paquier, V., 1900. Recherches géologiques dans le Diois et les Baronnies orientales. Travaux du laboratoire de
1388 Géologie de la Faculté des sciences de l'Université de Grenoble 5, 149–556.
1389 Paquier, V., 1905. Les rudistes urgoniens. Deuxième partie. Mémoire de la Société géologique de France,
1390 Paléontologie 13, 49–95.
1391 Parona, C.F., Bonarelli, G., 1897. Fossili Albiani d'Escragnolles, del Nizzardo e della Liguria occidentale.
1392 Paleontologica Ita1iana 2, 53–112.
1393 Pellat, E., 1903. Le Néocomien (Valanginien et Hauterivien) et le Barrémien entre Mons et Brouzet (Gard);
1394 quelques mots sur les faciès urgoniens de Martigues et d'Apt; sur l'Aptien des environs d'Uzès, et le
1395 Barrémien de Lussan (Gard). Bulletin Société géologique de France 4, 119–127.
1396 Pellat, E., Cossmann, N., 1907. Le Barrémien supérieur de Brouzet. Mémoire de la Société géologique de
1397 France, Paléontologie 25, 42 pp.
1398 Pictet, A., Delanoy, G., 2016. The Chabert Formation–a newly defined stratigraphic unit of late early Aptian age
1399 in the southern Ardèche, SE France. Archives des Sciences 69, 3–28.

1400 Pictet, A., Delanoy, G., Adatte T., Spangenberg, J.E., Baudouin, C., Boselli, P., Boselli, M., Kindler, P., Föllmi,
1401 K.B., 2015. Three successive phases of platform demise during the early Aptian and their association with
1402 the oceanic anoxic Selli episode (Ardèche, France). Palaeogeography, Palaeoclimatology, Palaeoecology
1403 418, 101–125.
1404 Pictet, A., Delamette, M., Matrion, B., 2016. The Perte-du-Rhône Formation, a new Cretaceous (Aptian–
1405 Cenomanian) lithostratigraphic unit in the Jura moutains (France and Switzerland). Swiss Journal of
1406 Geosciences 109, 20 pp.
1407 Puzos, M., 1832. Sur le *Scaphites Yvani*. Bulletin de la Société Géologique de la France, Paris 2, 355–356.
1408 Raddadi, M.C., 2005. Étude de la nature de la radioactivité gamma dans les roches carbonatées de plate-forme:
1409 analyses et interprétations environnementales, diagénétiques et géodynamiques. Géologie Alpine,
1410 Mémoire Haute Série 45, 164 pp.
1411 Reboulet, S., Rawson, P.F., Moreno-Bedmar, J.A., Aguirre-Urreta, M.B., Barragán, R., Bogomolov, Y.,
1412 Company, M., González-Arreola, C., Idakieva Stoyanova, V., Lukeneder, A., Matrion, B., Mitta, V.,
1413 Randrianaly, H., Vasícek, Z., Baraboshkin, E.J., Bert, D., Bersac, S., Bogdanova, T.N., Bulot, L.G., Latil,
1414 J.-L., Mikhailova, I.A., Ropolo, P., Szives, O., 2011. Report on the 4th International Meeting of the IUGS
1415 Lower Cretaceous Ammonite Working Group, the "Kilian Group" (Dijon, France, 30th August 2010).
1416 Cretaceous Research 32, 786–793.
1417 Reboulet, S., Szives, O., Aguirre-Urreta, B., Barragán, R., Company, M., Idakieva, V., Ivanov, M., Kakabadze,
1418 M.V., Moreno-Bedmar, J.A., Sandoval, J., Baraboshkin, E.J., Çağlar, M.K., Főzy, I., González-Arreola,
1419 C., Kenjo, S., Lukeneder, A., Raisossadat, S.N., Rawson, P.F., Tavera, J.M., 2014. Report on the 5th
1420 International Meeting of the IUGS Lower Cretaceous Ammonite Working Group, the Kilian Group
1421 (Ankara, Turkey, 31st August 2013). Cretaceous Research 50, 126–137.
1422 Rouchadzé, I., 1933. Les ammonites Aptiennes de la Géorgie occidentale. Bulletin de l'Institut géologique de
1423 Géorgie 1, 165–273.
1424 Renéville, De P., Raynaud, J.F., 1981. Palynologie du stratotype du Barrémien. Bulletin des Centres de
1425 recherches Exploration–Production Elf-Aquitaine 5, 1–29.
1426 Richet, R., 2011. High resolution 3D stratigraphic modeling of the Gresse-en-Vercors Lower Cretaceous
1427 carbonate platform (SE France): from digital outcrop modeling to carbonate sedimentary system
1428 characterization. (Thèse) Université de Provence, 175 pp.

1429 Rivier, F., 1960. Étude géologique des Monts de Vaucluse. Rapport COPEFA, Dept. Exploration Bassin
1430 Rhodanien, 1–31.
1431 Ropolo, P., Gonnet, R., Conte, G., 1999. The "*Pseudocrioceras* interval" and adjacent beds at La Bédoule (SE
1432 France): implications for highest Barremian/lowest Aptian biostratigraphy. Scripta Geologica, Special
1433 Issue 3, 159–213.
1434 Ropolo, P., Gonnet, R., Conte, G., 2000a. Le genre *Pseudocrioceras* dans les couches de passage du Barrémien
1435 supérieur/Bédoulien inférieur de Cassis–La Bédoule (SE France). Géologie Mediterranéenne XXV, 3-4
1436 (1998), 85–123.
1437 Ropolo, P., Conte, G., Gonnet, R., Masse, J.-P., Moullade, M., 2000b. Les faunes d'Ammonites du Barrémien
1438 supérieur/Aptien inférieur (Bédoulien) dans la région stratotypique de Cassis–La Bédoule (SE de la
1439 France): état des connaissances et propositions pour une zonation par Ammonites du Bédoulien type.
1440 Géologie Mediterranéenne XXV, 3-4 (1998), 167–175.
1441 Ropolo, P., Moullade, M., Gonnet, R., Conte, G., Tronchetti, G., 2006. The Deshayesitidae Stoyanov, 1949
1442 (Ammonoidea) of the Aptian stratotype region at Cassis-la Bédoule (SE France). Carnets de Géologie /
1443 Notebooks on Geology, Brest, Memoir 2006/01 (CG2006_M01), 46 pp.
1444 Sarkar, S., 1955. Révision des ammonites déroulées du Crétacé inferieur du Sud-est de la France. Mémoires de
1445 la Société géologique de France, Serie 5, Mémoire 72, 1–176.
1446 Scholle, P.A., Arthur, M.A., 1980. Carbon isotope fluctuations in Cretaceous pelagic limestones: Potential
1447 stratigraphic and petroleum exploration tool: American Association of Petroleum Geologists Bulletin 64,
1448 67–87.
1449 Spath, L.F., 1922. On Cretaceous Ammonoidea from Angola, collected by Professor J. W. Gregory, D.Sc.,
1450 F.R.S. Transactions of the Royal Society of Edinburgh 53, 91–160.
1451 Spath, L.F., 1923. A monograph of the Ammonoidea of the Gault (1923-1943), part I. Palaeontographical
1452 Society (1921), 1–72.
1453 Spath, L.F., 1924. On the ammonites of the Speeton Clay and the subdivisions of the Neocomian. Geological
1454 Magazine 61, 73–89.
1455 Stein, M., Föllmi, K.B., Westermann, S., Godet, A., Adatte, T., Matera, V., Fleitmann, D., Berner, Z., 2011.
1456 Progressive palaeoenvironmental change during the Late Barremian–Early Aptian as prelude to Oceanic
1457 Anoxic Event 1a: evidence from the Gorgo a Cerbara section (Umbria–Marche basin, central Italy).
1458 Palaeogeography, Palaeoclimatology, Palaeoecology 302, 396–406.

1459 Stein, M., Arnaud-Vanneau, A., Adatte, T., Fleitmann, D., Spangenberg, J.E., Föllmi, K., 2012a.
1460 Palaeoenvironmental and palaeoecological change on the northern Tethyan carbonate platform during the
1461 Late Barremian to earliest Aptian. Sedimentology 59, 939–963.
1462 Stein, M., Westermann, S., Adatte, T., Matera, V., Fleitmann, D., Spangenberg, J.E., Föllmi, K.B., 2012b. Late
1463 Barremian–Early Aptian palaeoenvironmental change: The Cassis–La Bédoule section, southeast France.
1464 Cretaceous Research 37, 209–222.
1465 Stoyanow, A. 1949. Lower Cretaceous stratigraphy in southern Arizona. Geological Society of America
1466 Memoir, 38, 169 p.
1467 Tendil, A.J.-B., Frau, C., Léonide, P., Fournier, F., Borgomano, J.R., Lanteaume, C., Masse, J.-P., Massonnat,
1468 G., Rolando, J.-R., accepted. Platform-to-basin anatomy of a Barremian–Aptian Tethyan carbonate
1469 system: new insights into the regional to global factors controlling the stratigraphic architecture of the
1470 Urgonian Provence platform (Southeast France). Cretaceous Research.
1471 Thieuloy, J.-P., 1979. *Matheronites limentinus* n. sp. (Ammonoidea) espèce-type d'un horizon-repère Barrémien
1472 supérieur du Vercors Méridional (Massif subalpin Français). Géobios, Mémoire spécial 3, 305–317.
1473 Thieuloy, J.-P., Girod, J.-P., 1964. L'Aptien et l'Albien fossilifères du synclinal d'Autrans (Vercors
1474 septentrional). Travaux du Laboratoire de Géologie de la Faculté des Sciences de Grenoble 40, 91–111.
1475 Vermeulen, J., 2005. Boundaries, ammonite fauna and main subdivisions of the stratotype of the Barremian. In:
1476 Adatte, T., Arnaud-Vanneau, A., Arnaud, H., Blanc-Aletru, M.-C., Bodin, S., Carrio-Schaffauser, E.,
1477 Föllmi, K., Godet, A., Raddadi, M.C., Vermeulen, J. 2005. The Hauterivian lower Aptian sequence
1478 stratigraphy from Jura platform to Vocontian basin: a multidisciplinary approach. Field-trip of the 7th
1479 International symposium on the Cretaceous (September 1–4, 2005). Géologie Alpine, Colloques et
1480 excursions 7, 181 pp.
1481 Vermeulen, J., Arnaud, H., Arnaud-Vanneau, A., Lahondere, J.-C., Lepinay, P., Massonnat, G., 2013.
1482 L'Hauterivien supérieur et le Barrémien inférieur de la région de Seynes et Belvézet (Gard). Annales du
1483 Muséum D'Histoire Naturelle de Nice 28, 1–16.
1484 Westermann, S., Stein, M., Matera, V., Fiet, N., Fleitmann, D., Adatte, T., Föllmi, K.B., 2013. Rapid changes in
1485 the redox conditions of the western Tethys Ocean during the early Aptian oceanic anoxic event.
1486 Geochimica et Cosmochimica Acta 121, 467–486.
1487 Wissler, L., Weissert, H., Masse, J.P., Bulot, L., 2002. Chemostratigraphic correlation of Barremian and lower
1488 Aptian ammonite zones and magnetic reversals. International Journal of Earth Sciences 91, 272–279.

Wissler, L., Funk, H., Weissert, H., 2003. Response of Early Cretaceous carbonate platforms to changes in atmospheric carbon dioxide levels. Palaeogeography, Palaeoclimatology, Palaeoecology 200, 187–205.

Zittel, K.A. Von, 1895. Grundzüge der Paläontologie (Paläozoologie). Munich and Leipzig, vii + 972 pp.

Figure list

Fig. 1. The standard Mediterranean ammonite zonation of the upper Hauterivian *pro parte* to lower Aptian (Reboulet et al., 2014) and the Vocontian depositional sequences (Arnaud, 2005b).

Fig. 2. Contrasting stratigraphic interpretations of the Urgonian-type lithostratigraphy – U^1, U^2 *sensu lato* and U^3 units *sensu* Leenhardt (1883) – with respect to the Barremian and Aptian stages.

Fig. 3. Regional extension of the Barremian–Aptian deposits in SE France and location of the surveyed outcrops and transects (see Fig. 5, 6 and 7). A detailed description of each sections can be found in the joint contribution of Tendil et al. (accepted).

Fig. 4. Temporal schematic evolution of the Provence platform during the Barremian–Aptian transition. A. lower Barremian, B. *T. vandenheckii–G. sartousiana pars* zones interval, C. upper *G. sartousiana* Zone, D. *I. giraudi* Zone, E. lower *M. sarasini* Zone, F. upper *M. sarasini–D. forbesi pars* zones interval, G. from the upper *D. forbesi* Zone.

Fig. 5. Platform-to-basin correlations of the eight ammonite bioevents of the Provence domain between Cassis–Roquefort-la-Bédoule and Brantes. The late Barremian regional drowning event, associated to the *Heteroceras* bioevent, is used as datum (flattening surface) for this cross section. Facies types are according to the joint contribution of Tendil et al. (accepted).

Fig. 6. Platform-to-basin correlations of the eight ammonite bioevents of the Provence domain between Cassis–Roquefort-la-Bédoule and Savoillan. The late Barremian regional drowning event, associated to the *Heteroceras* ammonite bioevent, is used as datum (flattening surface) for this cross section. Facies types are according to the joint contribution of Tendil et al. (accepted).

Fig. 7. Platform-to-basin correlations of the eight ammonite bioevents of the Provence domain between Cassis–Roquefort-la-Bédoule and Baudinard. The late Barremian regional drowning event, associated to the *Heteroceras* bioevent, is used as datum (flattening surface) for this cross section. Facies types are according to the joint contribution of Tendil et al. (accepted).

Fig. 8. Selected ammonites from the *Toxancyloceras vandenheckii* bioevent: *Moutoniceras* sp. – A–B. FSL.85850; *T. vandenheckii* – C. MPP-M-MV.8 from Mont Ventoux; *Toxancyloceras* sp. – D–E. MPP-A.45 (Masse *in* Frau coll.) from Roque Pourquière (Fontaine-de-Vaucluse). All specimens x1 except A x0.7.

Fig. 9. Selected ammonites from the first (A–D) and second (E–G) *Martelites* bioevent: *Kutatissites* sp. gr. *chreithiensis* (= *Ancyloceras* gr. *matheronianum in* Arnaud et al., 1998) – A–B. UJF-ID.10590 from the Lower *Orbitolina* Beds of the Subalpine platform (Roche Blanche, Chartreuse). *Kutatissites* sp. gr. *chreithiensis* – C–D. MPP-V-SC.c1 from Saint-Christol; *Pseudocrioceras* sp. – E–G. MPP-A.113 from Conque Verte (Gorges de La Nesque). All specimens x0.7.

Fig. 10. Selected ammonites from the *Camereiceras limentinum* bioevent: *Camereiceras limentinum* – A. MPP-M-MV.6 (plaster cast), B–C. MPP-M-MV.9 and H–I. MPP-A.102; *Janusites janus* – D–E. MPP-M-MV.2; *Gerhardtia galeatoides* – F. MPP-M-MV.16 (plaster cast) and G. MPP-M-MV.14. All specimens from Mont Ventoux except H–I from La Redde (Gorges de La Nesque). All specimens x1.

Fig. 11. Selected ammonites from the *Hemihoplites feraudianus* (A–C) and *Heteroceras* (D–G) bioevents: *Hemihoplites* sp. gr. *feraudianus* – A–B. MPP-A.14335 and C. MPP-SC.1 from Saint-Chamas; *Imerites giraudi* – D. MPP-APH.BAU.R28.1.1 from Baudinard and E–F. FSL.85837(80) from Sault; *Heteroceras emericianum* – D. FSL.85842(86) from Sault. All specimens x1.

Fig. 12. Selected ammonites from the first *Martelites* bioevent: *Martelites* gr. *sarasini–marteli* – A. FSL.105070 from Cassis–Roquefort-la-Bédoule, B–C. MPP-APH-BAU.R33.2 from Baudinard; D. MPP-V-BR.1 from Brantes. All specimens x1.

Fig. 13. Selected ammonites from the first *Martelites* bioevent: *Martelites* gr. *sarasini–marteli* – A–B. MPP-BAN.3 from Banon and C. MPP-V-SC.AA.1 from Azé Aven (Saint-Christol). All specimens x1.

Fig. 14. Selected ammonites from the second *Martelites* bioevent: *Martelites* gr. *sarasini–marteli* – A–B. MPP-V-BAN.BRX.1 from Banon, C–D. MPP-FSL.64209 from Mont Ventoux; E. MPP-V-MS.1 (plaster cast) from Montsalier and F. MPP-V-SV.1 (plaster cast) from Savoillan; *Martelites* sp. – E–F. MPP-A.88 from Simiane-la-Rotonde. All specimens x1.

Fig. 15. Selected ammonites from the first *Deshayesites* bioevent: *Deshayesites* sp. aff. *euglyphus* – A. MPP-B-VC.20 (bed 107), B. MPP-B-EM.250 and ?C. MPP-B-VC.24 (bed 107) from Cassis–Roquefort-la-Bédoule; *Deshayesites* gr. *luppovi* – D. MPP-B-VC.15 (bed 107), E. MPP-B-VC.25 (bed 107) from Cassis–Roquefort-la-Bédoule and ?F. *in situ* from Savoillan; *Deshayesites* sp. – G–H. MPP-V-FDV.1 from Fontaine-de-Vaucluse; *Pseudohaploceras matheroni* – I–J. MPP-V-PF.2 and *Macroscaphites yvani* – K–L. MPP-V-PF.3 from Petit Fribouquet. All specimens x1 except G–H x2.

Fig. 16. Selected ammonites from the first *Martelites* (A-B) and first *Deshayesites* (C) bioevents: *Procheloniceras* sp. gr. *sporadicum* – A–B. MPP.A.17 from Sault; *Procheloniceras* sp. gr. *dechauxi* – C. MPP-V-PF.1 from Petit Fribouquet. All specimens x0.75.

Fig. 17. Ammonite age-calibration of the North Provence Urgonian- and Aptian-type series developed in the present contribution and the previous interpretation (Masse, 1993, 1995; Masse & Fenerci-Masse, 2011, 2013a-c; Léonide et al., 2012, 2014).

Fig. 18. Revised litho-, bio- and chemostratigraphic correlations between type basinal sections of the South Provence (Cassis–Roquefort-la-Bédoule) and Vocontian basins (Angles–Combe Lambert–Glaise) and the southern Monts de Vaucluse platform series. Note that the demise of the Urgonian rudistid regime and its *Palorbitolina*-rich cover occurs long before the spreading (C2 *pro parte* – C3 isotopic carbon segments) and culmination (C3 *pro parte* – C6 isotopic carbon segments) of the OAE 1a. Scale bar is 5 m.

1578 Fig. 19. Revised ammonite age-calibration of the Urgonian Bas-Vivarais platform and comparison with previous
1579 datings (Clavel et al., 2007, 2013, 2014; Pictet et al., 2015).
1580
1581 Fig. 20. Revised ammonite age-calibration of the Urgonian Subalpine platform and comparison with previous
1582 datings (Clavel et al., 2007, 2013, 2014; Pictet et al., 2015).

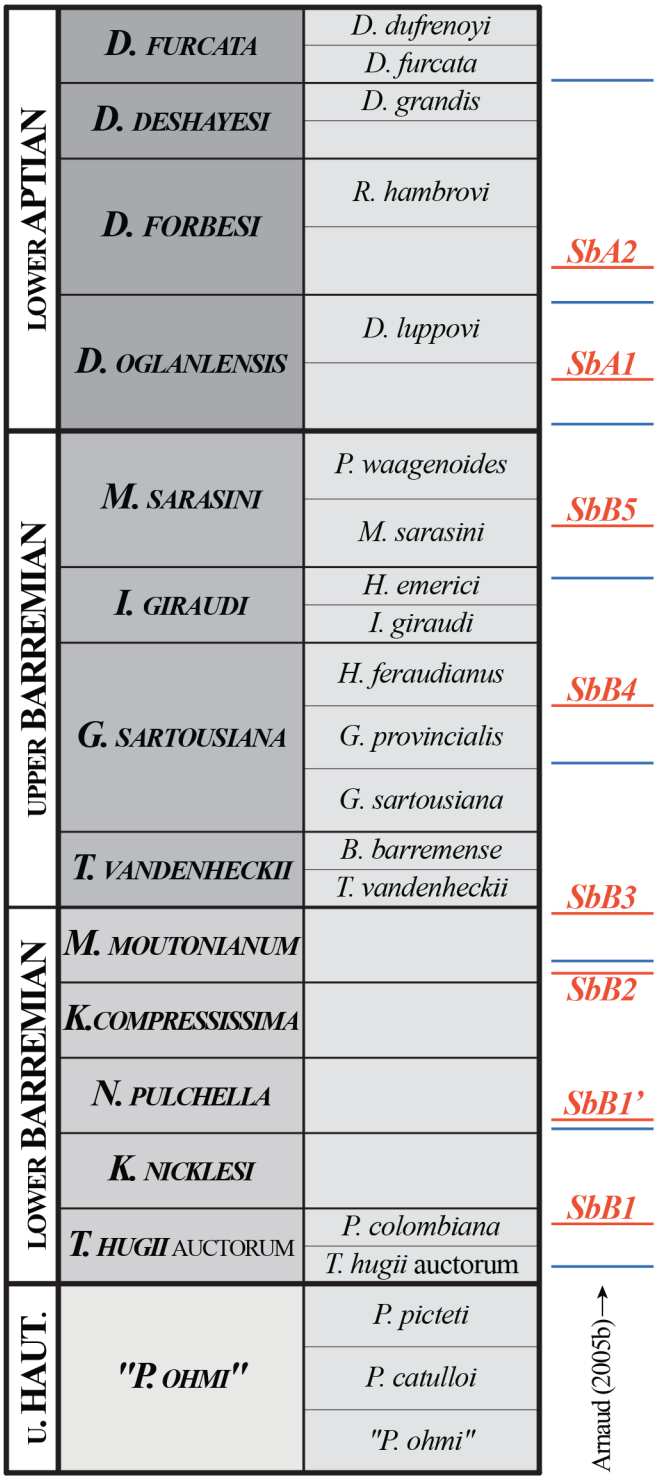
LOWER APTIAN
D. FURCATA
D. dufrenoyi
D. furcata
D. DESHAYESI
D. grandis
D. FORBESI
R. hambrovi
SbA2
D. OGLANLENSIS
D. luppovi
SbA1
UPPER BARREMIAN
M. SARASINI
P. waagenoides
M. sarasini
SbB5
I. GIRAUDI
H. emerici
I. giraudi
G. SARTOUSIANA
H. feraudianus
SbB4
G. provincialis
G. sartousiana
T. VANDENHECKII
B. barremense
T. vandenheckii
SbB3
LOWER BARREMIAN
M. MOUTONIANUM
SbB2
K.COMPRESSISSIMA
N. PULCHELLA
SbB1'
K. NICKLESI
SbB1
T. HUGII AUCTORUM
P. colombiana
T. hugii auctorum
U. HAUT.
"P. OHMI"
P. picteti
P. catulloi
"P. ohmi"
Arnaud (2005b)

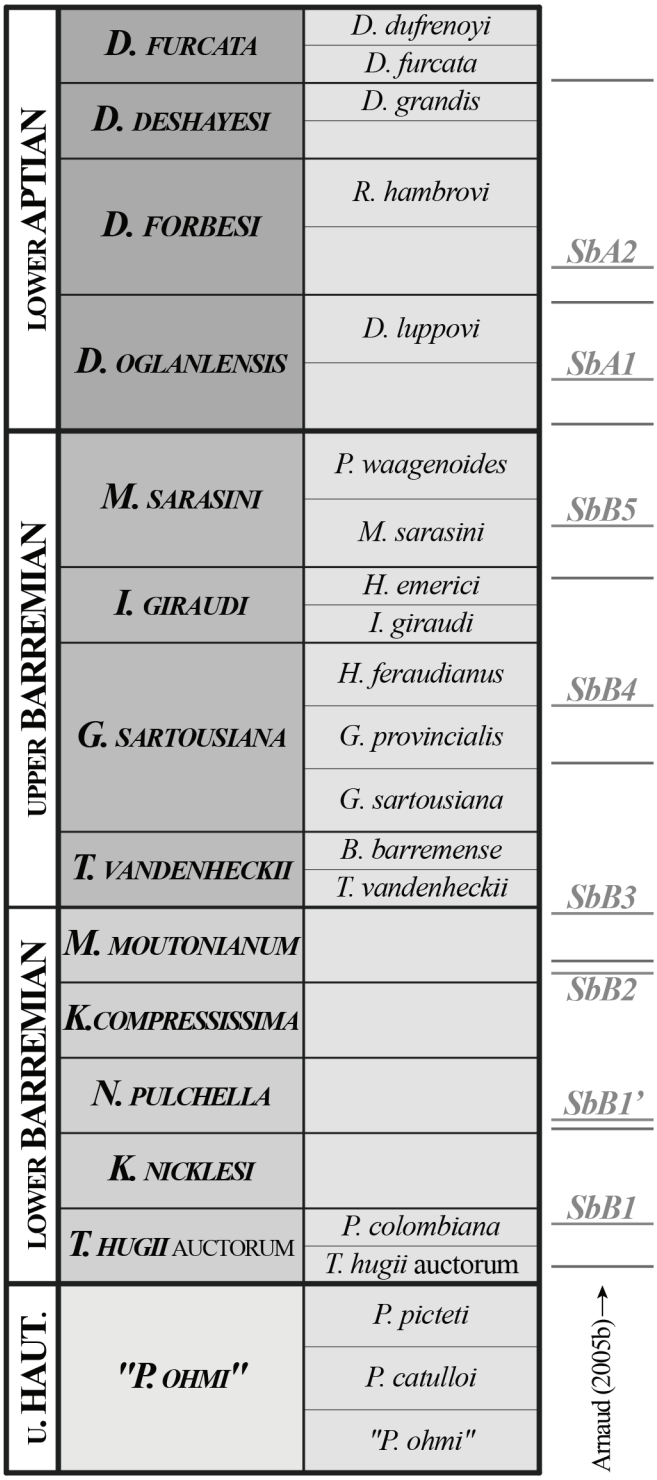
LOWER APTIAN
UPPER BARREMIAN
LOWER BARREMIAN
U. HAUT.
D. FURCATA
D. DESHAYESI
D. FORBESI
D. OGLANLENSIS
M. SARASINI
I. GIRAUDI
G. SARTOUSIANA
T. VANDENHECKII
M. MOUTONIANUM
K.COMPRESSISSIMA
N. PULCHELLA
K. NICKLESI
T. HUGII AUCTORUM
"P. OHMI"
D. dufrenoyi
D. furcata
D. grandis
R. hambrovi
D. luppovi
P. waagenoides
M. sarasini
H. emerici
I. giraudi
H. feraudianus
G. provincialis
G. sartousiana
B. barremense
T. vandenheckii
P. colombiana
T. hugii auctorum
P. picteti
P. catulloi
"P. ohmi"
SbA2
SbA1
SbB5
SbB4
SbB3
SbB2
SbB1'
SbB1
Arnaud (2005b)

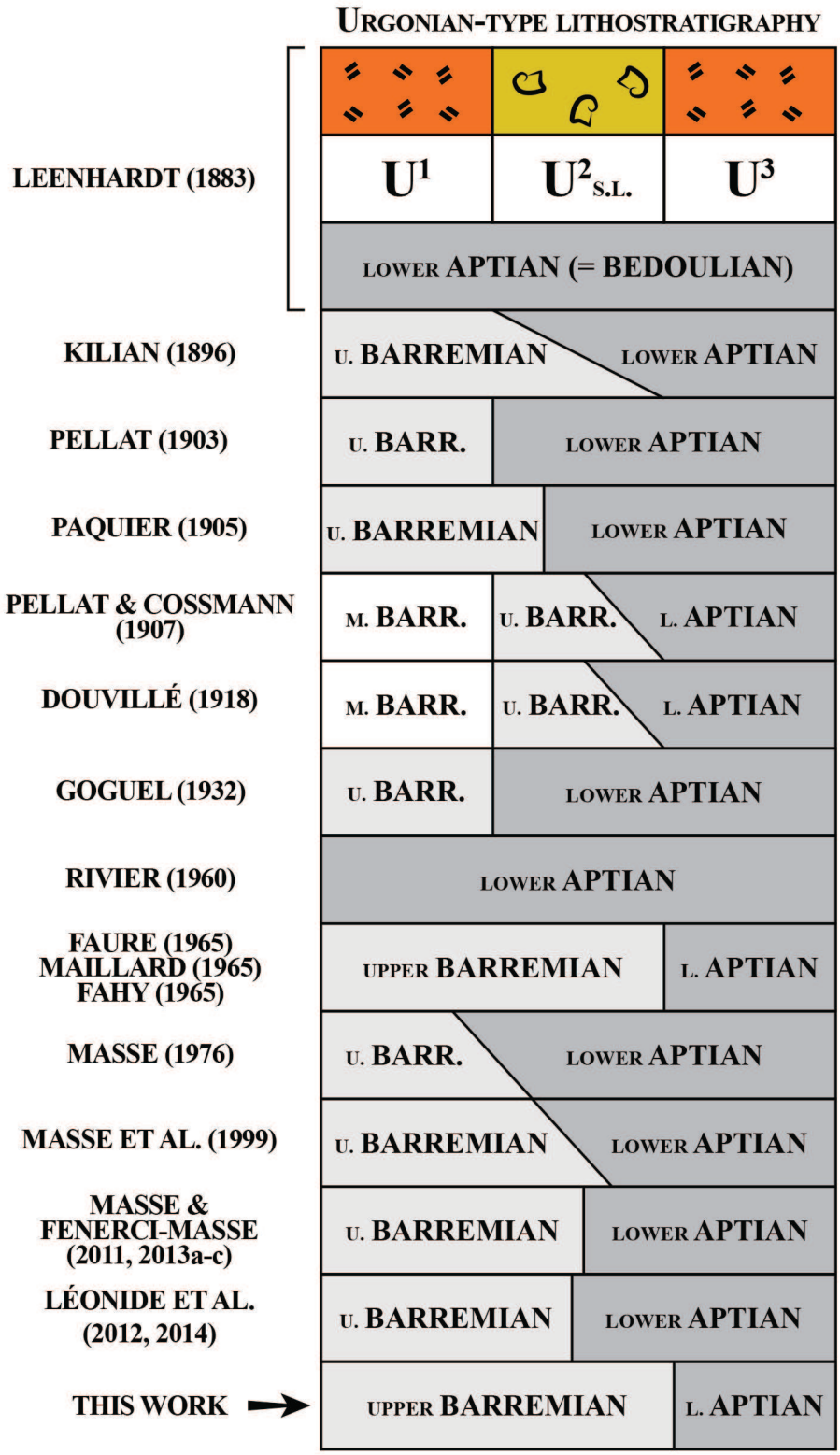
URGONIAN-TYPE LITHOSTRATIGRAPHY
LEENHARDT (1883)
U1
U2S.L.
U3
LOWER APTIAN (= BEDOULIAN)
KILIAN (1896)
U. BARREMIAN
LOWER APTIAN
PELLAT (1903)
U. BARR.
LOWER APTIAN
PAQUIER (1905)
U. BARREMIAN
LOWER APTIAN
PELLAT & COSSMANN (1907)
M. BARR.
U. BARR.
L. APTIAN
DOUVILLÉ (1918)
M. BARR.
U. BARR.
L. APTIAN
GOGUEL (1932)
U. BARR.
LOWER APTIAN
RIVIER (1960)
LOWER APTIAN
FAURE (1965)
MAILLARD (1965)
FAHY (1965)
UPPER BARREMIAN
L. APTIAN
MASSE (1976)
U. BARR.
LOWER APTIAN
MASSE ET AL. (1999)
U. BARREMIAN
LOWER APTIAN
MASSE & FENERCI-MASSE (2011, 2013a-c)
U. BARREMIAN
LOWER APTIAN
LÉONIDE ET AL. (2012, 2014)
U. BARREMIAN
LOWER APTIAN
THIS WORK
UPPER BARREMIAN
L. APTIAN

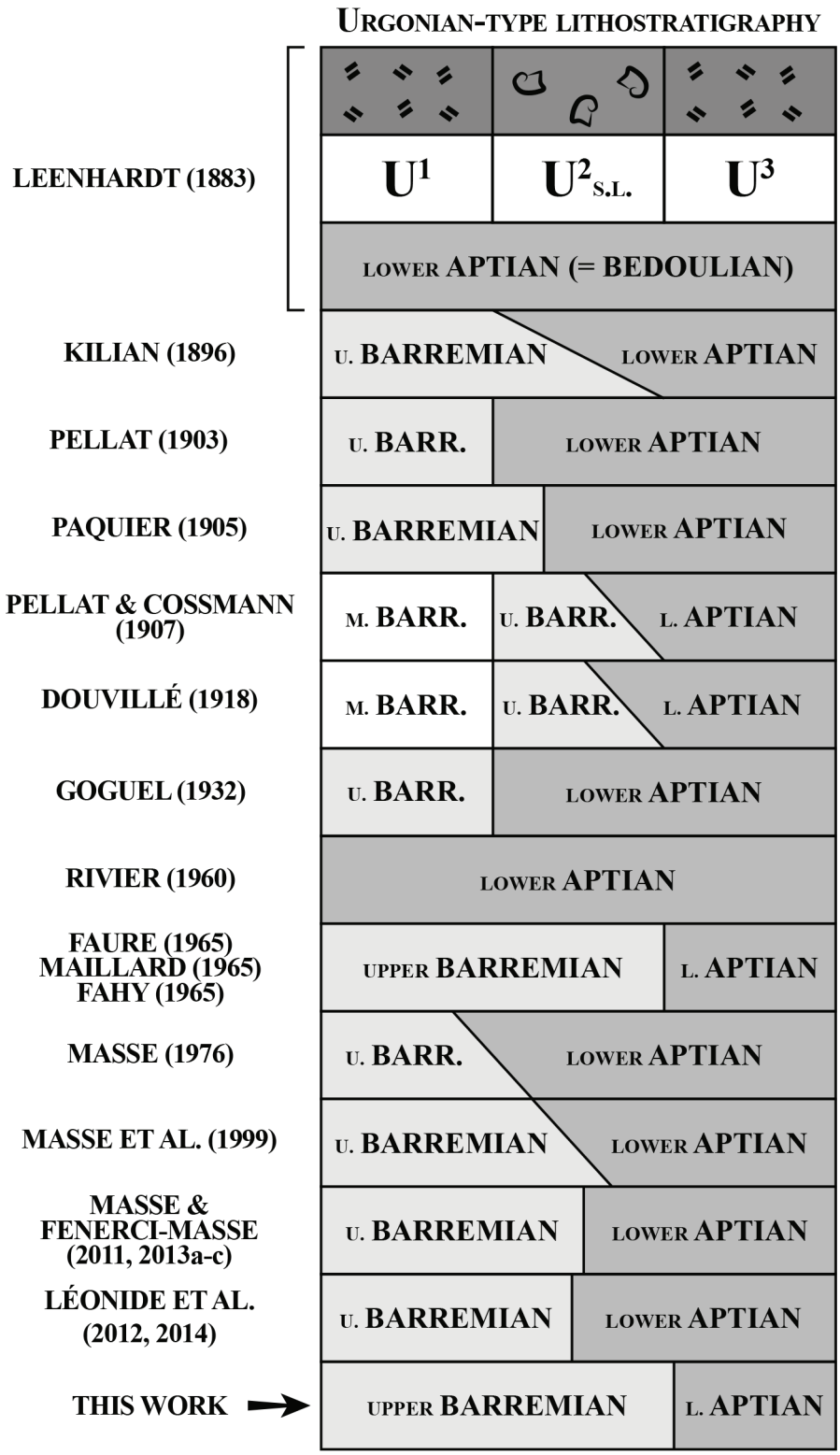
URGONIAN-TYPE LITHOSTRATIGRAPHY
LEENHARDT (1883)
U1
U2S.L.
U3
LOWER APTIAN (= BEDOULIAN)
KILIAN (1896)
U. BARREMIAN
LOWER APTIAN
PELLAT (1903)
U. BARR.
LOWER APTIAN
PAQUIER (1905)
U. BARREMIAN
LOWER APTIAN
PELLAT & COSSMANN (1907)
M. BARR.
U. BARR.
L. APTIAN
DOUVILLÉ (1918)
M. BARR.
U. BARR.
L. APTIAN
GOGUEL (1932)
U. BARR.
LOWER APTIAN
RIVIER (1960)
LOWER APTIAN
FAURE (1965)
MAILLARD (1965)
FAHY (1965)
UPPER BARREMIAN
L. APTIAN
MASSE (1976)
U. BARR.
LOWER APTIAN
MASSE ET AL. (1999)
U. BARREMIAN
LOWER APTIAN
MASSE & FENERCI-MASSE (2011, 2013a-c)
U. BARREMIAN
LOWER APTIAN
LÉONIDE ET AL. (2012, 2014)
U. BARREMIAN
LOWER APTIAN
THIS WORK
UPPER BARREMIAN
L. APTIAN

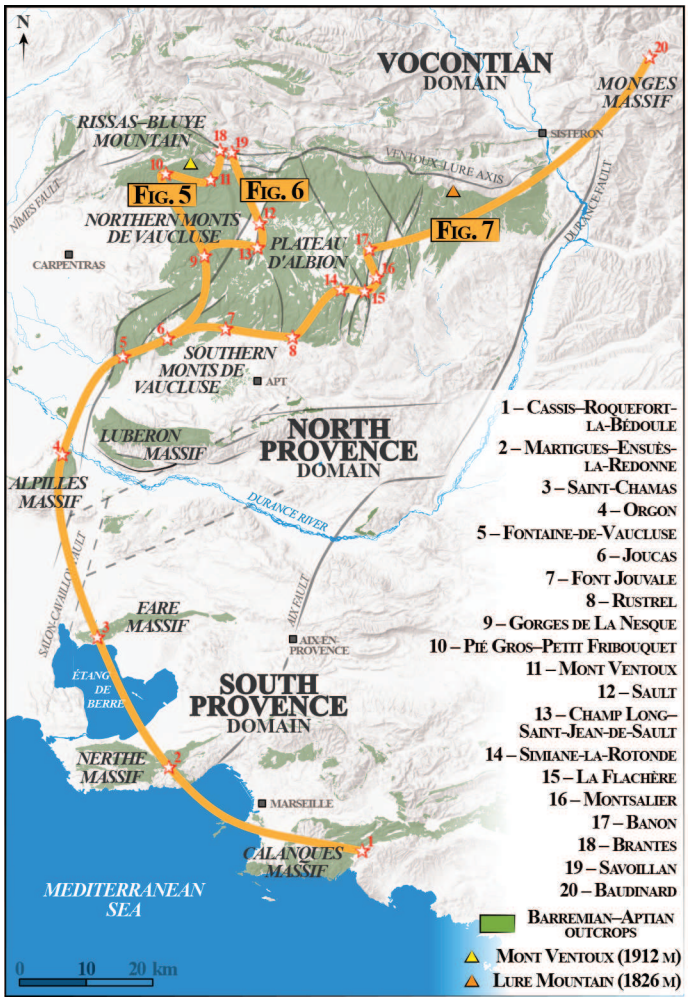
N
VOCONTIAN
DOMAIN
MONGES
MASSIF
SISTERON
RISSAS–BLUYE
MOUNTAIN
VENTOUX-LURE AXIS
NÎMES FAULT
DURANCE FAULT
FIG. 5
FIG. 6
FIG. 7
NORTHERN MONTS
DE VAUCLUSE
PLATEAU
D'ALBION
CARPENTRAS
SOUTHERN
MONTS DE
VAUCLUSE
APT
LUBERON
MASSIF
NORTH
PROVENCE
DOMAIN
ALPILLES
MASSIF
DURANCE RIVER
SALON-CAVAILLON FAULT
ARC FAULT
FARE
MASSIF
AIX-EN-
PROVENCE
ÉTANG
DE
BERRE
SOUTH
PROVENCE
DOMAIN
NERTHE
MASSIF
MARSEILLE
CALANQUES
MASSIF
MEDITERRANEAN
SEA
0 10 20 km
1 – CASSIS–ROQUEFORT-LA-BÉDOULE
2 – MARTIGUES–ENSUÈS-LA-REDONNE
3 – SAINT-CHAMAS
4 – ORGON
5 – FONTAINE-DE-VAUCLUSE
6 – JOUCAS
7 – FONT JOUVALE
8 – RUSTREL
9 – GORGES DE LA NESQUE
10 – PIÉ GROS–PETIT FRIBOUQUET
11 – MONT VENTOUX
12 – SAULT
13 – CHAMP LONG–SAINT-JEAN-DE-SAULT
14 – SIMIANE-LA-ROTONDE
15 – LA FLACHÈRE
16 – MONTSALIER
17 – BANON
18 – BRANTES
19 – SAVOILLAN
20 – BAUDINARD
BARREMIAN–APTIAN OUTCROPS
MONT VENTOUX (1912 M)
LURE MOUNTAIN (1826 M)

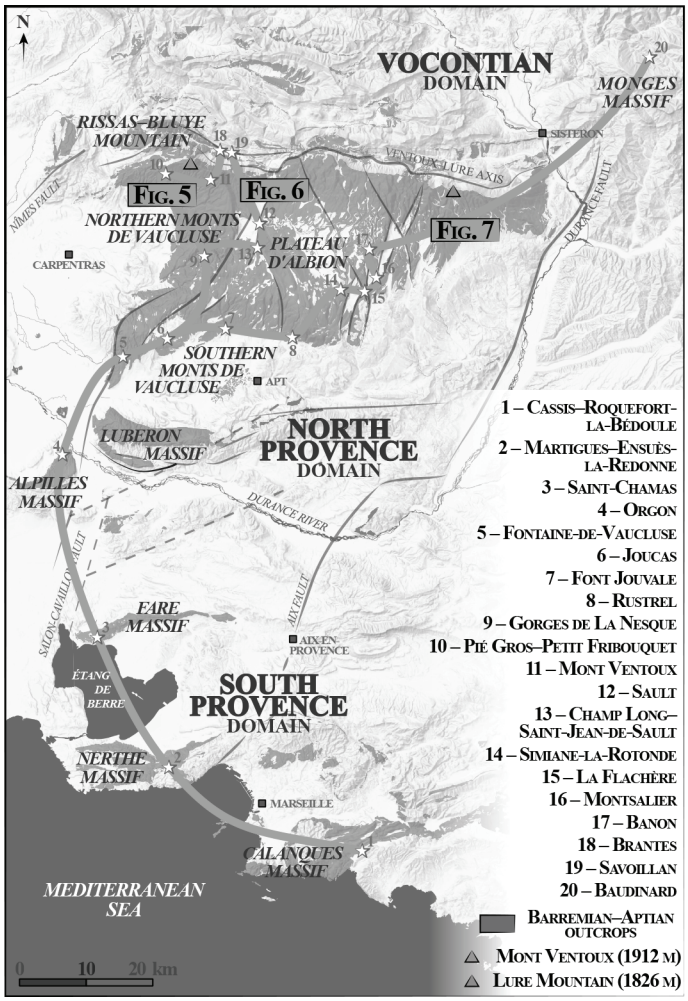
N
VOCONTIAN DOMAIN
MONGES MASSIF
RISSAS–BLUYE MOUNTAIN
SISTERON
VENTOUX-LURE AXIS
DURANCE FAULT
NÎMES FAULT
FIG. 5
FIG. 6
FIG. 7
NORTHERN MONTS DE VAUCLUSE
PLATEAU D'ALBION
CARPENTRAS
SOUTHERN MONTS DE VAUCLUSE
APT
LUBERON MASSIF
NORTH PROVENCE DOMAIN
ALPILLES MASSIF
DURANCE RIVER
SALON-CAVAILLON FAULT
AIX FAULT
FARE MASSIF
AIX-EN-PROVENCE
ÉTANG DE BERRE
SOUTH PROVENCE DOMAIN
NERTHE MASSIF
MARSEILLE
CALANQUES MASSIF
MEDITERRANEAN SEA
0 10 20 km
1 – CASSIS–ROQUEFORT-LA-BÉDOULE
2 – MARTIGUES–ENSUÈS-LA-REDONNE
3 – SAINT-CHAMAS
4 – ORGON
5 – FONTAINE-DE-VAUCLUSE
6 – JOUCAS
7 – FONT JOUVALE
8 – RUSTREL
9 – GORGES DE LA NESQUE
10 – PIÉ GROS–PETIT FRIBOUQUET
11 – MONT VENTOUX
12 – SAULT
13 – CHAMP LONG–SAINT-JEAN-DE-SAULT
14 – SIMIANE-LA-ROTONDE
15 – LA FLACHÈRE
16 – MONTSALIER
17 – BANON
18 – BRANTES
19 – SAVOILLAN
20 – BAUDINARD
BARREMIAN–APTIAN OUTCROPS
MONT VENTOUX (1912 M)
LURE MOUNTAIN (1826 M)

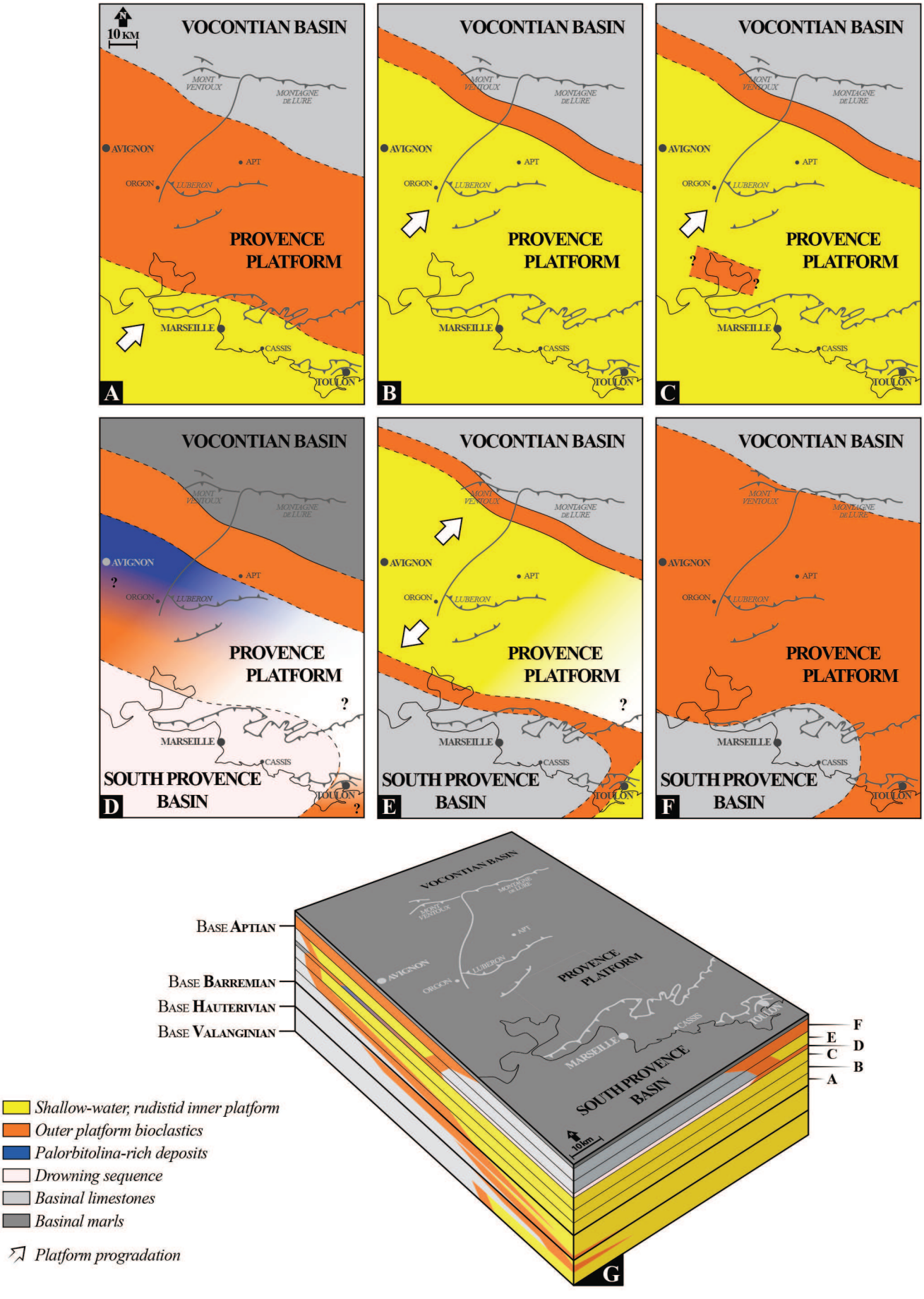
VOCONTIAN BASIN
PROVENCE PLATFORM
SOUTH PROVENCE BASIN
MONT VENTOUX
MONTAGNE DE LURE
AVIGNON
APT
ORGON
LUBERON
MARSEILLE
CASSIS
TOULON
10 KM
A
B
C
D
E
F
G
BASE APTIAN
BASE BARREMIAN
BASE HAUTERIVIAN
BASE VALANGINIAN
Shallow-water, rudistid inner platform
Outer platform bioclastics
Palorbitolina-rich deposits
Drowning sequence
Basinal limestones
Basinal marls
Platform progradation

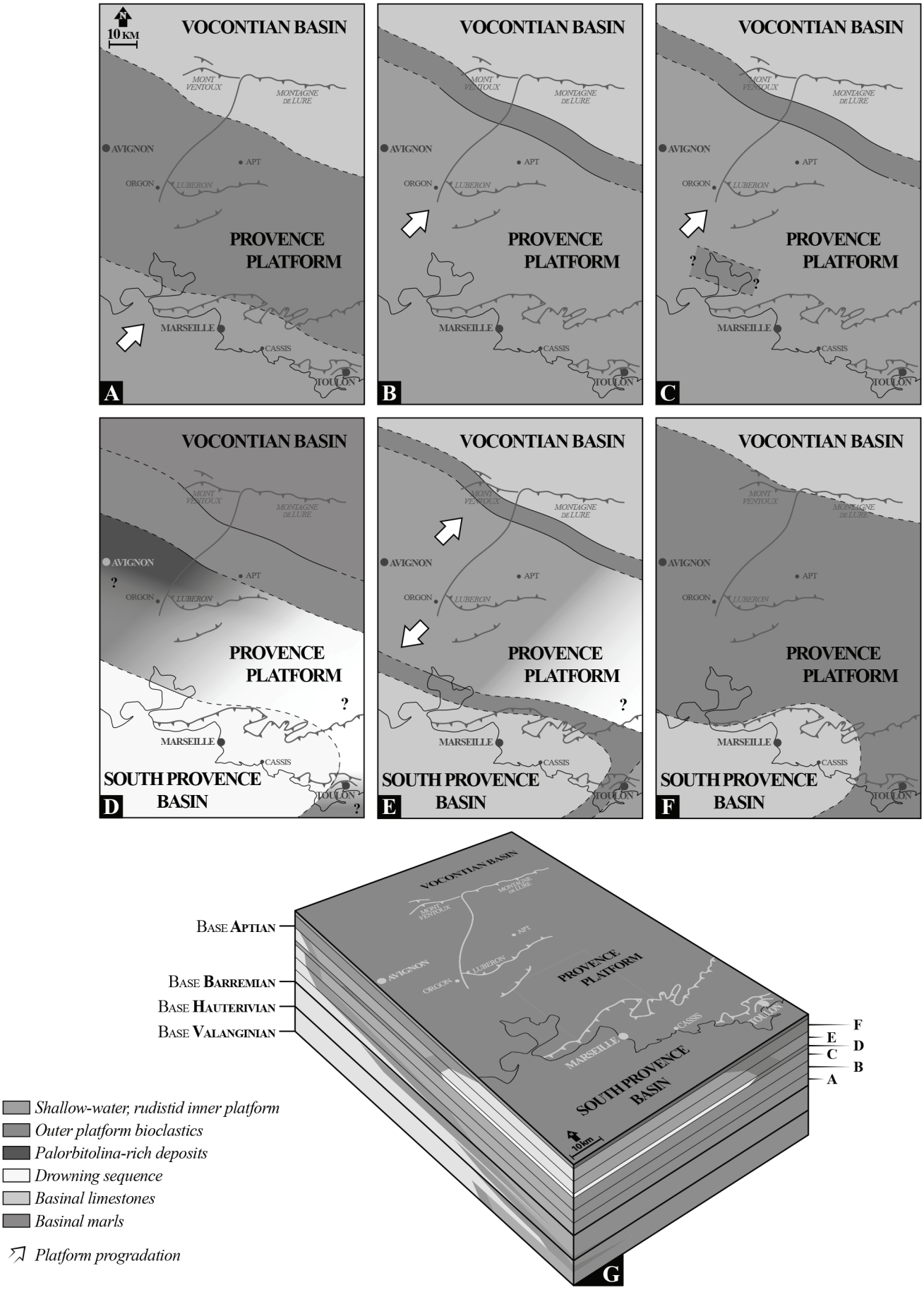
VOCONTIAN BASIN
PROVENCE PLATFORM
SOUTH PROVENCE BASIN
MONT VENTOUX
MONTAGNE DE LURE
AVIGNON
APT
ORGON
LUBERON
MARSEILLE
CASSIS
TOULON
10 KM
A
B
C
D
E
F
G
BASE APTIAN
BASE BARREMIAN
BASE HAUTERIVIAN
BASE VALANGINIAN
Shallow-water, rudistid inner platform
Outer platform bioclastics
Palorbitolina-rich deposits
Drowning sequence
Basinal limestones
Basinal marls
Platform progradation

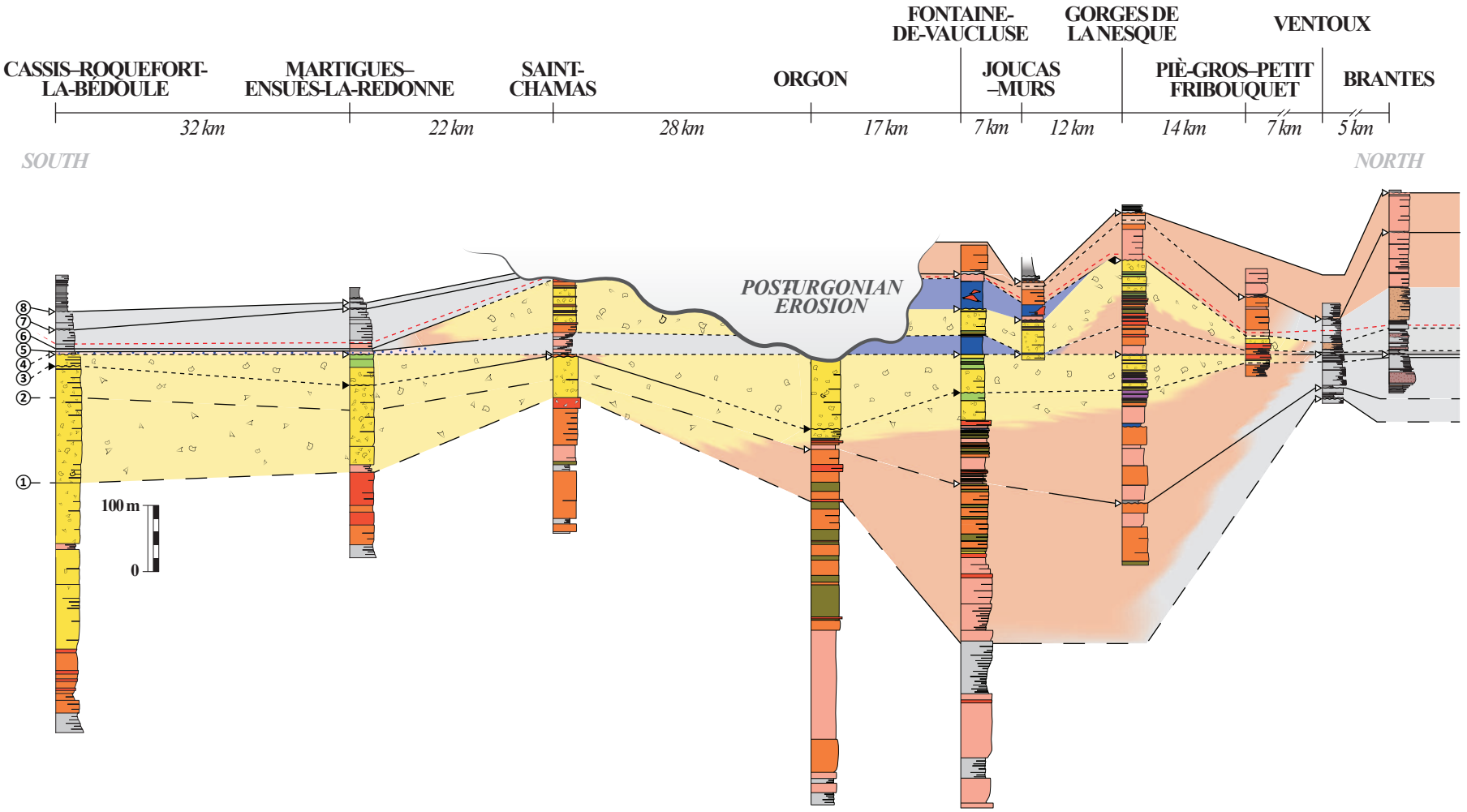
CASSIS–ROQUEFORT-LA-BÉDOULE
MARTIGUES–ENSUÈS-LA-REDONNE
SAINT-CHAMAS
ORGON
FONTAINE-DE-VAUCLUSE
JOUCAS–MURS
GORGES DE LA NESQUE
PIÈ-GROS–PETIT FRIBOUQUET
VENTOUX
BRANTES
32 km
22 km
28 km
17 km
7 km
12 km
14 km
7 km
5 km
SOUTH
NORTH
POST-URGONIAN EROSION
100 m
0
FACIES TYPES
Inner platform
Beach–fenestrate facies
Peloidal–foraminiferal facies
Rudist facies
Rudstone facies
Outer platform
Coral facies
Ooidal facies
Calcarenitic facies
Slope
Calcisiltite facies
Finely laminated calcisiltite facies
Platform-derived bioclastic facies
Basin
Basinal limestone facies
Marl facies
Gastropod-/bivalve-rich facies
Orbitolinid facies
SKELETAL & NON-SKELETAL CONSTITUENTS
Agriopleura
Requieniid–monopleurid
Caprinid
Offneria simplex (caprinid)
CHARACTERISTIC SURFACES
Subaerial exposure
Drowning surface
CORRELATIONS
Ammonite-based time line
Ammonite-derived time line
Poorly-constrained time line
Putative B/A boundary
AMMONITE BIO-EVENTS
⑧ 2nd Deshayesites bio-event
⑦ 1st Deshayesites bio-event
⑥ 2nd Martelites bio-event
⑤ 1st Martelites bio-event
④ Heteroceras bio-event
③ Hemihoplites feraudianus bio-event
② Camereiceras limentinum bio-event
① Toxancyloceras vandenheckii bio-event

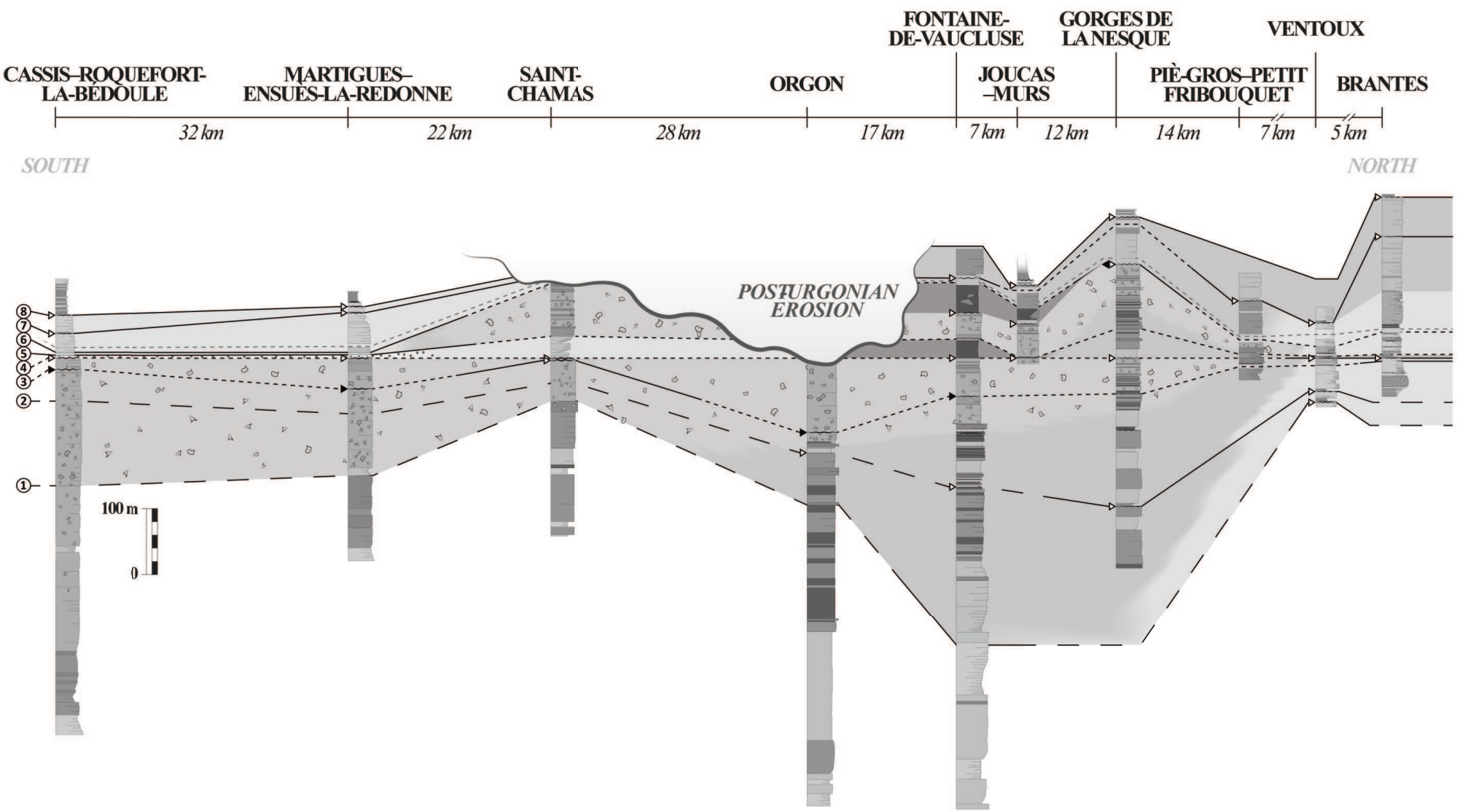
CASSIS–ROQUEFORT-LA-BÉDOULE
MARTIGUES–ENSUES-LA-REDONNE
SAINT-CHAMAS
ORGON
FONTAINE-DE-VAUCLUSE
JOUCAS–MURS
GORGES DE LA NESQUE
PIÈ-GROS–PETIT FRIBOUQUET
VENTOUX
BRANTES
32 km
22 km
28 km
17 km
7 km
12 km
14 km
7 km
5 km
SOUTH
NORTH
POSTURGONIAN EROSION
100 m
0
FACIES TYPES
Inner platform
Beach–fenestrate facies
Peloidal–foraminiferal facies
Rudist facies
Rudstone facies
Outer platform
Coral facies
Ooidal facies
Calcarenitic facies
Slope
Calcisiltite facies
Finely laminated calcisiltite facies
Platform-derived bioclastic facies
Basin
Basinal limestone facies
Marl facies
Gastropod-/bivalve-rich facies
Orbitolinid facies
SKELETAL & NON-SKELETAL CONSTITUENTS
Agriopleura
Requieniid–monopleurid
Caprinid
Offneria simplex (caprinid)
CHARACTERISTIC SURFACES
Subaerial exposure
Drowning surface
CORRELATIONS
Ammonite-based time line
Ammonite-derived time line
Poorly-constrained time line
Putative B/A boundary
AMMONITE BIO-EVENTS
⑧ 2nd Deshayesites bio-event
⑦ 1st Deshayesites bio-event
⑥ 2nd Martelites bio-event
⑤ 1st Martelites bio-event
④ Heteroceras bio-event
③ Hemihoplites feraudianus bio-event
② Camereiceras limentinum bio-event
① Toxancyloceras vandenheckii bio-event

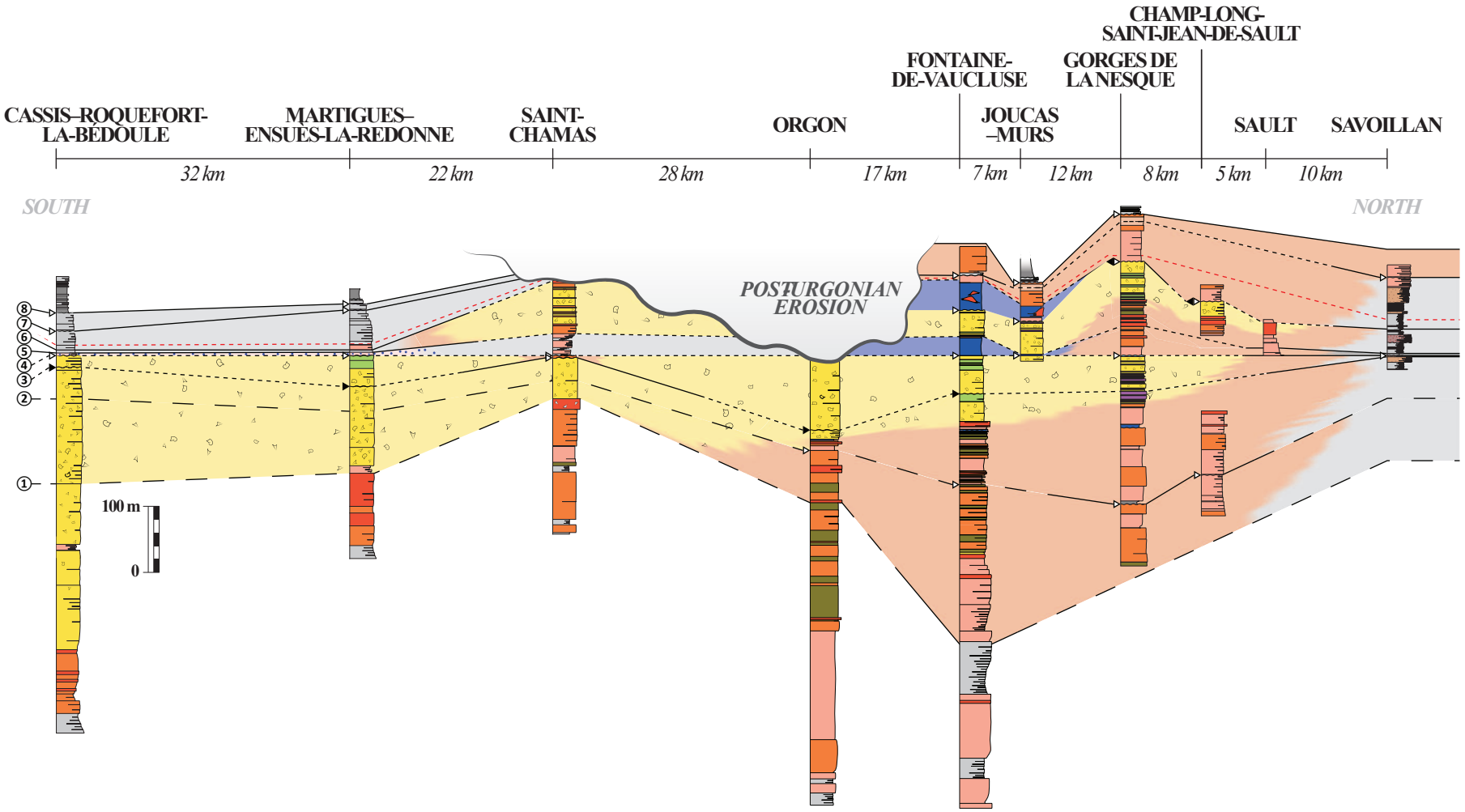

FACIES TYPES

Inner platform
- ***Beach–fenestrate*** *facies*
- ***Peloidal–foraminiferal*** *facies*
- ***Rudist*** *facies*

Outer platform
- ***Rudstone*** *facies*
- ***Coral*** *facies*
- ***Ooidal*** *facies*
- ***Calcarenitic*** *facies*

Slope
- ***Calcisiltite*** *facies*
- ***Finely laminated calcisiltite*** *facies*
- ***Platform-derived bioclastic*** *facies*

Basin
- ***Basinal limestone*** *facies*
- ***Marl*** *facies*

- ***Gastropod-/bivalve-rich*** *facies*
- ***Orbitolinid*** *facies*

SKELETAL & NON-SKELETAL CONSTITUENTS

- ***Agriopleura***
- ***Requieniid–monopleurid***
- ***Caprinid***
- ***Offneria simplex (caprinid)***

CHARACTERISTIC SURFACES

- ***Subaerial exposure***
- ***Drowning surface***

CORRELATIONS

- ***Ammonite-based time line***
- ***Ammonite-derived time line***
- ***Poorly-constrained time line***
- ***Putative B/A boundary***

AMMONITE BIO-EVENTS

⑧ ***2nd Deshayesites*** *bio-event*
⑦ ***1st Deshayesites*** *bio-event*
⑥ ***2nd Martelites*** *bio-event*
⑤ ***1st Martelites*** *bio-event*
④ ***Heteroceras*** *bio-event*
③ ***Hemihoplites feraudianus*** *bio-event*
② ***Camereiceras limentinum*** *bio-event*
① ***Toxancyloceras vandenheckii*** *bio-event*

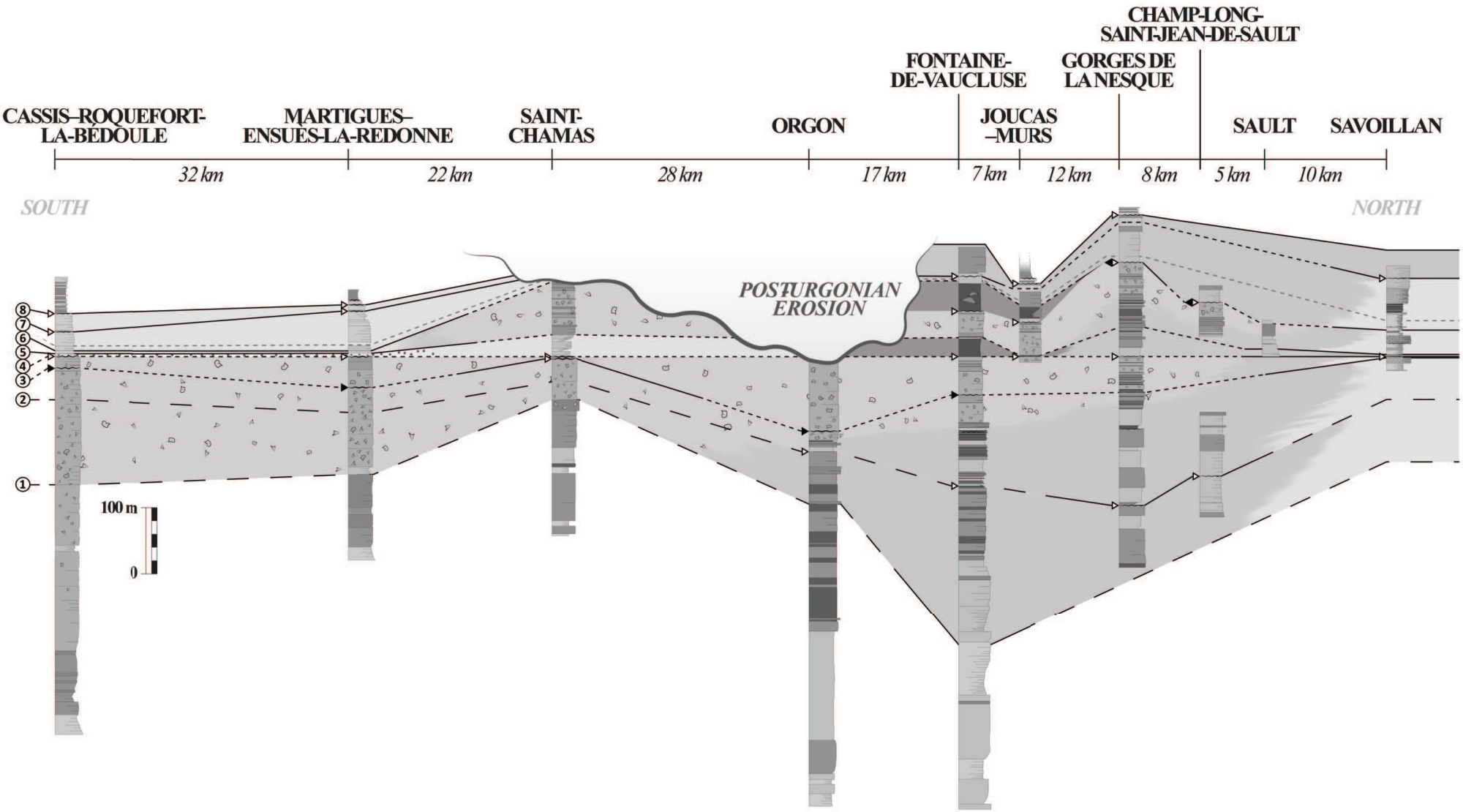

FACIES TYPES

Inner platform
- ***Beach–fenestrate*** *facies*
- ***Peloidal–foraminiferal*** *facies*
- ***Rudist*** *facies*
- ***Rudstone*** *facies*

Outer platform
- ***Coral*** *facies*
- ***Ooidal*** *facies*
- ***Calcarenitic*** *facies*

Slope
- ***Calcisiltite*** *facies*
- ***Finely laminated calcisiltite*** *facies*
- ***Platform-derived bioclastic*** *facies*

Basin
- ***Basinal limestone*** *facies*
- ***Marl*** *facies*

- ***Gastropod-/bivalve-rich*** *facies*
- ***Orbitolinid*** *facies*

SKELETAL & NON-SKELETAL CONSTITUENTS

- ***Agriopleura***
- ***Requieniid–monopleurid***
- ***Caprinid***
- ***Offneria simplex (caprinid)***

CHARACTERISTIC SURFACES

- ***Subaerial exposure***
- ***Drowning surface***

CORRELATIONS

- ***Ammonite-based time line***
- ***Ammonite-derived time line***
- ***Poorly-constrained time line***
- ***Putative B/A boundary***

AMMONITE BIO-EVENTS

⑧ ***2nd Deshayesites*** *bio-event*
⑦ ***1st Deshayesites*** *bio-event*
⑥ ***2nd Martelites*** *bio-event*
⑤ ***1st Martelites*** *bio-event*
④ ***Heteroceras*** *bio-event*
③ ***Hemihoplites feraudianus*** *bio-event*
② ***Camereiceras limentinum*** *bio-event*
① ***Toxancyloceras vandenheckii*** *bio-event*

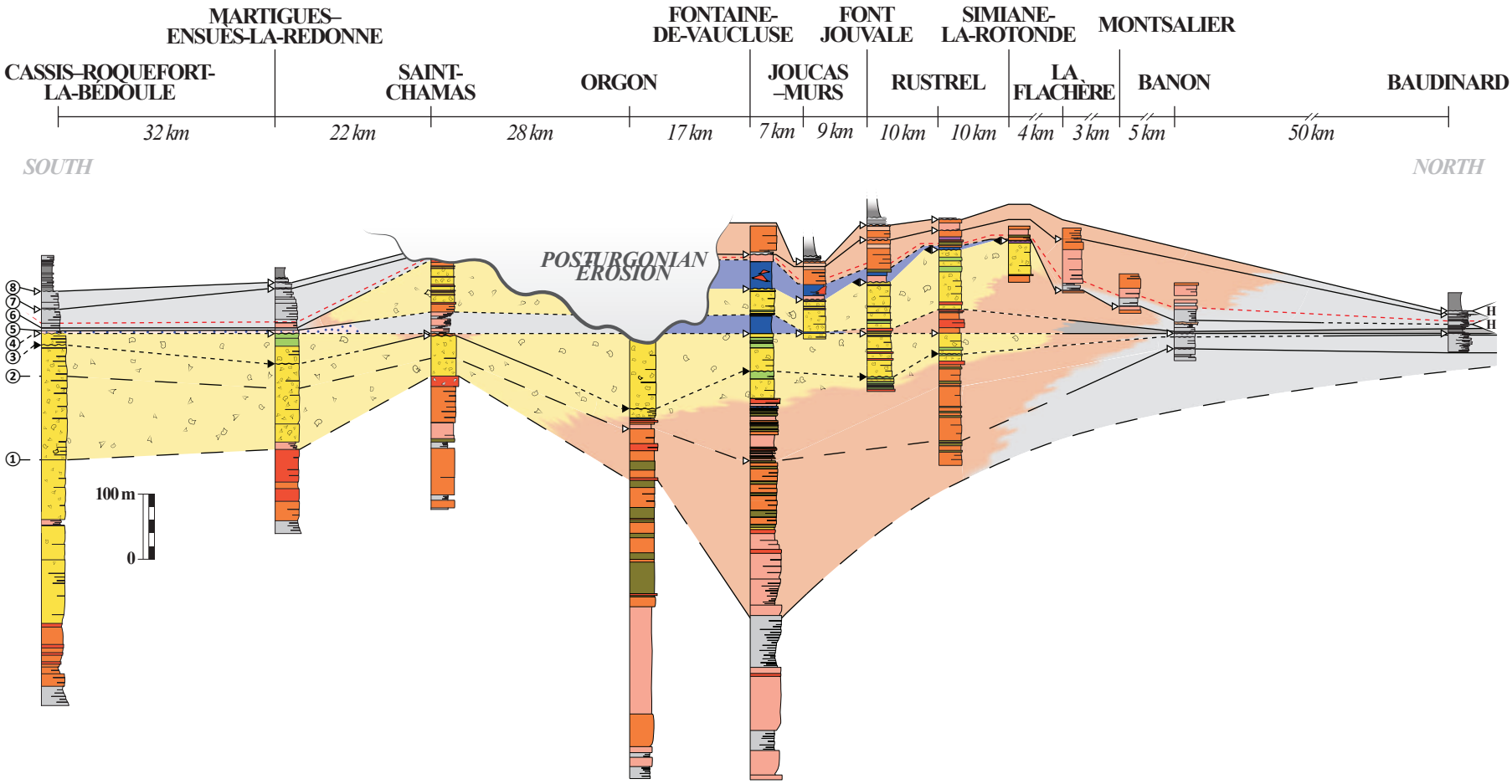
CASSIS–ROQUEFORT-LA-BÉDOULE
MARTIGUES–ENSUES-LA-REDONNE
SAINT-CHAMAS
ORGON
FONTAINE-DE-VAUCLUSE
JOUCAS–MURS
FONT JOUVALE
RUSTREL
SIMIANE-LA-ROTONDE
LA FLACHÈRE
MONTSALIER
BANON
BAUDINARD
32 km
22 km
28 km
17 km
7 km
9 km
10 km
10 km
4 km
3 km
5 km
50 km
SOUTH
NORTH
POSTTURGONIAN EROSION
100 m
0
FACIES TYPES
Inner platform
Beach–fenestrate facies
Peloidal–foraminiferal facies
Rudist facies
Outer platform
Rudstone facies
Coral facies
Ooidal facies
Calcarenitic facies
Slope
Calcisiltite facies
Finely laminated calcisiltite facies
Platform-derived bioclastic facies
Basin
Basinal limestone facies
Marl facies
Gastropod-/bivalve-rich facies
Orbitolinid facies
SKELETAL & NON-SKELETAL CONSTITUENTS
Agriopleura
Requieniid–monopleurid
Caprinid
Offneria simplex (caprinid)
CHARACTERISTIC SURFACES
Subaerial exposure
Drowning surface
H Depositional hiatus
CORRELATIONS
Ammonite-based time line
Ammonite-derived time line
Poorly-constrained time line
Putative B/A boundary
AMMONITE BIO-EVENTS
⑧ 2nd Deshayesites bio-event
⑦ 1st Deshayesites bio-event
⑥ 2nd Martelites bio-event
⑤ 1st Martelites bio-event
④ Heteroceras bio-event
③ Hemihoplites feraudianus bio-event
② Camereiceras limentinum bio-event
① Toxancyloceras vandenheckii bio-event

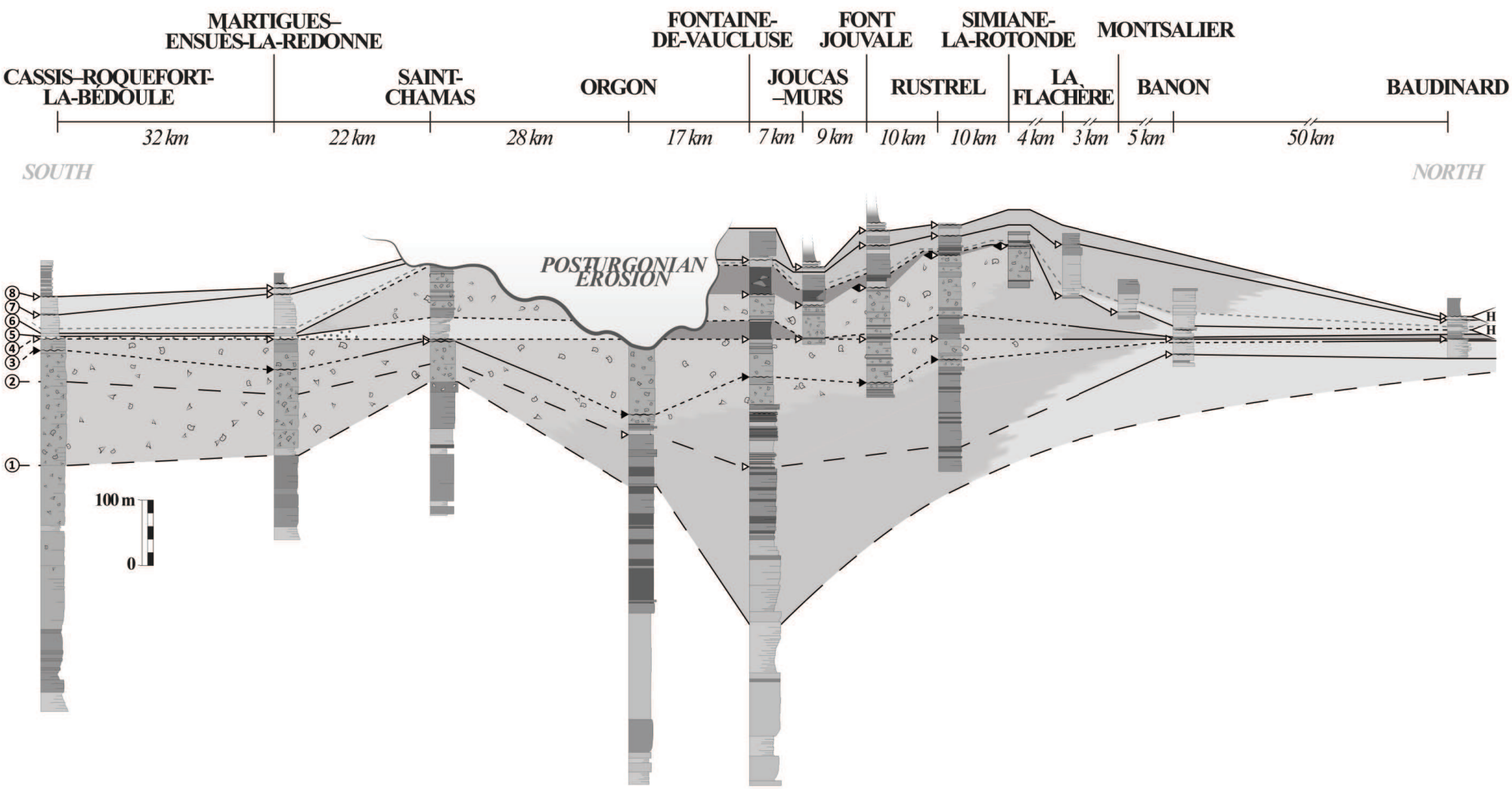

FACIES TYPES

Inner platform
- ***Beach–fenestrate*** *facies*
- ***Peloidal–foraminiferal*** *facies*
- ***Rudist*** *facies*
- ***Rudstone*** *facies*

Outer platform
- ***Coral*** *facies*
- ***Ooidal*** *facies*
- ***Calcarenitic*** *facies*

Slope
- ***Calcisiltite*** *facies*
- ***Finely laminated calcisiltite*** *facies*
- ***Platform-derived bioclastic*** *facies*

Basin
- ***Basinal limestone*** *facies*
- ***Marl*** *facies*

- ***Gastropod-/bivalve-rich*** *facies*
- ***Orbitolinid*** *facies*

SKELETAL & NON-SKELETAL CONSTITUENTS

- ***Agriopleura***
- ***Requieniid–monopleurid***
- ***Caprinid***
- ***Offneria simplex (caprinid)***

CHARACTERISTIC SURFACES

- ▶ ***Subaerial exposure***
- ▷ ***Drowning surface***
- H ***Depositional hiatus***

CORRELATIONS

- ***Ammonite-based time line***
- ***Ammonite-derived time line***
- ***Poorly-constrained time line***
- ***Putative B/A boundary***

AMMONITE BIO-EVENTS

- ⑧ ***2nd Deshayesites*** *bio-event*
- ⑦ ***1st Deshayesites*** *bio-event*
- ⑥ ***2nd Martelites*** *bio-event*
- ⑤ ***1st Martelites*** *bio-event*
- ④ ***Heteroceras*** *bio-event*
- ③ ***Hemihoplites feraudianus*** *bio-event*
- ② ***Camereiceras limentinum*** *bio-event*
- ① ***Toxancyloceras vandenheckii*** *bio-event*


C
A
10 mm
D
E
B

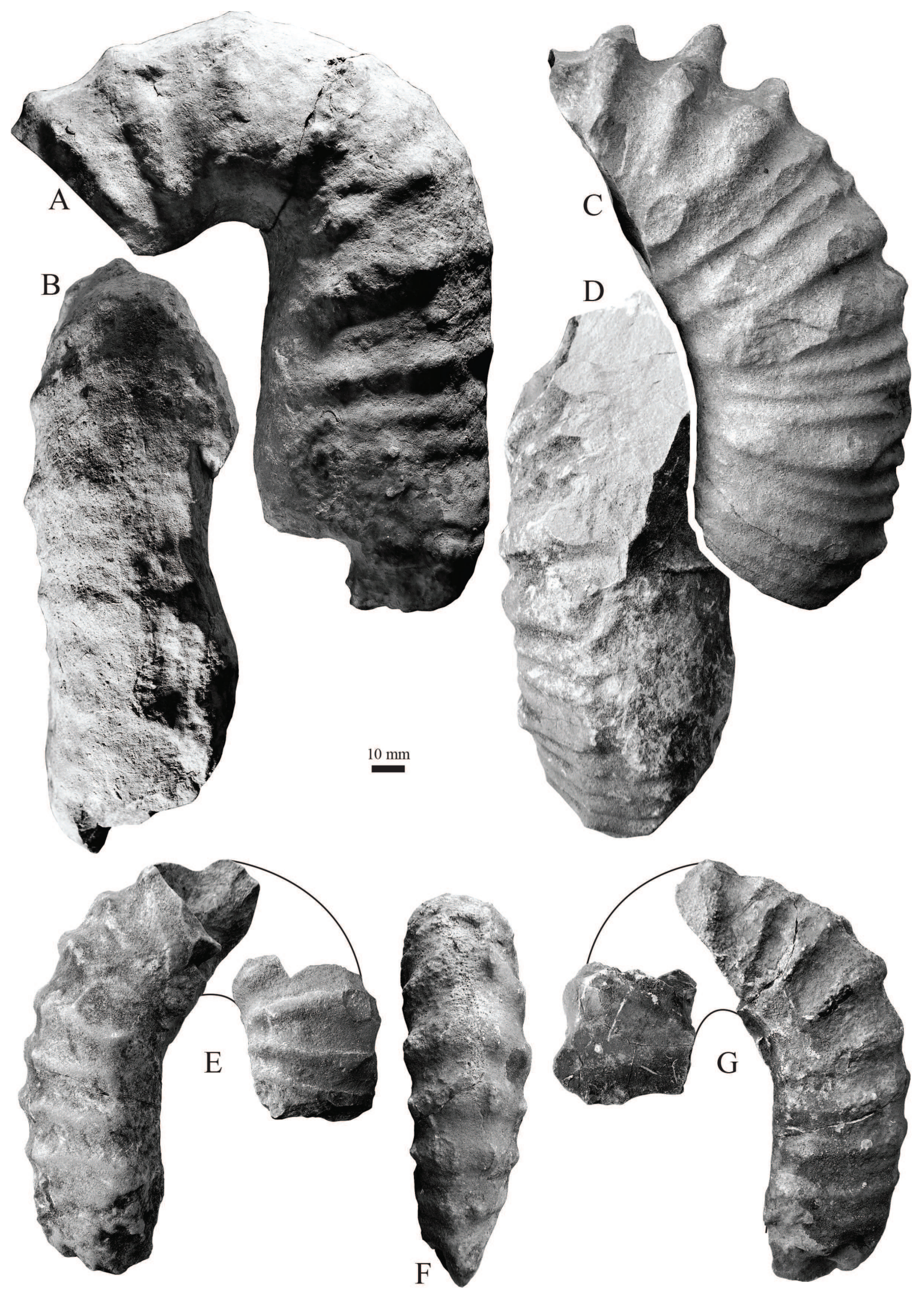
A
B
C
D
10 mm
E
F
G

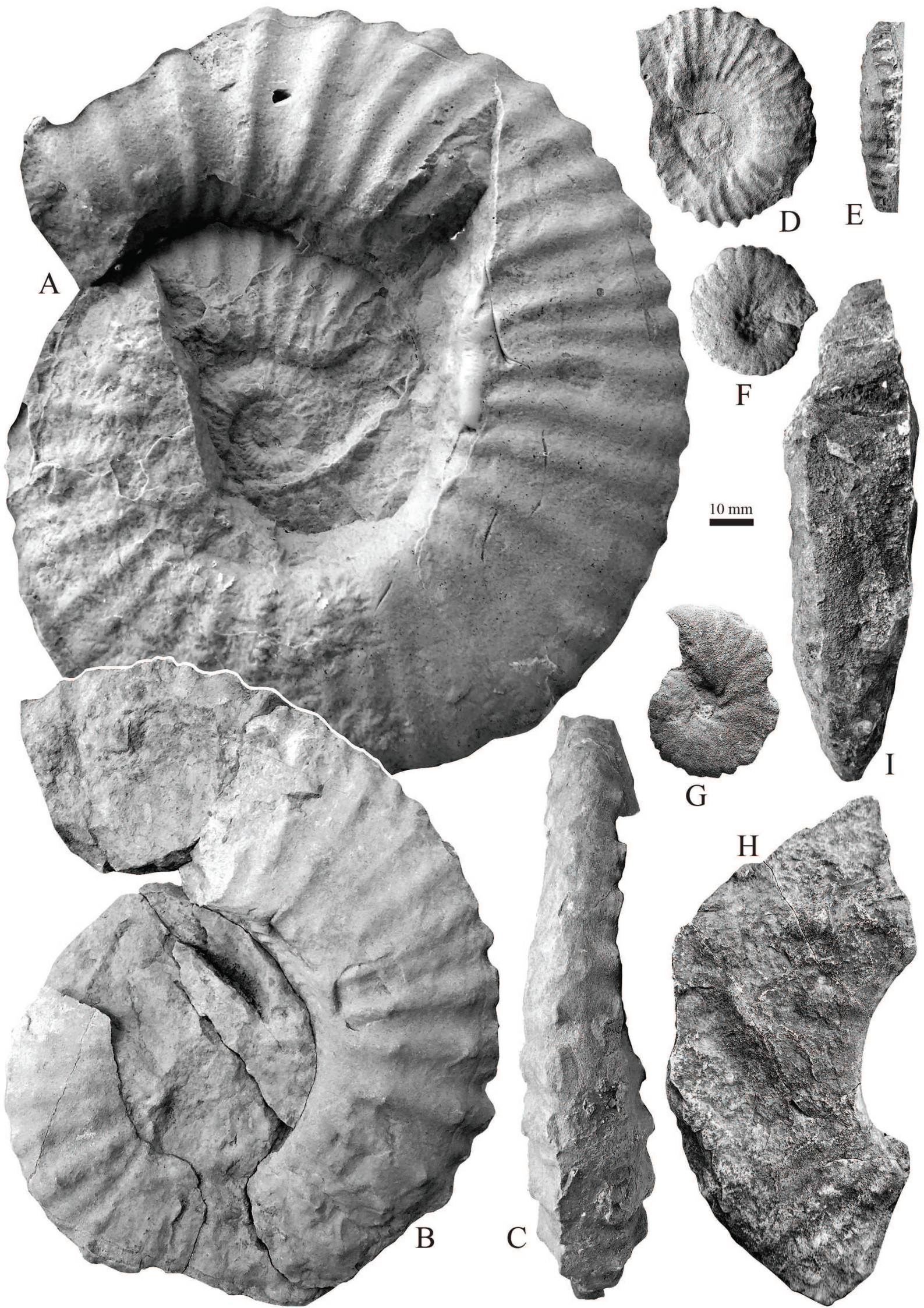
A
B
C
D
E
F
G
H
I
10 mm

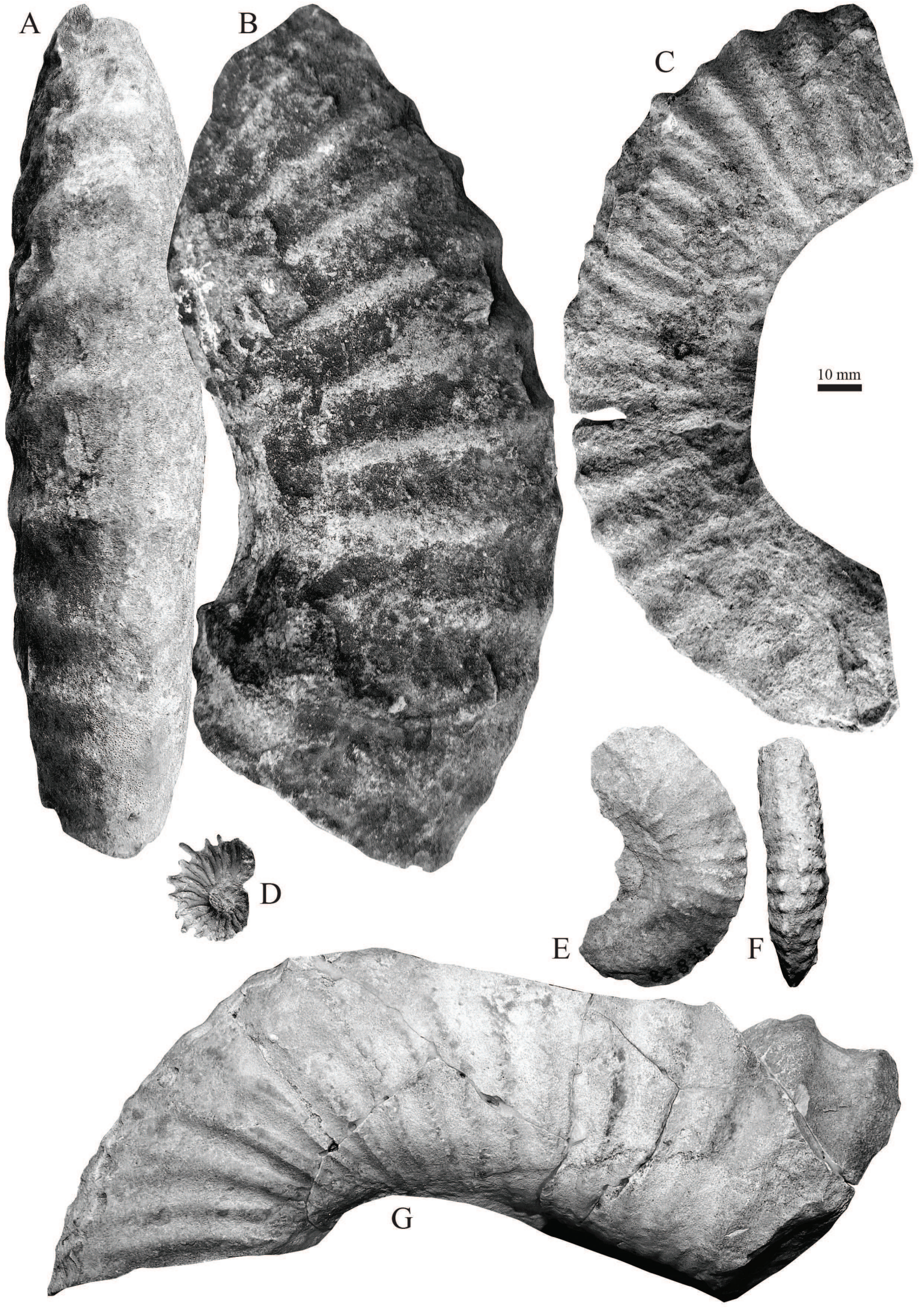
A
B
C
10 mm
D
E
F
G

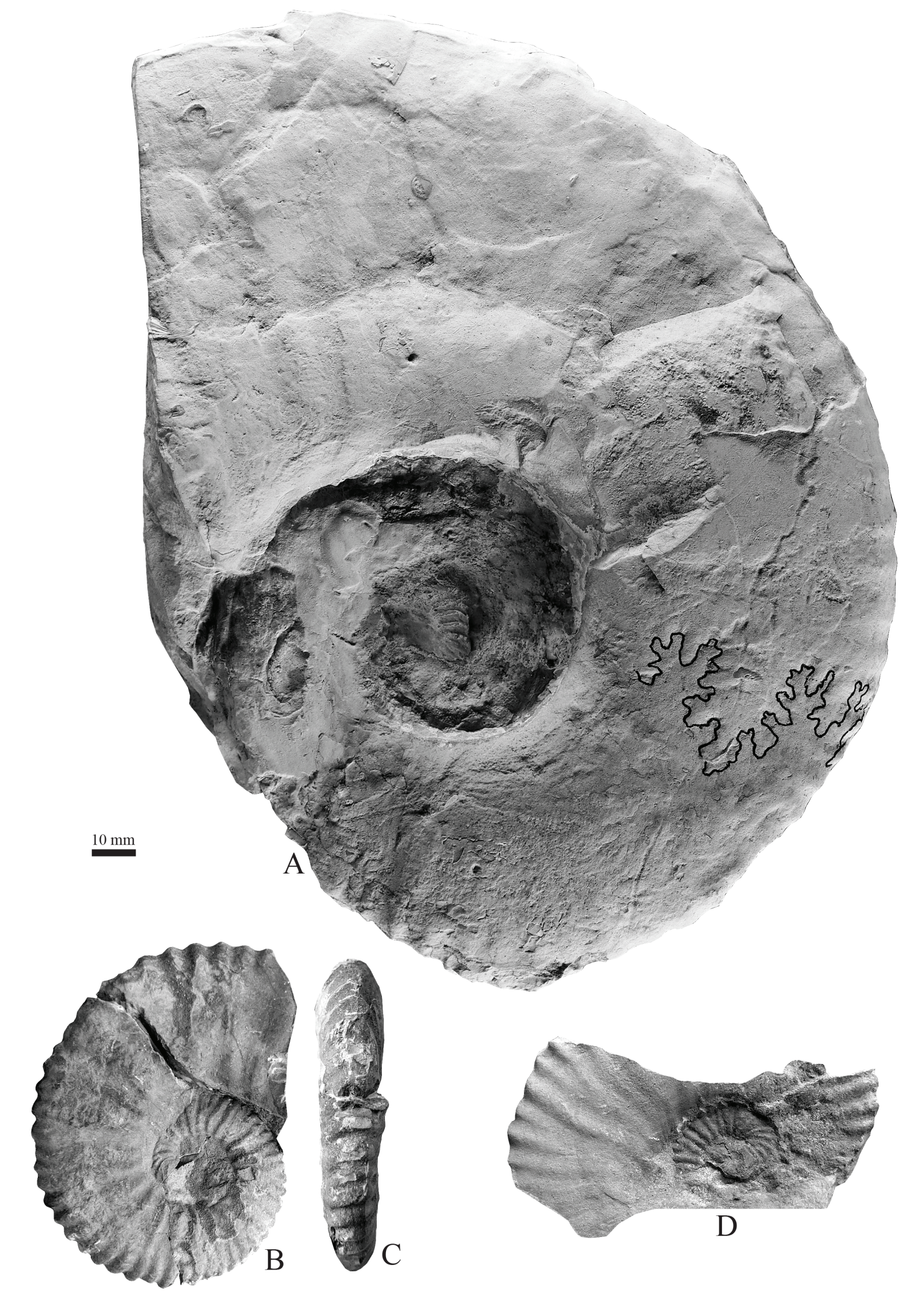
10 mm
A
B
C
D

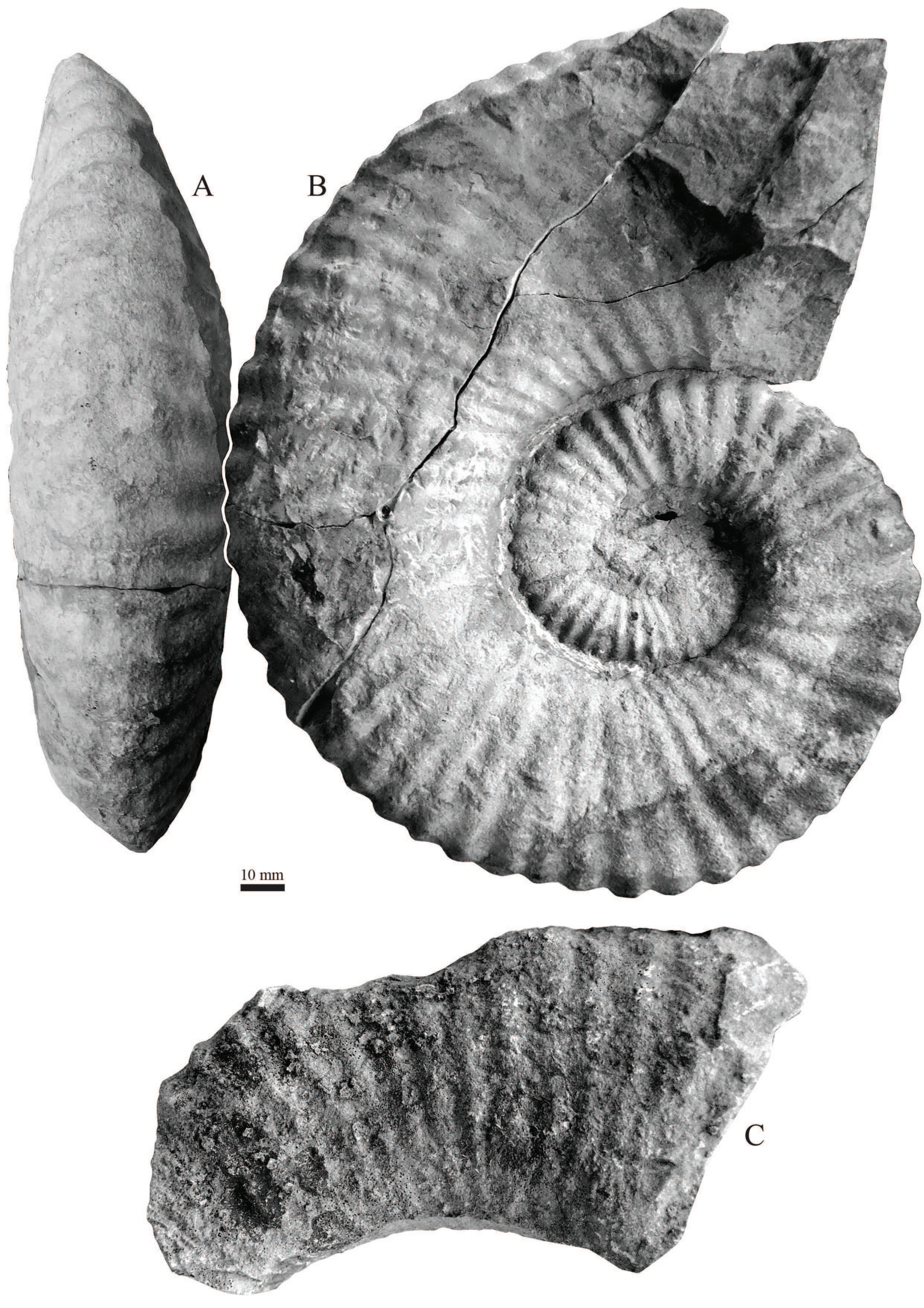
A
B
10 mm
C

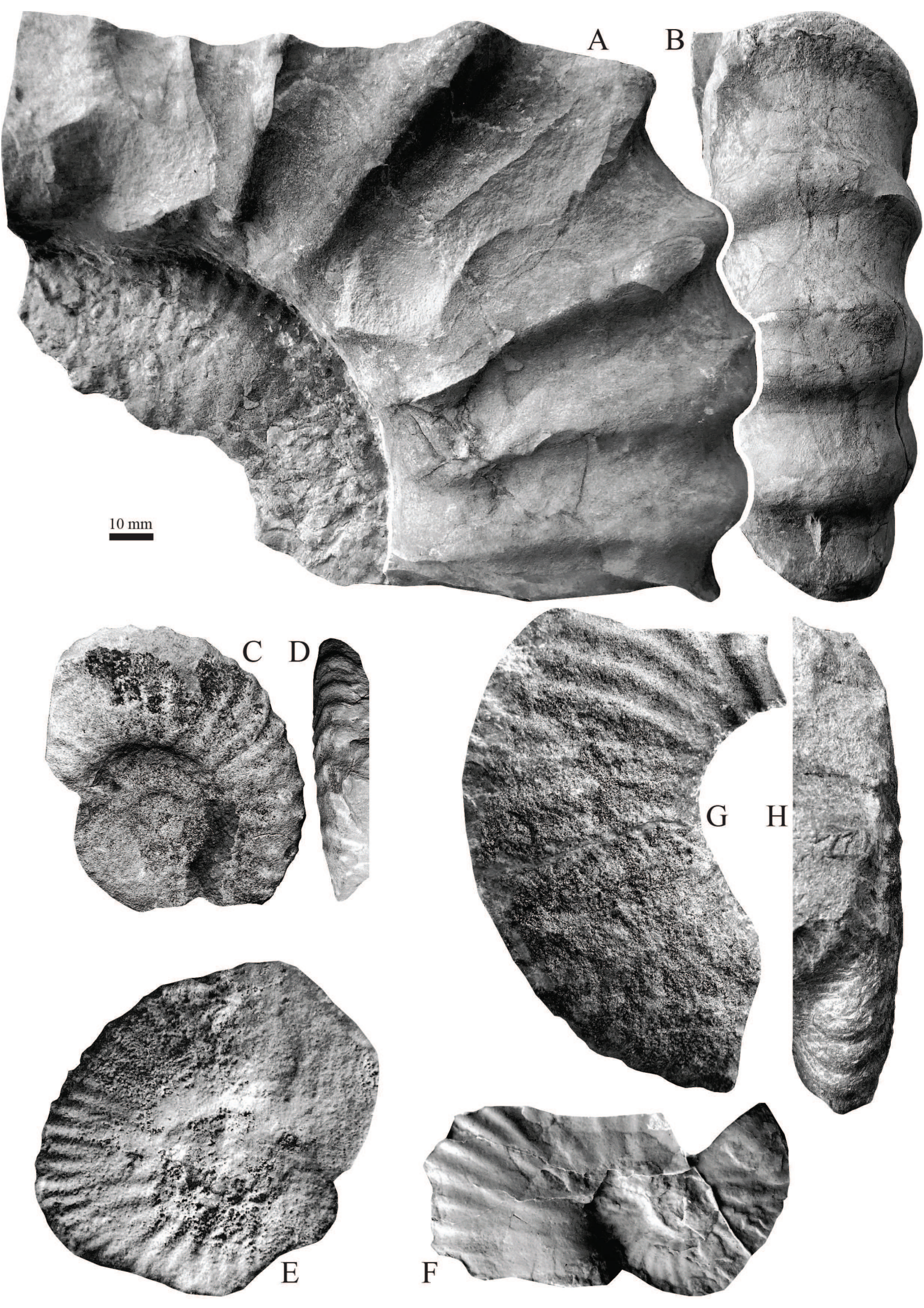
A
B
10 mm
C
D
G
H
E
F

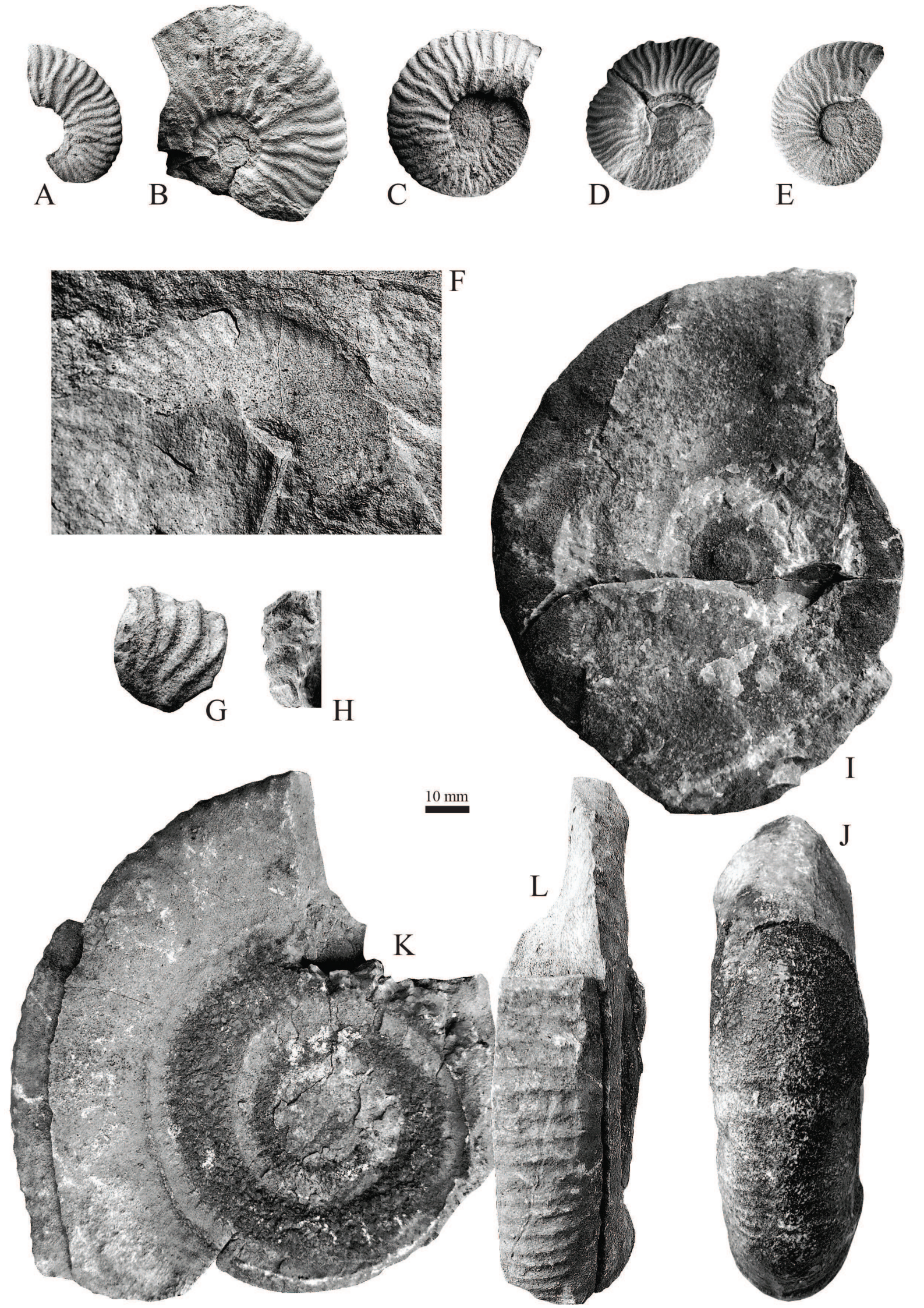
A
B
C
D
E
F
G
H
I
10 mm
J
K
L

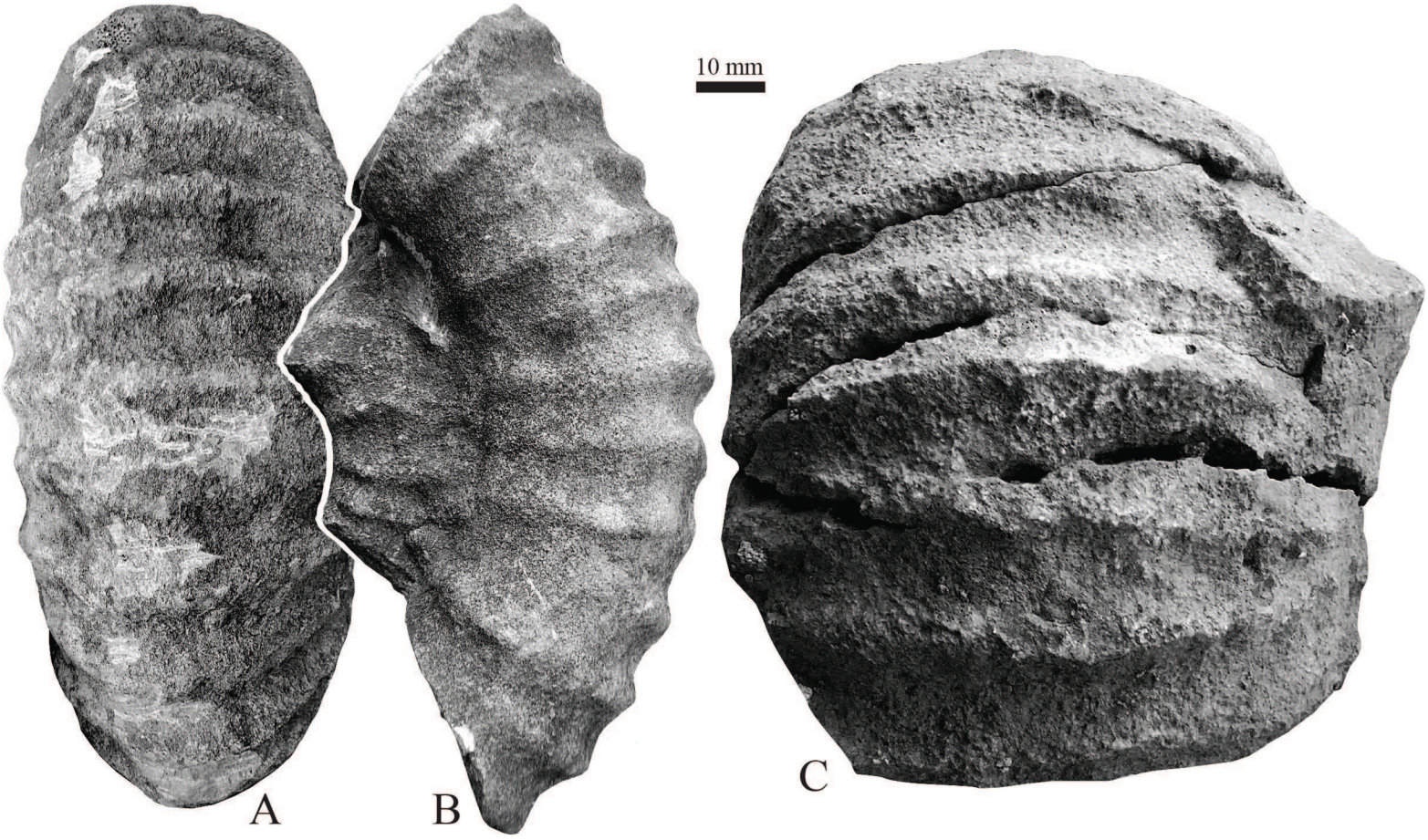
10 mm
A
B
C

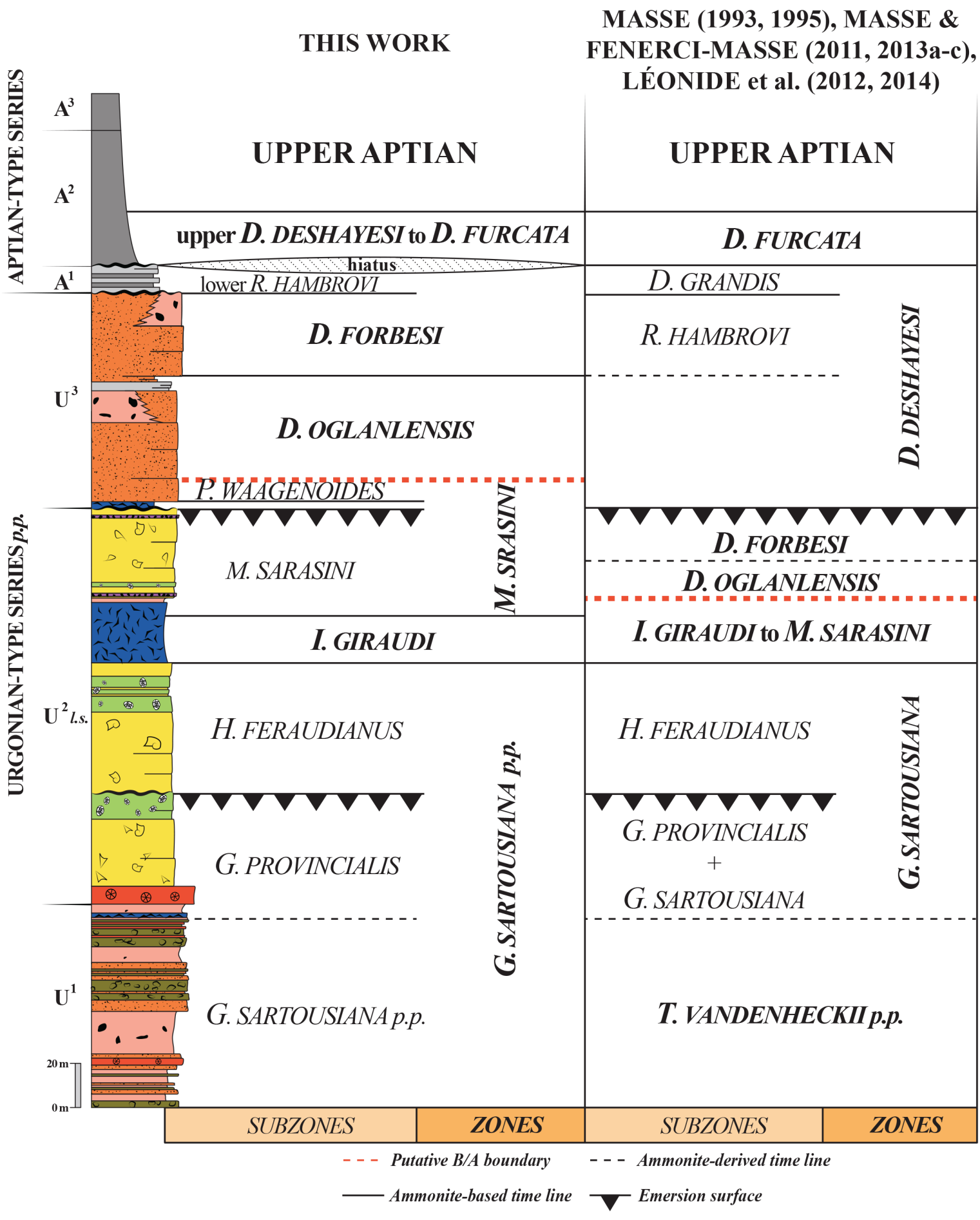
THIS WORK
MASSE (1993, 1995), MASSE & FENERCI-MASSE (2011, 2013a-c), LÉONIDE et al. (2012, 2014)
APTIAN-TYPE SERIES
URGONIAN-TYPE SERIES p.p.
A3
A2
A1
U3
U2 l.s.
U1
20 m
0 m
UPPER APTIAN
UPPER APTIAN
upper D. DESHAYESI to D. FURCATA
D. FURCATA
hiatus
lower R. HAMBROVI
D. GRANDIS
D. FORBESI
R. HAMBROVI
D. DESHAYESI
D. OGLANLENSIS
P. WAAGENOIDES
M. SARASINI
M. SRASINI
D. FORBESI
D. OGLANLENSIS
I. GIRAUDI
I. GIRAUDI to M. SARASINI
H. FERAUDIANUS
H. FERAUDIANUS
G. SARTOUSIANA p.p.
G. PROVINCIALIS
G. PROVINCIALIS + G. SARTOUSIANA
G. SARTOUSIANA
G. SARTOUSIANA p.p.
T. VANDENHECKII p.p.
SUBZONES
ZONES
SUBZONES
ZONES
Putative B/A boundary
Ammonite-derived time line
Ammonite-based time line
Emersion surface

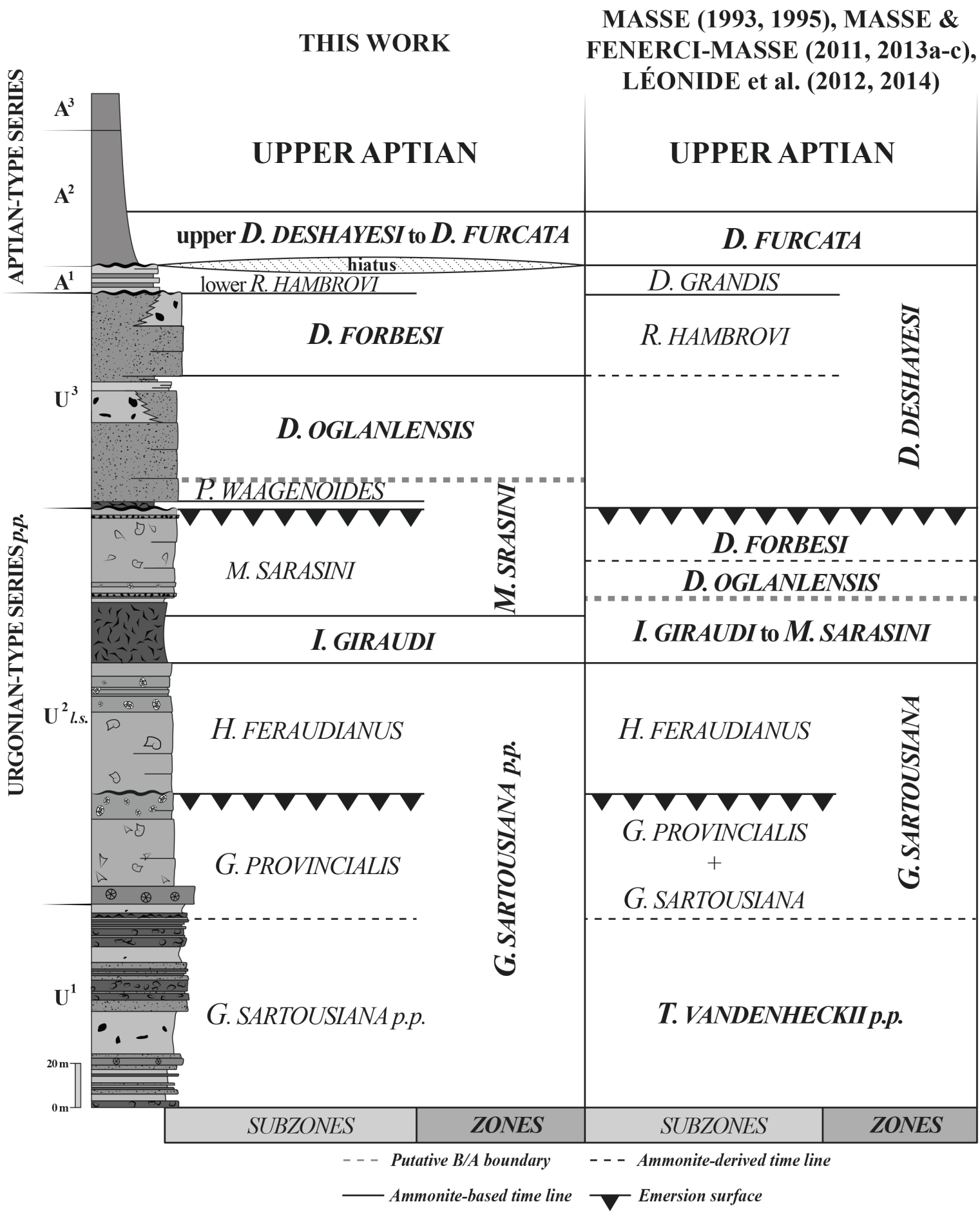
THIS WORK
MASSE (1993, 1995), MASSE & FENERCI-MASSE (2011, 2013a-c), LÉONIDE et al. (2012, 2014)
APTIAN-TYPE SERIES
URGONIAN-TYPE SERIES p.p.
A3
A2
A1
U3
U2 l.s.
U1
20 m
0 m
UPPER APTIAN
UPPER APTIAN
upper D. DESHAYESI to D. FURCATA
D. FURCATA
hiatus
lower R. HAMBROVI
D. GRANDIS
D. FORBESI
R. HAMBROVI
D. DESHAYESI
D. OGLANLENSIS
P. WAAGENOIDES
M. SARASINI
M. SRASINI
D. FORBESI
D. OGLANLENSIS
I. GIRAUDI
I. GIRAUDI to M. SARASINI
H. FERAUDIANUS
H. FERAUDIANUS
G. SARTOUSIANA p.p.
G. PROVINCIALIS
G. PROVINCIALIS + G. SARTOUSIANA
G. SARTOUSIANA
G. SARTOUSIANA p.p.
T. VANDENHECKII p.p.
SUBZONES
ZONES
SUBZONES
ZONES
Putative B/A boundary
Ammonite-derived time line
Ammonite-based time line
Emersion surface

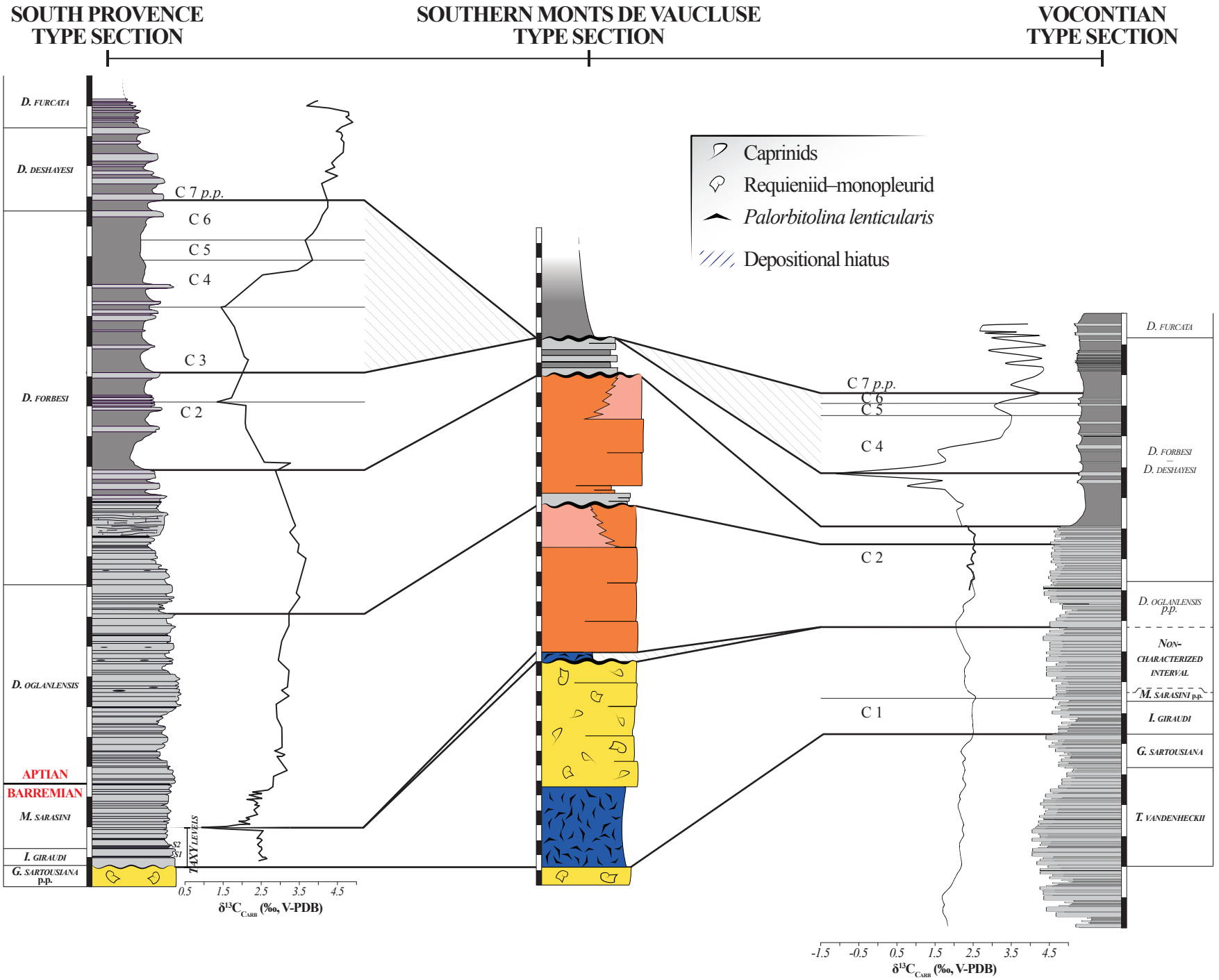
SOUTH PROVENCE TYPE SECTION
SOUTHERN MONTS DE VAUCLUSE TYPE SECTION
VOCONTIAN TYPE SECTION
Caprinids
Requieniid–monopleurid
Palorbitolina lenticularis
Depositional hiatus
D. FURCATA
D. DESHAYESI
D. FORBESI
D. OGLANLENSIS
APTIAN
BARREMIAN
M. SARASINI
I. GIRAUDI
G. SARTOUSIANA p.p.
C 7 p.p.
C 6
C 5
C 4
C 3
C 2
C 1
THAXY LEVELS
S2
S1
0.5 1.5 2.5 3.5 4.5
δ13CCARB (‰, V-PDB)
D. FORBESI – D. DESHAYESI
D. OGLANLENSIS p.p.
NON-CHARACTERIZED INTERVAL
M. SARASINI p.p.
T. VANDENHECKII
-1.5 -0.5 0.5 1.5 2.5 3.5 4.5
δ13CCARB (‰, V-PDB)

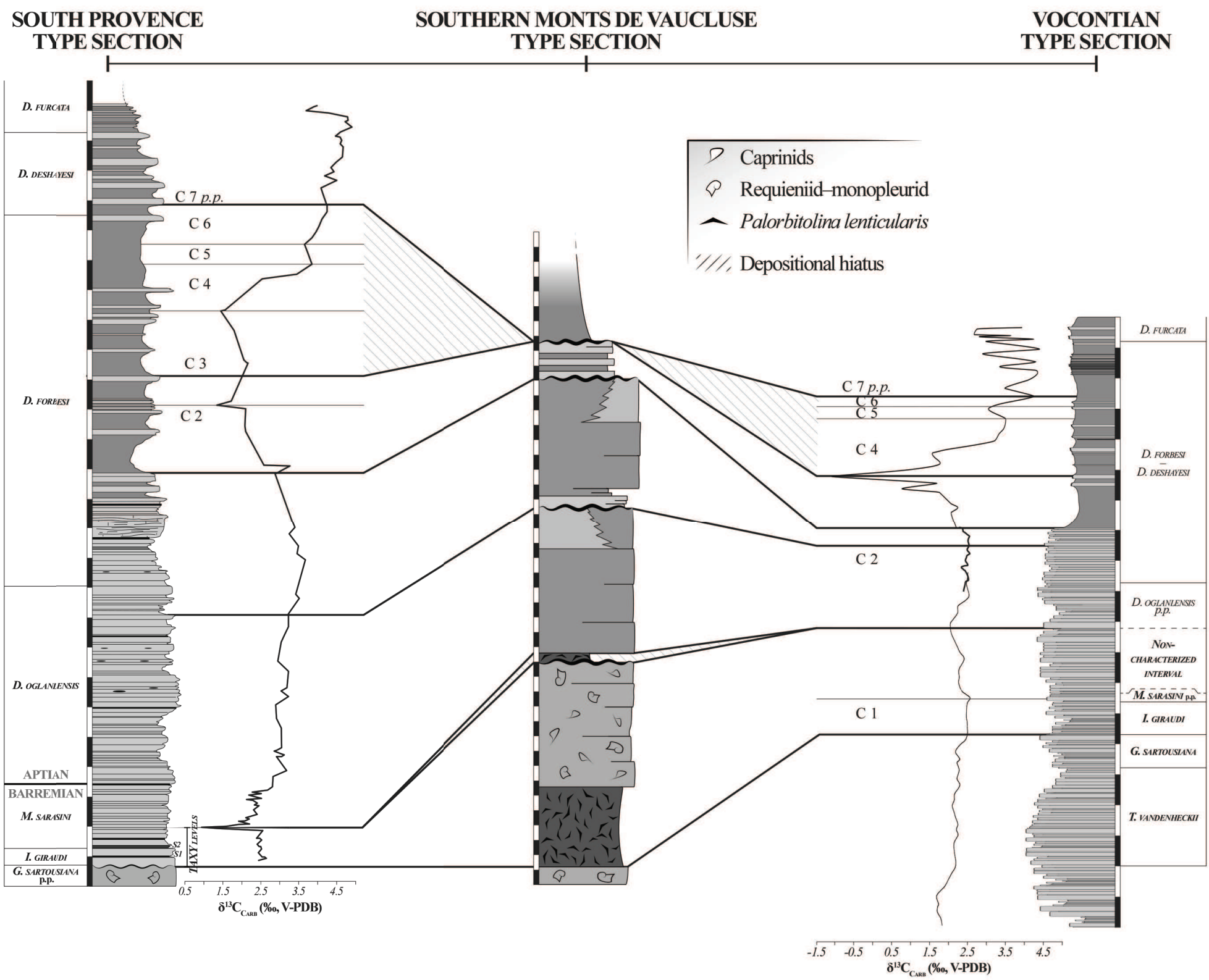
SOUTH PROVENCE TYPE SECTION
SOUTHERN MONTS DE VAUCLUSE TYPE SECTION
VOCONTIAN TYPE SECTION
Caprinids
Requieniid–monopleurid
Palorbitolina lenticularis
Depositional hiatus
D. FURCATA
D. DESHAYESI
D. FORBESI
D. OGLANLENSIS
APTIAN
BARREMIAN
M. SARASINI
I. GIRAUDI
G. SARTOUSIANA p.p.
C 7 p.p.
C 6
C 5
C 4
C 3
C 2
C 1
S2
S1
THIXY LEVELS
0.5 1.5 2.5 3.5 4.5
δ13CCARB (‰, V-PDB)
D. FURCATA
D. FORBESI – D. DESHAYESI
D. OGLANLENSIS p.p.
NON-CHARACTERIZED INTERVAL
M. SARASINI p.p.
I. GIRAUDI
G. SARTOUSIANA
T. VANDENHECKII
-1.5 -0.5 0.5 1.5 2.5 3.5 4.5
δ13CCARB (‰, V-PDB)

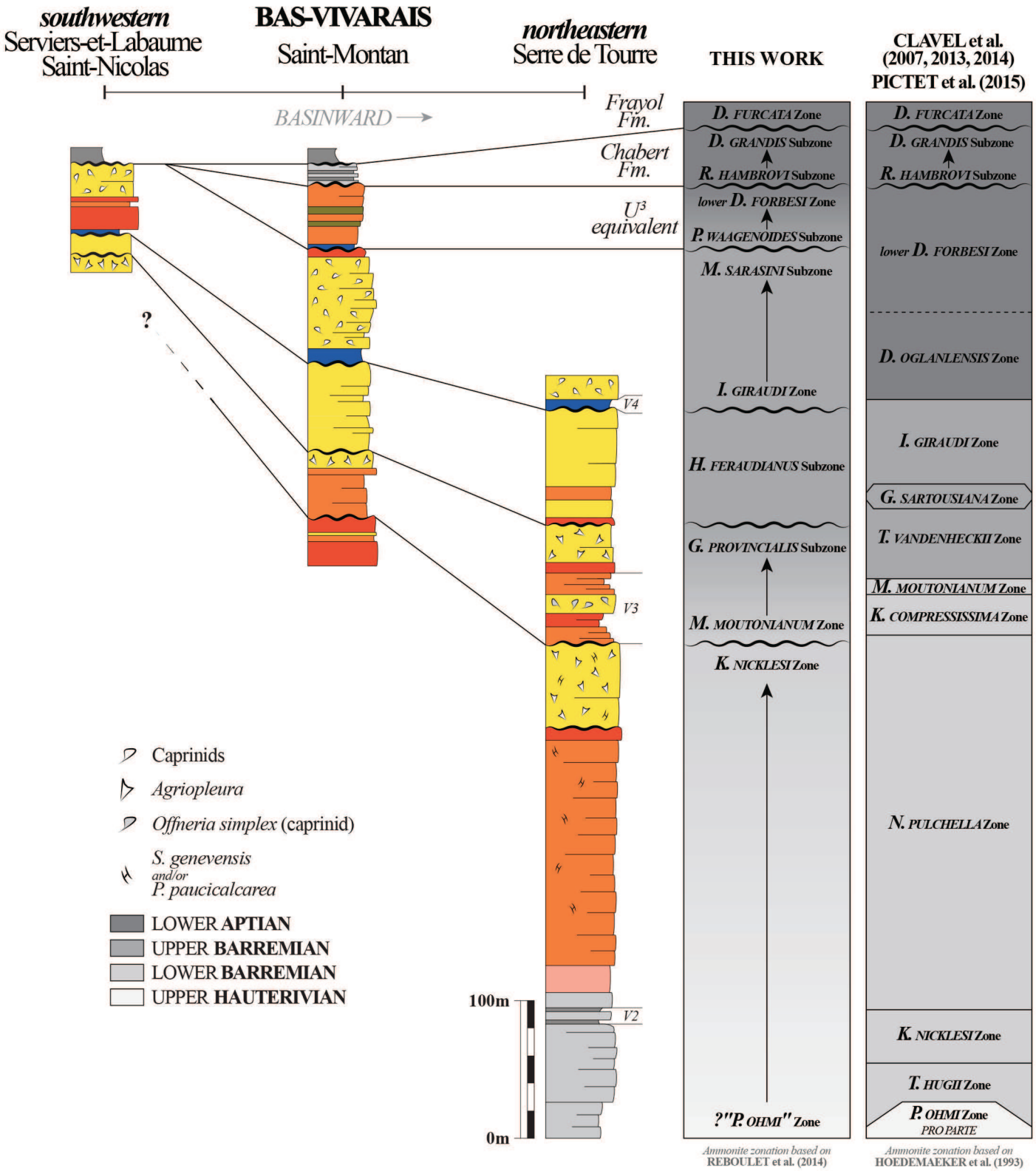
southwestern
Serviers-et-Labaume
Saint-Nicolas
BAS-VIVARAIS
Saint-Montan
northeastern
Serre de Tourre
BASINWARD
Frayol Fm.
Chabert Fm.
U3 equivalent
?
V4
V3
V2
100m
0m
Caprinids
Agriopleura
Offneria simplex (caprinid)
S. genevensis
and/or
P. paucicalcarea
LOWER APTIAN
UPPER BARREMIAN
LOWER BARREMIAN
UPPER HAUTERIVIAN
THIS WORK
D. FURCATA Zone
D. GRANDIS Subzone
R. HAMBROVI Subzone
lower D. FORBESI Zone
P. WAAGENOIDES Subzone
M. SARASINI Subzone
I. GIRAUDI Zone
H. FERAUDIANUS Subzone
G. PROVINCIALIS Subzone
M. MOUTONIANUM Zone
K. NICKLESI Zone
?"P. OHMI" Zone
Ammonite zonation based on
REBOULET et al. (2014)
CLAVEL et al.
(2007, 2013, 2014)
PICTET et al. (2015)
D. FURCATA Zone
D. GRANDIS Subzone
R. HAMBROVI Subzone
lower D. FORBESI Zone
D. OGLANLENSIS Zone
I. GIRAUDI Zone
G. SARTOUSIANA Zone
T. VANDENHECKII Zone
M. MOUTONIANUM Zone
K. COMPRESSISSIMA Zone
N. PULCHELLA Zone
K. NICKLESI Zone
T. HUGII Zone
P. OHMI Zone
PRO PARTE
Ammonite zonation based on
HOEDEMAEKER et al. (1993)

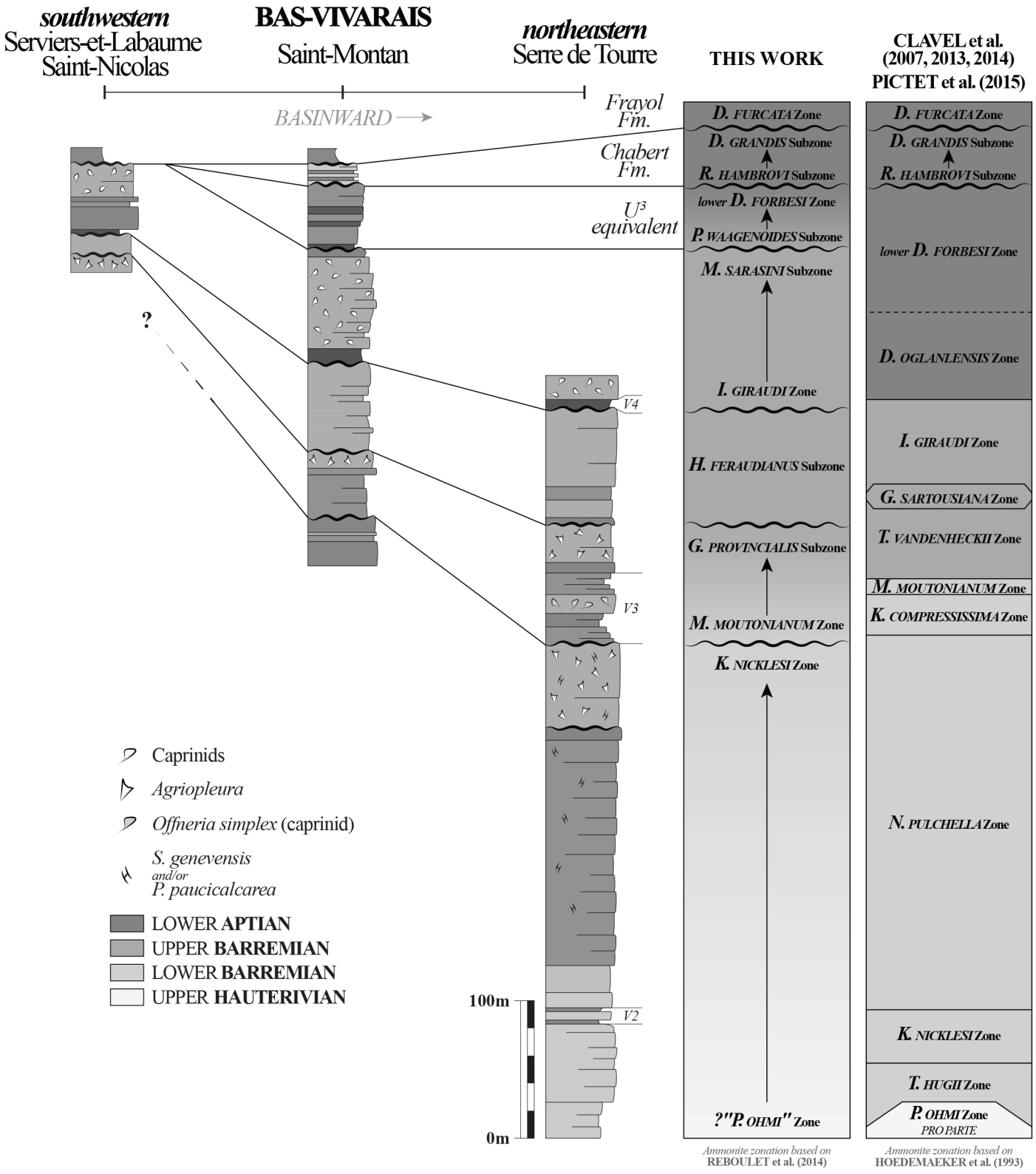
southwestern
Serviers-et-Labaume
Saint-Nicolas
BAS-VIVARAIS
Saint-Montan
northeastern
Serre de Tourre
BASINWARD
Frayol Fm.
Chabert Fm.
U3 equivalent
?
V4
V3
V2
100m
0m
Caprinids
Agriopleura
Offneria simplex (caprinid)
S. genevensis
and/or
P. paucicalcarea
LOWER APTIAN
UPPER BARREMIAN
LOWER BARREMIAN
UPPER HAUTERIVIAN
THIS WORK
D. FURCATA Zone
D. GRANDIS Subzone
R. HAMBROVI Subzone
lower D. FORBESI Zone
P. WAAGENOIDES Subzone
M. SARASINI Subzone
I. GIRAUDI Zone
H. FERAUDIANUS Subzone
G. PROVINCIALIS Subzone
M. MOUTONIANUM Zone
K. NICKLESI Zone
?"P. OHMI" Zone
Ammonite zonation based on
REBOULET et al. (2014)
CLAVEL et al.
(2007, 2013, 2014)
PICTET et al. (2015)
D. FURCATA Zone
D. GRANDIS Subzone
R. HAMBROVI Subzone
lower D. FORBESI Zone
D. OGLANLENSIS Zone
I. GIRAUDI Zone
G. SARTOUSIANA Zone
T. VANDENHECKII Zone
M. MOUTONIANUM Zone
K. COMPRESSISSIMA Zone
N. PULCHELLA Zone
K. NICKLESI Zone
T. HUGII Zone
P. OHMI Zone
PRO PARTE
Ammonite zonation based on
HOEDEMAEKER et al. (1993)

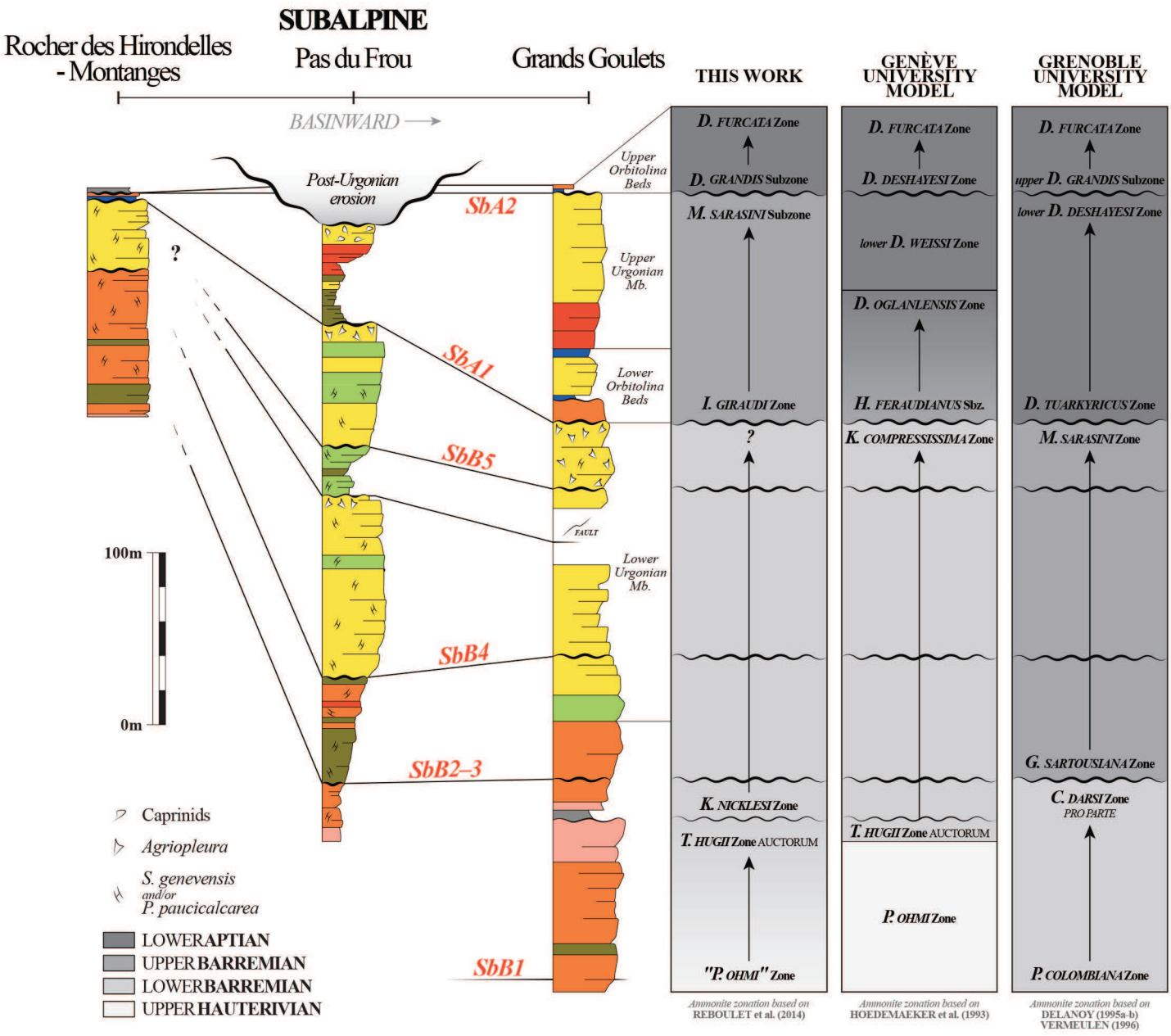
SUBALPINE
Rocher des Hirondelles - Montanges
Pas du Frou
Grands Goulets
BASINWARD
Post-Urgonian erosion
SbA2
SbA1
SbB5
SbB4
SbB2–3
SbB1
?
FAULT
Upper Orbitolina Beds
Upper Urgonian Mb.
Lower Orbitolina Beds
Lower Urgonian Mb.
100m
0m
Caprinids
Agriopleura
S. genevensis and/or P. paucicalcarea
LOWER APTIAN
UPPER BARREMIAN
LOWER BARREMIAN
UPPER HAUTERIVIAN
THIS WORK
D. FURCATA Zone
D. GRANDIS Subzone
M. SARASINI Subzone
I. GIRAUDI Zone
?
K. NICKLESI Zone
T. HUGII Zone AUCTORUM
"P. OHMI" Zone
Ammonite zonation based on REBOULET et al. (2014)
GENÈVE UNIVERSITY MODEL
D. FURCATA Zone
D. DESHAYESI Zone
lower D. WEISSI Zone
D. OGLANLENSIS Zone
H. FERAUDIANUS Sbz.
K. COMPRESSISSIMA Zone
T. HUGII Zone AUCTORUM
P. OHMI Zone
Ammonite zonation based on HOEDEMAEKER et al. (1993)
GRENOBLE UNIVERSITY MODEL
D. FURCATA Zone
upper D. GRANDIS Subzone
lower D. DESHAYESI Zone
D. TUARKYRICUS Zone
M. SARASINI Zone
G. SARTOUSIANA Zone
C. DARSI Zone PRO PARTE
P. COLOMBIANA Zone
Ammonite zonation based on DELANOY (1995a-b) VERMEULEN (1996)

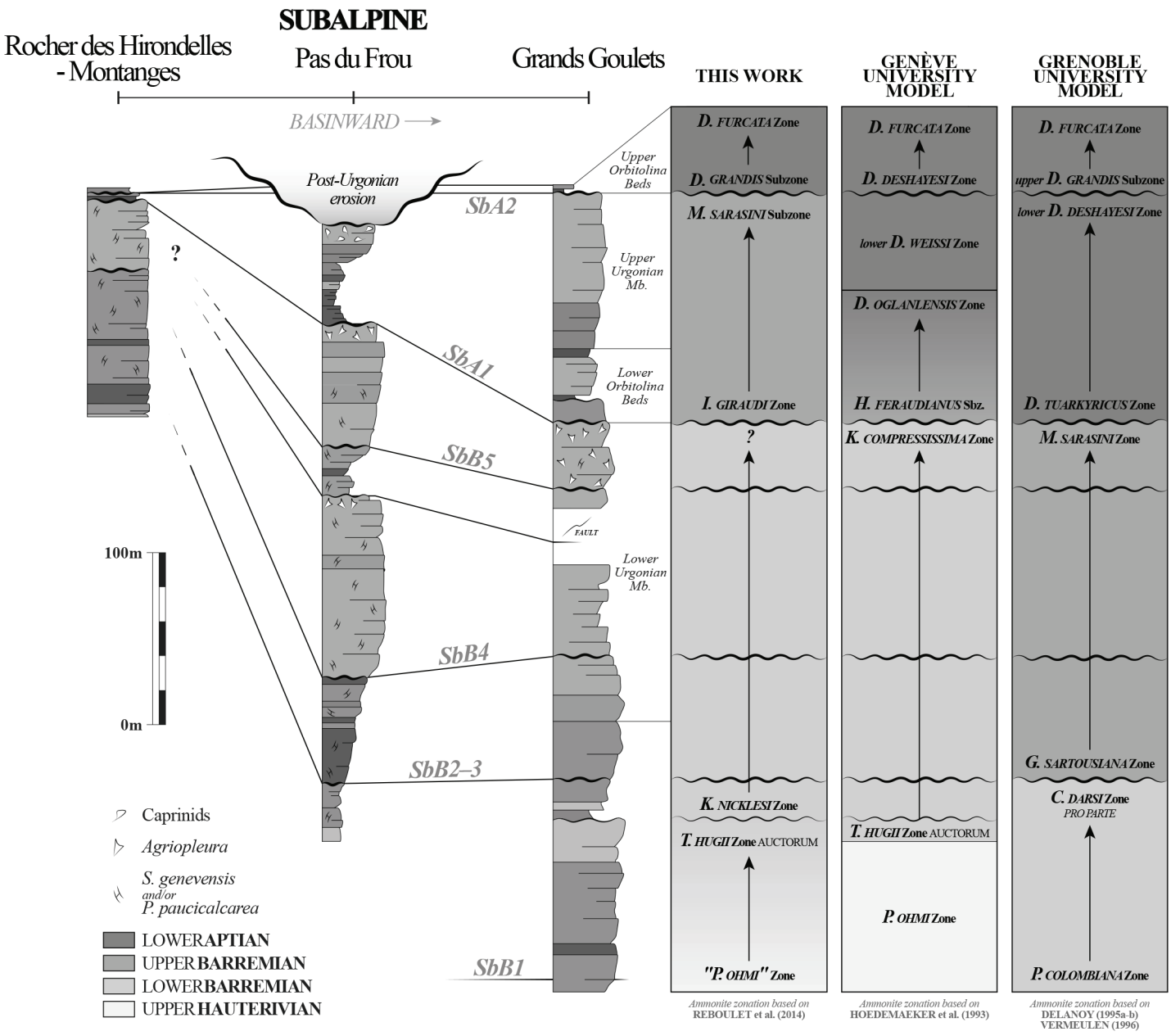
SUBALPINE
Rocher des Hirondelles - Montanges
Pas du Frou
Grands Goulets
BASINWARD
Post-Urgonian erosion
SbA2
SbA1
SbB5
SbB4
SbB2–3
SbB1
?
FAULT
Upper Orbitolina Beds
Upper Urgonian Mb.
Lower Orbitolina Beds
Lower Urgonian Mb.
100m
0m
Caprinids
Agriopleura
S. genevensis and/or P. paucicalcarea
LOWER APTIAN
UPPER BARREMIAN
LOWER BARREMIAN
UPPER HAUTERIVIAN
THIS WORK
D. FURCATA Zone
D. GRANDIS Subzone
M. SARASINI Subzone
I. GIRAUDI Zone
?
K. NICKLESI Zone
T. HUGII Zone AUCTORUM
"P. OHMI" Zone
Ammonite zonation based on REBOULET et al. (2014)
GENÈVE UNIVERSITY MODEL
D. FURCATA Zone
D. DESHAYESI Zone
lower D. WEISSI Zone
D. OGLANLENSIS Zone
H. FERAUDIANUS Sbz.
K. COMPRESSISSIMA Zone
T. HUGII Zone AUCTORUM
P. OHMI Zone
Ammonite zonation based on HOEDEMAEKER et al. (1993)
GRENOBLE UNIVERSITY MODEL
D. FURCATA Zone
upper D. GRANDIS Subzone
lower D. DESHAYESI Zone
D. TUARKYRICUS Zone
M. SARASINI Zone
G. SARTOUSIANA Zone
C. DARSI Zone PRO PARTE
P. COLOMBIANA Zone
Ammonite zonation based on DELANOY (1995a, b) VERMEULEN (1996)